



Universiteit
Leiden
The Netherlands

Inhibitor discovery of phospholipases and N-acyltransferases

Zhou, J.

Citation

Zhou, J. (2020, November 11). *Inhibitor discovery of phospholipases and N-acyltransferases*. Retrieved from <https://hdl.handle.net/1887/138014>

Version: Publisher's Version

License: [Licence agreement concerning inclusion of doctoral thesis in the Institutional Repository of the University of Leiden](#)

Downloaded from: <https://hdl.handle.net/1887/138014>

Note: To cite this publication please use the final published version (if applicable).

Cover Page



Universiteit Leiden



The handle <http://hdl.handle.net/1887/138014> holds various files of this Leiden University dissertation.

Author: Zhou, J.

Title: Inhibitor discovery of phospholipases and N-acyltransferases

Issue date: 2020-11-11

Inhibitor Discovery of Phospholipases and *N*-acyltransferases

PROEFSCHRIFT

ter verkrijging van

de graad van Doctor aan de Universiteit Leiden,

op gezag van Rector Magnificus prof. mr. C.J.J.M. Stolker,

volgens het besluit van het College voor Promoties

te verdedigen op 11 november 2020

klokke 11:15 uur

door

周 娟

Juan Zhou

Geboren te Henan, China in 1985

Promotiecommissie

Promotores: Prof. dr. Mario van der Stelt
Prof. dr. Herman S. Overkleeft

Overige leden: Prof. dr. J. J. C. Neefjes
Prof. dr. J. Brouwer
Prof. dr. J. M. F. G. Aerts
Prof. dr. S. H. L. Verhelst
Mw. Dr. J. Meijerink

Cover design: Juan Zhou

Printed by Ridderprint

Table of Contents

Chapter 1	5
General introduction	
Chapter 2	21
Development and application of ABPP assay to identify PLAAT3 inhibitors	
Chapter 3	35
Structure-activity relationship of α -ketoamides on phospholipase-acyltransferases: discovery of LEI-110	
Chapter 4	51
Biochemical and cellular profiling of LEI110	
Chapter 5	65
Development of a PLA2G4E assay and subsequent application in hit identification	
Chapter 6	79
Summary and future prospects	
Summary in Chinese	87
Curriculum Vitae	89
List of publications	90

1

General introduction

1.1 Introduction

The plant *Cannabis sativa* and its extracts, such as marijuana and hashish, have been used for recreational and medicinal purposes for a long time.¹ Marijuana has both psychological and physical effects. It modulates neurotransmission in the brain, resulting in changes in mood, appetite, memory, motor coordination and other behavioral responses.² In 1964, Δ^9 -tetrahydrocannabinol (Δ^9 -THC) (Figure 1) was purified and characterized as the major psychoactive component of *Cannabis sativa*.³ The cannabinoid receptor type 1 (CB1R) was identified as a target protein of THC in 1990.⁴ The CB1R is a member of the G-protein-coupled receptor family and is expressed in the peripheral nervous system and central nervous system.⁵ In 1993, a second THC-responsive protein, the cannabinoid receptor type 2 (CB2R), was discovered.⁶ CBR2 is expressed predominantly in peripheral immune cells.^{7,8}

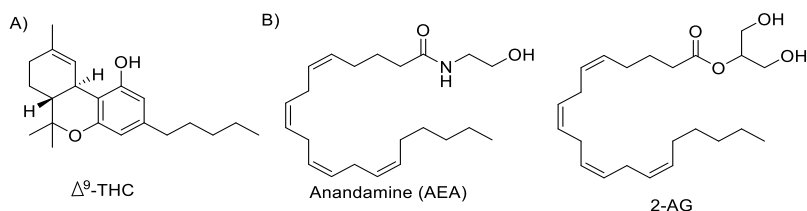


Figure 1. Chemical structures of (A) the plant natural product, Δ^9 -THC and (B) the endocannabinoids, 2-arachidonoylglycerol (2-AG) and *N*-arachidonoylethanolamine (also known as anandamide, AEA).

The finding that Δ^9 -THC, a plant natural product, interacts with mammalian receptor proteins, suggested the existence of endogenous cannabinoid receptor ligands. Indeed, in 1992, two years after the discovery of the CB1R, anandamide (or *N*-arachidonoylethanolamine, AEA, Figure 1B) was isolated from pig brain as the first endogenous cannabinoid ligand.⁹ In 1995, 2-arachidonoylglycerol (2-AG, Figure 1B), previously known as a common intermediate in the metabolisms of glycerophospholipids and triglyceride, was reported as a second endogenous ligand for both cannabinoid receptors.¹⁰

In the past decades several *N*-acylethanolamines (NAEs) structurally related to AEA have been discovered (Figure 2B).^{11,12} These NAEs are involved in various physiological processes, such as anti-inflammation,¹³ neuroprotection,¹⁴ anorexic effects¹⁵ and anti-proliferative effects.¹⁶⁻¹⁹ Unlike AEA, these NAEs do not bind to cannabinoid receptors,²⁰ but exert their biological activities via binding to other receptors pathways.¹⁹

Palmitoylethanolamide (PEA) was discovered in 1957.²¹ Accumulation of PEA has been observed during inflammation.^{13,22} The nuclear receptor peroxisome proliferator-activated receptor-alpha (PPAR-alpha) has been identified as the main target through which PEA exerts its anti-inflammatory effect.²³ PEA agonizes PPAR-alpha and alters the expression of a number of target genes. It is this signaling process that is thought to be behind the observed neuroprotective

property of PEA.²⁴ Besides PPAR-alpha, PEA can also bind to cannabinoid-like G-coupled receptors GPR55 and GPR119.²²

Oleylethanolamide (OEA) is an endogenous agonist for PPAR-alpha and stimulates lipolysis.²⁵ OEA may also function as an endogenous ligand for GPR119.^{26, 27} OEA regulates feeding and body weight in mice^{14, 28} and pythons.²⁹ It was reported that OEA could promote longevity of the life span in *Caenorhabditis elegans* probably via binding to nuclear receptor NHR-80.³⁰

Stearoylethanolamide (SEA) is a saturated analogue of OEA. In LPS-induced pulmonary inflammation, SEA shows an anti-inflammatory effect, because it inhibited the translocation of NF- κ B, a critical transcription factor for the expression of many cytokines, into the nucleus of rat peritoneal macrophages.³¹ Zhukov and coworkers found that in an inflammatory rat model, the administration of SEA could accelerate the healing process of skin burn.³² In addition, SEA was shown to restore the morphine-induced alterations of brain phospholipid composition and the restoration of brain phospholipid composition was associated with a decline in morphine dependence.^{33, 34} Recently, it was shown that SEA protects the brain from inflammation and improves memory in mice.³⁵

Docosahexaenylethanolamide (DHEA) is a conjugate of docosahexaenoic acid and ethanolamine. Like other members of NAEs, DHEA also has anti-inflammatory properties.³⁶⁻³⁸ DHEA displayed anti-proliferative activity in LNCaP and PC3 prostate cancer cells¹⁶ and promoted neurite growth and synaptogenesis.³⁹

1.2 Biosynthetic pathways of NAEs

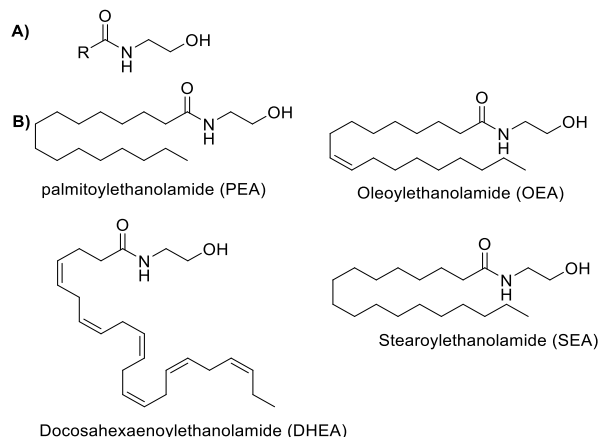


Figure 2. (A) General chemical structures of NAEs. R represents various acyl groups. (B) Chemical structures of PEA, OEA, DHEA and SEA.

NAEs are derived from phospholipids in a couple of chemical transformations as shown in figure 3.^{12, 20, 40, 41} First, *N*-acyltransferases (NAT) acylate the amine of phosphatidylethanolamine (PE) to produce *N*-acyl-phosphatidylethanolamine (NAPE). There are two classes of NATs: Ca^{2+} -dependent NAT (Ca-NAT) and Ca^{2+} -independent NATs (PLAAT1-5).⁴²

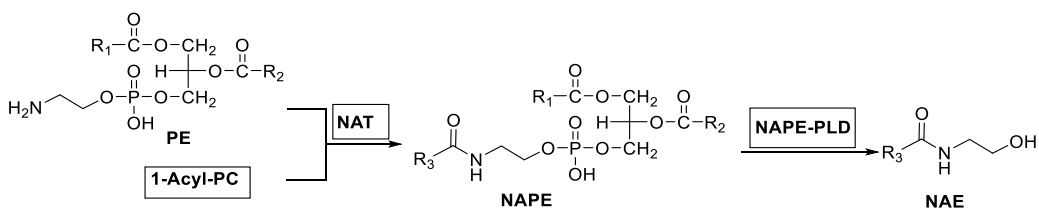


Figure 3. The NAPE-PLD-dependent pathway for the biosynthesis of NAEs.

The phosphodiester bond in NAPEs, generated by PLAATs or PLA2G4E, is subsequently hydrolyzed by a NAPE-selective phospholipase D (NAPE-PLD) yielding various NAEs.⁴³⁻⁴⁵ NAEs can also be generated from NAPE via NAPE-PLD-independent pathways, which were first proposed in 1984.⁴⁶ Studies on mice genetically lacking NAPE-PLD further confirmed the existence of other pathways.⁴⁷⁻⁴⁹ For example, NAPE can be deacylated by ABHD4 to yield glycerophospho-*N*-acyl-ethanolamine (GP-NAE), which is a substrate for GDE1 or GDE4 (Figure 4, route 1).⁵⁰⁻⁵² In a second pathway, cytosolic phospholipase A2 (cPLA₂) hydrolyzes NAPE to LysoNAPE, which is directly cleaved by GDE4 or GDE7 to produce NAEs.⁵³ In a third pathway, NAPE is hydrolyzed to phospho-NAE by phospholipase C (PLC) and NAEs are liberated via SHIP1 or PTPN22.^{42, 54, 55}

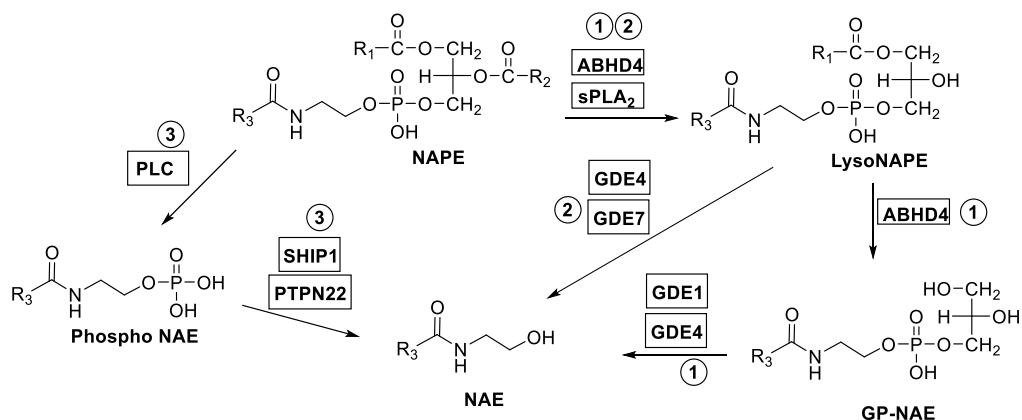


Figure 4. The NAPE-PLD-dependent pathways for the biosynthesis of NAEs.

Alternatively, NAEs can also be generated from another type of NAPE, the plasmalogen-NAPE (pNAPE) (Figure 5).^{42, 48} pNAPE serve as a substrate in both NAPE-PLD-dependent (Figure 5, route 1) and NAPE-PLD-independent pathways (Figure 5, route 2). The formation of lyso-pNAPE is catalyzed by ABHD4 or sPLA₂ and GDE1, 4, and 7 may hydrolyze Lyso-pNAPE yielding AEA.^{51, 56}

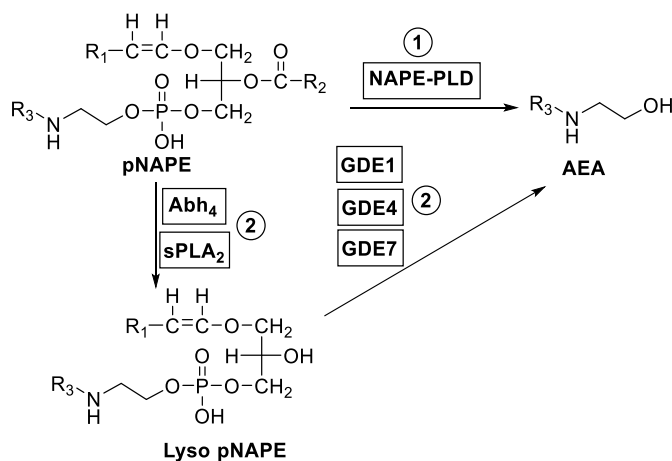


Figure 5. The biosynthetic pathway of NAEs from pNPPE.

The enzyme responsible for the Ca²⁺-dependent formation of NAEs remained elusive until Cravatt and colleagues showed that PLA2G4E (also known as cPLA₂ε) was able to transfer an acyl chain from the *sn*-1 position of phosphatidylcholine (PC) to the amine of phosphatidylethanolamine (PE), thereby producing NAEs.⁵⁷ PLA2G4E was previously discovered in a comprehensive homology search against murine genome and EST data bases and annotated as a phospholipase (PLA).⁵⁸ It belongs to the cytosolic phospholipase A2 group IV (PLA2G4) proteins, a subfamily from the PLA2 proteins, which catalyzes the hydrolysis of the

sn-2 acyl bond of phospholipids, thereby releasing fatty acids. This leads to a signaling cascade initiated by lipid second messengers, which regulates a wide variety of physiological responses and plays an important role in diseases, such as cancer.⁵⁹ There are six members in this protein family, namely PLA2G4A, PLA2G4B, PLA2G4C, PLA2G4D, PLA2G4E and PLA2G4F, which are structurally similar. They contain a N-terminal C2 domain and a C-terminal catalytic domain. The C2 domain has a binding site for intracellular Ca²⁺. Upon binding of calcium, the protein is transported from the cytosol to the Golgi membrane, which is needed for catalytic activity.⁶⁰ The catalytic pocket contains a Ser/Asp dyad, which is located in the α/β hydrolase domain.^{60, 61} In contrast to the other family members, PLA2G4E has a strong preference for catalyzing the *N*-acyltransferase reactions over phospholipid hydrolysis.⁵⁷

The human phospholipase A/acyl transferase (PLAAT1-5) family consists of five members (namely, PLA/AT 1-5).^{62, 63} They are the products of the *Hrasls* genes.⁶⁴ PLAATs possess Ca²⁺-independent phospholipase activity *in vitro* with both phosphatidylcholine (PC) and phosphatidylethanolamine (PE) acting as substrates. All members also exhibit O-acyl transferase activity with preference for the *sn*-1 position of lysophosphatidylcholine (lyso PC) as well as *N*-acyltransferase activity with the ability to produce *N*-acylphosphatidylethanolamines (NAPEs) through transfer of the acyl chain from the *sn*-1 position of glycerophospholipids to the amine function of PE.⁶³ All enzymes, except PLAAT3, show a preference for PLA1 activity over PLA2 activity.

PLAAT3 (also known as PLA2G16) is the most studied PLAAT protein. The protein is mostly expressed in white adipose tissue and to a lesser extent in brown adipose tissue.⁶⁵ The enzyme exhibits predominant PLA activity over O-acyltransferase or *N*-acyltransferase activities. It is in fact responsible for the majority of phospholipase activity in adipocytes.⁶³ The *in vivo* relevance of PLAAT3 has not been studied extensively, but a mouse model constitutively lacking the *Hrasls3* gene has been generated.⁶⁵ Ablation of PLAAT3 prevented obesity caused by high fat diet or leptin deficiency, thus establishing PLAAT3 as a potential target for the treatment of obesity. The PLAAT3 deficient mice exhibited a higher rate of lipolysis, due to decreased levels of prostaglandin E2 (PGE2) that were most likely caused by a decrease in arachidonic acid levels. Increased fatty acid oxidation in adipose tissue was also reported.

1.3 Activity-based protein profiling (ABPP)

Activity-based protein profiling is a powerful chemical biological technique that uses chemical probes which can covalently binds to catalytic amino acid of the target protein.⁶⁶ It allows efficient lead discovery studies by assessing inhibitor activity and selectivity in complex proteomes.⁶⁷ The activity-based probe (ABP) contains a warhead, a recognition part and a linker part, which is conjugated to a fluorophore or biotin reporter tag for fluorescent- or mass-spectrometry-based detection, respectively. The main advantage of ABPP is that the activity-based probe monitors the abundance of active proteins, thereby taking into account post-translational modifications and protein-protein-interactions. In comparative ABPP, the abundance and diversity of active enzymes in various biological samples are compared. In this setting, new enzyme activities can also be discovered or the presence of unexpected ones can be revealed. When a competitive ABPP is performed, the method can also be applied to screen the inhibitors for specific enzyme or to identify the bind targets of small-molecular inhibitor. In the field of serine hydrolases, various ABPs have been developed to decipher the physiological functions of these enzymes, discover new serine hydrolases or screen inhibitors.⁶⁸ MB064 is a β -lactone-based probe (structure shown in Figure 5), which has been developed and applied as a broad-spectrum serine hydrolase probe for the identification of highly potent and selective diacylglycerol lipase inhibitors.^{69, 70} In addition, MB064 was instrumental in the discovery of the off-target profile of the fatty acid amide hydrolase inhibitor BIA 10-2474 that caused the death of a volunteer in a clinical phase 1 study.⁷¹ The β -lactone warhead covalently reacts with the catalytic serine in many serine hydrolases, forming an acyl-enzyme intermediate. Interestingly, MB064 has also been reported to form thioester bonds with the catalytic cysteine of various enzymes.⁷² In this thesis, MB064 is also used to develop assays to screen and modify inhibitors for PLAATs and PLA2G4E.

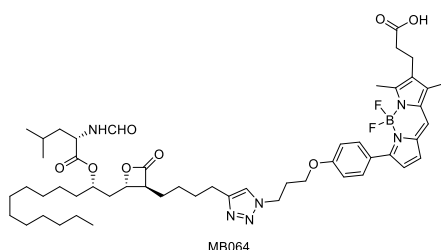


Figure 5. Chemical structure of probe MB064.

1.4 Aim and outline of this thesis

The aim of this thesis is to develop an activity-based protein profiling method to monitor the activity of PLAAT3 and the Ca²⁺-dependent N-acyltransferase that catalyzes the first step in NAE production and to identify inhibitors for these enzymes. In **Chapter 2**, the fluorescent activity-based probe MB064 is shown to label recombinant and endogenously expressed PLAAT3. Competitive activity-based protein profiling (ABPP) using MB064 enabled the discovery of α -ketoamides as the first PLAAT3 inhibitors. **Chapter 3** presents the systematic optimization of the initially discovered α -ketoamide hit. In the end, LEI110 is identified as the most potent and selective inhibitor that is available for PLAAT3. In **Chapter 4**, the biological activity of LEI110 is investigated. Gel-based ABPP and chemical proteomics showed that LEI110 is a selective pan-inhibitor of the PLAAT family of thiol hydrolases (i.e., PLAAT1, PLAAT2, PLAAT4 and PLAAT5). Molecular dynamic simulations of LEI110 in the reported crystal structure of PLAAT3 provided insight in the potential ligand–protein interactions to explain its binding mode. **Chapter 5** reports the development of an ABPP assay to study the Ca²⁺-dependent NAT, PLA2G4E, again using probe MB064. After optimizing the labeling conditions, a compound library is screened for PLA2G4E inhibitors. Several inhibitors for PLA2G4E were identified. **Chapter 6** provides a summary of the research described in this thesis and provides some future prospects.

1.5 References

1. Ligresti, A.; De Petrocellis, L.; Di Marzo, V., From Phytocannabinoids to Cannabinoid Receptors and Endocannabinoids: Pleiotropic Physiological and Pathological Roles Through Complex Pharmacology. *Physiol. Rev.* **2016**, *96* (4), 1593-659.
2. Rinder, I. D., The effects of marijuana: a social psychological interpretation. *Psychiatry* **1978**, *41* (2), 202-6.
3. Gaoni, Y.; Mechoulam, R., Isolation, structure, and partial synthesis of an active constituent of Hashish. *J. Am. Chem. Soc.* **1964**, *86* (8), 1646-1647.
4. Matsuda, L. A.; Lolait, S. J.; Brownstein, M. J.; Young, A. C.; Bonner, T. I., Structure of a cannabinoid receptor and functional expression of the cloned cDNA. *Nature* **1990**, *346* (6284), 561-4.
5. Van Waes, V.; Beverley, J. A.; Siman, H.; Tseng, K. Y.; Steiner, H., CB1 Cannabinoid receptor expression in the striatum: association with corticostriatal circuits and developmental regulation. *Front. Pharmacol.* **2012**, *3*, 21.
6. Munro, S.; Thomas, K. L.; Abu-Shaar, M., Molecular characterization of a peripheral receptor for cannabinoids. *Nature* **1993**, *365* (6441), 61-5.
7. Galiegue, S.; Mary, S.; Marchand, J.; Dussossoy, D.; Carriere, D.; Carayon, P.; Bouaboula, M.; Shire, D.; Le Fur, G.; Casellas, P., Expression of central and peripheral cannabinoid receptors in human immune tissues and leukocyte subpopulations. *Eur. J. Biochem.* **1995**, *232* (1), 54-61.
8. Ashton, J. C.; Friberg, D.; Darlington, C. L.; Smith, P. F., Expression of the cannabinoid CB2 receptor in the rat cerebellum: an immunohistochemical study. *Neurosci. Lett.* **2006**, *396* (2), 113-6.
9. Devane, W. A.; Hanus, L.; Breuer, A.; Pertwee, R. G.; Stevenson, L. A.; Griffin, G.; Gibson, D.; Mandelbaum, A.; Etinger, A.; Mechoulam, R., Isolation and structure of a brain constituent that binds to the cannabinoid receptor. *Science* **1992**, *258* (5090), 1946-9.
10. Mechoulam, R.; Ben-Shabat, S.; Hanus, L.; Ligumsky, M.; Kaminski, N. E.; Schatz, A. R.; Gopher, A.; Almog, S.; Martin, B. R.; Compton, D. R.; et al., Identification of an endogenous 2-monoglyceride, present in canine gut, that binds to cannabinoid receptors. *Biochem. Pharmacol.* **1995**, *50* (1), 83-90.
11. Schmid, H. H. O.; Schmid, P. C.; Natarajan, V., N-Acylated glycerophospholipids and their derivatives. *Prog. Lipid Res.* **1990**, *29* (1), 1-43.
12. Hansen, H. S.; Moesgaard, B.; Hansen, H. H.; Petersen, G., N-Acylethanolamines and precursor phospholipids — relation to cell injury. *Chem. Phys. Lipids* **2000**, *108* (1), 135-150.
13. Didier, M. L.; Severine, V.; Kent-Olov, J.; Christopher, J. F., The palmitoylethanolamide family: a new class of anti-inflammatory agents ? *Curr. Med. Chem.* **2002**, *9* (6), 663-674.

14. Lo Verme, J.; Gaetani, S.; Fu, J.; Oveisi, F.; Burton, K.; Piomelli, D., Regulation of food intake by oleoylethanolamide. *Cell. Mol. Life Sci.* **2005**, *62* (6), 708.
15. Rodríguez de Fonseca, F.; Navarro, M.; Gómez, R.; Escuredo, L.; Nava, F.; Fu, J.; Murillo-Rodríguez, E.; Giuffrida, A.; LoVerme, J.; Gaetani, S.; Kathuria, S.; Gall, C.; Piomelli, D., An anorexic lipid mediator regulated by feeding. *Nature* **2001**, *414* (6860), 209-212.
16. Brown, I.; Cascio, M. G.; Wahle, K. W. J.; Smoum, R.; Mechoulam, R.; Ross, R. A.; Pertwee, R. G.; Heys, S. D., Cannabinoid receptor-dependent and -independent anti-proliferative effects of omega-3 ethanolamides in androgen receptor-positive and -negative prostate cancer cell lines. *Carcinogenesis* **2010**, *31* (9), 1584-1591.
17. Berdyshev, E. V.; Schmid, P. C.; Krebsbach, R. J.; Kuwae, T.; Huang, C.; Ma, W. Y.; Dong, Z.; Schmid, H. H., Role of N-acylethanolamines in cell signaling. *World Rev. Nutr. Diet.* **2001**, *88*, 207-14.
18. Coulon, D.; Faure, L.; Salmon, M.; Wattedet, V.; Bessoule, J. J., N-Acylethanolamines and related compounds: aspects of metabolism and functions. *Plant Sci.* **2012**, *184*, 129-40.
19. Tsuboi, K.; Uyama, T.; Okamoto, Y.; Ueda, N., Endocannabinoids and related N-acylethanolamines: biological activities and metabolism. *Inflamm. Regen.* **2018**, *38*, 28.
20. Schmid, H. H. O.; Berdyshev, E. V., Cannabinoid receptor-inactive N-acylethanolamines and other fatty acid amides: metabolism and function. *Prostag. Leukotr. Ess.* **2002**, *66* (2), 363-376.
21. Petrosino, S.; Iuvone, T.; Di Marzo, V., N-palmitoyl-ethanolamine: biochemistry and new therapeutic opportunities. *Biochimie* **2010**, *92* (6), 724-727.
22. Godlewski, G.; Offertáler, L.; Wagner, J. A.; Kunos, G., Receptors for acylethanolamides—GPR55 and GPR119. *Prostag. Oth. Lipid M.* **2009**, *89* (3), 105-111.
23. Lo Verme, J.; Fu, J.; Astarita, G.; La Rana, G.; Russo, R.; Calignano, A.; Piomelli, D., The nuclear receptor peroxisome proliferator-activated receptor- α mediates the anti-inflammatory actions of palmitoylethanolamide. *Mol. Pharmacol.* **2005**, *67* (1), 15-9.
24. Fidaleo, M.; Fanelli, F.; Ceru, M. P.; Moreno, S., Neuroprotective properties of peroxisome proliferator-activated receptor α (PPAR α) and its lipid ligands. *Curr Med Chem* **2014**, *21* (24), 2803-21.
25. Gaetani, S.; Kaye, W. H.; Cuomo, V.; Piomelli, D., Role of endocannabinoids and their analogues in obesity and eating disorders. *Eat. Weight Disord.* **2008**, *13* (3), e42-8.
26. Overton, H. A.; Babbs, A. J.; Doel, S. M.; Fyfe, M. C. T.; Gardner, L. S.; Griffin, G.; Jackson, H. C.; Procter, M. J.; Rasamison, C. M.; Tang-Christensen, M.; Widdowson, P. S.; Williams, G. M.; Reynet, C., Deorphanization of a G protein-coupled receptor for oleoylethanolamide and its use in the discovery of small-molecule hypophagic agents. *Cell Metab.* **2006**, *3* (3), 167-175.
27. Brown, A. J., Novel cannabinoid receptors. *Br. J. Pharmacol.* **2007**, *152* (5), 567-75.

28. Gaetani, S.; Oveisi, F.; Piomelli, D., Modulation of meal pattern in the rat by the anorexic lipid mediator oleoylethanolamide. *Neuropsychopharmacology* **2003**, *28* (7), 1311-1316.
29. Astarita, G.; Rourke, B. C.; Andersen, J. B.; Fu, J.; Kim, J. H.; Bennett, A. F.; Hicks, J. W.; Piomelli, D., Postprandial increase of oleoylethanolamide mobilization in small intestine of the Burmese python (*Python molurus*). *Am. J. Physiol.-Reg. I.* **2006**, *290* (5), R1407-R1412.
30. Folick, A.; Oakley, H. D.; Yu, Y.; Armstrong, E. H.; Kumari, M.; Sanor, L.; Moore, D. D.; Ortlund, E. A.; Zechner, R.; Wang, M. C., Lysosomal signaling molecules regulate longevity in *Caenorhabditis elegans*. *Science* **2015**, *347* (6217), 83-86.
31. Berdyshev, A. G.; Kosiakova, H. V.; Onopchenko, O. V.; Panchuk, R. R.; Stoika, R. S.; Hula, N. M., N-Stearoylethanolamine suppresses the pro-inflammatory cytokines production by inhibition of NF- κ B translocation. *Prostag. Oth. Lipid M.* **2015**, *121*, 91-96.
32. A. D. Zhukov, A. G. B., G. V. Kosiakova, V. M. Klimashevskiy, T. M. Gorid'ko, O. F. Meged, N. M. Hula, N-stearoylethanolamine effect on the level of 11-hydroxycorticosteroids, cytokines IL-1 β , IL-6 and TNF α in rats with nonspecific inflammation caused by thermal burn of skin. *Ukr. Biochem. J.* **2014**, *86* (3), 88-97.
33. Hula, N. M.; Hulii, M. F.; Kharchenko, N. K.; Horid'ko, T. M.; Marhitych, V. M., Neuroprotective effect of N-acylethanolamines in chronic morphine dependence. III. Influence on the content of neurotransmitters in the rat brain. *Ukr. Biokhim. Zh.* **2005**, *77* (1), 47-51.
34. Hula, N. M.; Marhitych, V. M.; Artamonov, M. V.; Zhukov, O. D.; Horid'ko, T. M.; Klimashevs'kyi, V. M., Neuroprotective effect of N-acylethanolamines in chronic morphine dependence. I. Rat brain phospholipids as a target of their action. *Ukr. Biokhim. Zh.* **2004**, *76* (5), 123-31.
35. Lykhmus, O.; Uspenska, K.; Koval, L.; Lytovchenko, D.; Voytenko, L.; Horid'ko, T.; Kosiakova, H.; Gula, N.; Komisarenko, S.; Skok, M., N-Stearoylethanolamine protects the brain and improves memory of mice treated with lipopolysaccharide or immunized with the extracellular domain of α 7 nicotinic acetylcholine receptor. *Int. Immunopharmacol.* **2017**, *52*, 290-296.
36. Balvers, M. G.; Verhoeckx, K. C.; Meijerink, J.; Bijlsma, S.; Rubingh, C. M.; Wortelboer, H. M.; Witkamp, R. F., Time-dependent effect of in vivo inflammation on eicosanoid and endocannabinoid levels in plasma, liver, ileum and adipose tissue in C57BL/6 mice fed a fish-oil diet. *Int Immunopharmacol* **2012**, *13* (2), 204-14.
37. Balvers, M. G.; Verhoeckx, K. C.; Plastina, P.; Wortelboer, H. M.; Meijerink, J.; Witkamp, R. F., Docosahexaenoic acid and eicosapentaenoic acid are converted by 3T3-L1 adipocytes to N-acyl ethanolamines with anti-inflammatory properties. *Biochim. Biophys. Acta* **2010**, *1801* (10), 1107-14.

38. Meijerink, J.; Plastina, P.; Vincken, J. P.; Poland, M.; Attya, M.; Balvers, M.; Gruppen, H.; Gabriele, B.; Witkamp, R. F., The ethanolamide metabolite of DHA, docosahexaenylethanolamine, shows immunomodulating effects in mouse peritoneal and RAW264.7 macrophages: evidence for a new link between fish oil and inflammation. *Br. J. Nutr.* **2011**, *105* (12), 1798-807.
39. Kim, H.-Y.; Spector, A. A.; Xiong, Z.-M., A synaptogenic amide N-docosahexaenylethanolamide promotes hippocampal development. *Prostag. Oth. Lipid M.* **2011**, *96* (1), 114-120.
40. Sugiura, T.; Kobayashi, Y.; Oka, S.; Waku, K., Biosynthesis and degradation of anandamide and 2-arachidonoylglycerol and their possible physiological significance. *Prostagl. Leukotr. Ess.* **2002**, *66* (2), 173-192.
41. Schmid, H. H. O., Pathways and mechanisms of N-acylethanolamine biosynthesis: can anandamide be generated selectively? *Chem. Phys. Lipids* **2000**, *108* (1), 71-87.
42. Hussain, Z.; Uyama, T.; Tsuboi, K.; Ueda, N., Mammalian enzymes responsible for the biosynthesis of N-acylethanolamines. *BBA-Mol. Cell Biol. L.* **2017**, *1862* (12), 1546-1561.
43. Magotti, P.; Bauer, I.; Igarashi, M.; Babagoli, M.; Marotta, R.; Piomelli, D.; Garau, G., Structure of human N-acylphosphatidylethanolamine-hydrolyzing phospholipase D: regulation of fatty acid ethanolamide biosynthesis by bile acids. *Structure* **2015**, *23* (3), 598-604.
44. Okamoto, Y.; Morishita, J.; Tsuboi, K.; Tonai, T.; Ueda, N., Molecular characterization of a phospholipase D generating anandamide and its congeners. *J. Biol. Chem.* **2004**, *279* (7), 5298-305.
45. Wang, J.; Ueda, N., Biology of endocannabinoid synthesis system. *Prostag. Oth. Lipid M.* **2009**, *89* (3), 112-119.
46. Natarajan, V.; Schmid, P. C.; Reddy, P. V.; Schmid, H. H. O., Catabolism of N-acylethanolamine phospholipids by dog brain preparations. *J. Neurochem.* **1984**, *42* (6), 1613-1619.
47. Leung, D.; Saghatelian, A.; Simon, G. M.; Cravatt, B. F., Inactivation of N-acyl phosphatidylethanolamine phospholipase D reveals multiple mechanisms for the biosynthesis of endocannabinoids. *Biochemistry* **2006**, *45* (15), 4720-4726.
48. Tsuboi, K.; Okamoto, Y.; Ikematsu, N.; Inoue, M.; Shimizu, Y.; Uyama, T.; Wang, J.; Deutsch, D. G.; Burns, M. P.; Ulloa, N. M.; Tokumura, A.; Ueda, N., Enzymatic formation of N-acylethanolamines from N-acylethanolamine plasmalogen through N-acylphosphatidylethanolamine-hydrolyzing phospholipase D-dependent and -independent pathways. *BBA-Mol. Cell Biol. L.* **2011**, *1811* (10), 565-577.

49. Leishman, E.; Mackie, K.; Luquet, S.; Bradshaw, H. B., Lipidomics profile of a NAPE-PLD KO mouse provides evidence of a broader role of this enzyme in lipid metabolism in the brain. *BBA-Mol. Cell Biol. L.* **2016**, *1861* (6), 491-500.
50. Simon, G. M.; Cravatt, B. F., Endocannabinoid biosynthesis proceeding through glycerophospho-N-acyl ethanolamine and a role for alpha/beta-hydrolase 4 in this pathway. *J. Biol. Chem.* **2006**, *281* (36), 26465-72.
51. Rahman, I. A. S.; Tsuboi, K.; Hussain, Z.; Yamashita, R.; Okamoto, Y.; Uyama, T.; Yamazaki, N.; Tanaka, T.; Tokumura, A.; Ueda, N., Calcium-dependent generation of N-acylethanolamines and lysophosphatidic acids by glycerophosphodiesterase GDE7. *BBA-Mol. Cell Biol. L.* **2016**, *1861* (12, Part A), 1881-1892.
52. Simon, G. M.; Cravatt, B. F., Anandamide biosynthesis catalyzed by the phosphodiesterase GDE1 and detection of glycerophospho-N-acyl ethanolamine precursors in mouse brain. *J. Biol. Chem.* **2008**, *283* (14), 9341-9.
53. Sun, Y. X.; Tsuboi, K.; Okamoto, Y.; Tonai, T.; Murakami, M.; Kudo, I.; Ueda, N., Biosynthesis of anandamide and N-palmitoylethanolamine by sequential actions of phospholipase A2 and lysophospholipase D. *Biochem. J.* **2004**, *380* (Pt 3), 749-56.
54. Liu, J.; Wang, L.; Harvey-White, J.; Osei-Hyiaman, D.; Razdan, R.; Gong, Q.; Chan, A. C.; Zhou, Z.; Huang, B. X.; Kim, H.-Y.; Kunos, G., A biosynthetic pathway for anandamide. *Proc. Natl. Acad. Sci. U. S. A.* **2006**, *103* (36), 13345-13350.
55. Liu, J.; Wang, L.; Harvey-White, J.; Huang, B. X.; Kim, H. Y.; Luquet, S.; Palmiter, R. D.; Krystal, G.; Rai, R.; Mahadevan, A.; Razdan, R. K.; Kunos, G., Multiple pathways involved in the biosynthesis of anandamide. *Neuropharmacology* **2008**, *54* (1), 1-7.
56. Tsuboi, K.; Okamoto, Y.; Rahman, I. A. S.; Uyama, T.; Inoue, T.; Tokumura, A.; Ueda, N., Glycerophosphodiesterase GDE4 as a novel lysophospholipase D: a possible involvement in bioactive N-acylethanolamine biosynthesis. *BBA-Mol. Cell Biol. L.* **2015**, *1851* (5), 537-548.
57. Ogura, Y.; Parsons, W. H.; Kamat, S. S.; Cravatt, B. F., A calcium-dependent acyltransferase that produces N-acyl phosphatidylethanolamines. *Nat. Chem. Biol.* **2016**, *12* (9), 669-71.
58. Ohto, T.; Uozumi, N.; Hirabayashi, T.; Shimizu, T., Identification of novel cytosolic phospholipase A2s, murine cPLA2 δ , ϵ , and ζ , Which form a gene cluster with cPLA2 β . *J. Biol.* **2005**, *280* (26), 24576-24583.
59. Lucas, K. K.; Dennis, E. A., Distinguishing phospholipase A2 types in biological samples by employing group-specific assays in the presence of inhibitors. *Prostag. Oth. Lipid M.* **2005**, *77* (1-4), 235-48.
60. Dennis, E. A.; Cao, J.; Hsu, Y. H.; Magrioti, V.; Kokotos, G., Phospholipase A2 enzymes: physical structure, biological function, disease implication, chemical inhibition, and therapeutic intervention. *Chem. Rev.* **2011**, *111* (10), 6130-85.

61. Ghosh, M.; Tucker, D. E.; Burchett, S. A.; Leslie, C. C., Properties of the Group IV phospholipase A2 family. *Prog. Lipid Res.* **2006**, *45* (6), 487-510.
62. Jin, X.-H.; Uyama, T.; Wang, J.; Okamoto, Y.; Tonai, T.; Ueda, N., cDNA cloning and characterization of human and mouse Ca²⁺-independent phosphatidylethanolamine N-acyltransferases. *Biochimica et BBA-Mol. Cell Biol. L.* **2009**, *1791* (1), 32-38.
63. Uyama, T.; Ikematsu, N.; Inoue, M.; Shinohara, N.; Jin, X. H.; Tsuboi, K.; Tonai, T.; Tokumura, A.; Ueda, N., Generation of N-acylphosphatidylethanolamine by members of the phospholipase A/acyltransferase (PLA/AT) family. *J. Biol. Chem.* **2012**, *287* (38), 31905-19.
64. Mardian, E. B.; Bradley, R. M.; Duncan, R. E., The HRASLS (PLA/AT) subfamily of enzymes. *J. Biomed. Sci.* **2015**, *22* (1), 99.
65. Jaworski, K.; Ahmadian, M.; Duncan, R. E.; Sarkadi-Nagy, E.; Varady, K. A.; Hellerstein, M. K.; Lee, H.-Y.; Samuel, V. T.; Shulman, G. I.; Kim, K.-H.; de Val, S.; Kang, C.; Sul, H. S., AdPLA ablation increases lipolysis and prevents obesity induced by high-fat feeding or leptin deficiency. *Nat. Med.* **2009**, *15*, 159.
66. Liu, Y. S.; Patricelli, M. P.; Cravatt, B. F., Activity-based protein profiling: the serine hydrolases. *Proc. Natl. Acad. Sci. U. S. A.* **1999**, *96* (26), 14694-14699.
67. Niphakis, M. J.; Cravatt, B. F., Enzyme inhibitor discovery by activity-based protein profiling. *Annu. Rev. Biochem.* **2014**, *83*, 341-377.
68. Simon, G. M.; Cravatt, B. F., Activity-based proteomics of enzyme superfamilies: serine hydrolases as a case study. *J. Biol. Chem.* **2010**, *285* (15), 11051-5.
69. Baggelaar, M. P.; Janssen, F. J.; van Esbroeck, A. C. M.; den Dulk, H.; Allara, M.; Hoogendoorn, S.; McGuire, R.; Florea, B. I.; Meeuwenoord, N.; van den Elst, H.; van der Marel, G. A.; Brouwer, J.; Di Marzo, V.; Overkleeft, H. S.; van der Stelt, M., Development of an activity-based probe and in silico design reveal highly selective inhibitors for diacylglycerol lipase- α in brain. *Angew. Chem.-Int. Edit.* **2013**, *52* (46), 12081-12085.
70. Baggelaar, M. P.; Chameau, P. J. P.; Kantae, V.; Hummel, J.; Hsu, K. L.; Janssen, F.; van der Wel, T.; Soethoudt, M.; Deng, H.; den Dulk, H.; Allara, M.; Florea, B. I.; Di Marzo, V.; Wadman, W. J.; Kruse, C. G.; Overkleeft, H. S.; Hankemeier, T.; Werkman, T. R.; Cravatt, B. F.; van der Stelt, M., Highly selective, reversible inhibitor identified by comparative chemoproteomics modulates diacylglycerol lipase activity in neurons. *J. Am. Chem. Soc.* **2015**, *137* (27), 8851-8857.
71. van Esbroeck, A. C. M.; Janssen, A. P. A.; Cognetta, A. B.; Ogasawara, D.; Shpak, G.; van der Kroeg, M.; Kantae, V.; Baggelaar, M. P.; de Vrij, F. M. S.; Deng, H.; Allara, M.; Fezza, F.; Lin, Z.; van der Wel, T.; Soethoudt, M.; Mock, E. D.; den Dulk, H.; Baak, I. L.; Florea, B. I.; Hendriks, G.; de Petrocellis, L.; Overkleeft, H. S.; Hankemeier, T.; De Zeeuw, C. I.; Di Marzo, V.; Maccarrone, M.; Cravatt, B. F.; Kushner, S. A.; van der Stelt, M., Activity-based protein profiling reveals off-target proteins of the FAAH inhibitor BIA 10-2474. *Science* **2017**, *356* (6342), 1084-1087.

72. Yang, P. Y.; Liu, K.; Ngai, M. H.; Lear, M. J.; Wenk, M. R.; Yao, S. Q., Activity-based proteome profiling of potential cellular targets of Orlistat - an FDA-approved drug with anti-tumor activities. *J. Am. Chem. Soc.* **2010**, *132* (2), 656-666.

2

**Development and application of an ABPP assay to identify
PLAAT3 inhibitors**

2.1 Introduction

Phospholipase A acyltransferase 3 (PLAAT3, or PLA2G16), was first isolated from murine fibroblasts as a product of the HRASLS-gene (H-RAS-like suppressor) family, which also includes the phospholipase/acyltransferases, namely phospholipid-metabolizing enzyme A-C1 (A-C1, or PLAAT1), HRAS-like suppressor 2 (HRASLS2, or PLAAT2), retinoid acid receptor responder protein 3 (RARRES3, or PLAAT4) and Ca²⁺-independent *N*-acyltransferase (iNAT, or PLAAT5).¹⁻³ PLAAT3 is an intercellular, single-pass transmembrane cysteine hydrolase with a molecular weight of 18 kDa with as major activity the hydrolysis of the sn-2 fatty acyl chain of phosphatidylcholine.^{4, 5} PLAAT3 has a papain-fold motive consisting of three α -helices and five antiparallel β -sheets organized in a circular permutation and a conserved catalytic triad consisting of Cys113, His23 and His35 as determined by X-ray crystallography (PDB code: 4DOT) and site-directed mutagenesis studies.⁶⁻⁹

PLAAT3 is found in various cell lines (e.g. HepG2)^{10, 11} and adipose tissue.^{12, 13} Its expression is induced during adipocyte differentiation.^{14, 15} In mouse models, PLAAT3 has been shown to play an important role in the development of obesity.¹⁶ The nuclear receptor PPAR γ (peroxisome proliferator-activated receptor) regulates the function and formation of adipose tissue and PLAAT3 was identified as the downstream target of PPAR γ with a role in adipogenesis.¹² PLAAT3 (also known as HRSL3 or H-REV107-1) is also a member of a class II tumor suppressor gene family and it functions as tumor suppressor by regulating the activity of proto-oncogenes.^{1, 17, 18} In tumor cell lines and experimental tumors, the growth-inhibitory activity of tumor and downregulation of PLAAT3 were observed¹⁹ and PLAAT3 was shown to be involved in the oncogenic network which mediate the growth and survival of ovarian cancer cells.¹⁷ PLAAT3 is also involved in clearance of the virus in host cells.^{18, 20} The authors first created a Haplobank from haploid mouse embryonic stem cells lines and the subsequent reverse genetic screening led to the identification of PLAAT3 as a host factor which is required for cytotoxicity by rhinoviruses.¹⁸ In another genome-wide screening, PLAAT3 was identified as picornavirus host factor because it can facilitate the viral genome translocation and prevent clearance.²¹ Taken together, these studies highlight the therapeutic potential of PLAAT3. However, to date, there are no PLAAT3 inhibitors reported that can be used as pharmacological tools to validate PLAAT3 as a therapeutic target.

Currently, no ABPs have been reported for PLAAT3 that could enable inhibitor discovery. In this chapter, it is shown that MB064 (Figure 1A) labels PLAAT3 in an activity-dependent manner and is able to visualize endogenous PLAAT3 in adipose tissue. Screening of a focused lipase inhibitor library using ABPP resulted in the identification of an α -ketoamide (compound **1**, Figure 1B) as a selective PLAAT3 inhibitor.

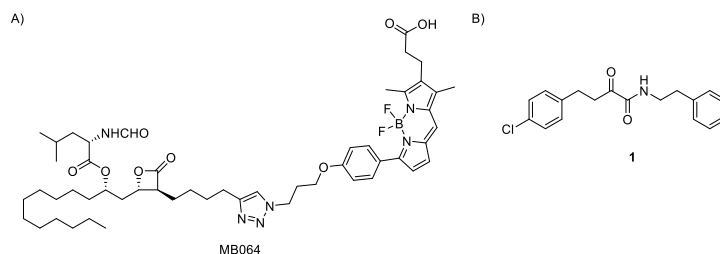


Figure 1. Chemical structures of probe MB064 and compound 1.

2.2 Results and discussion

To test whether MB064 could also label PLAAT3, proteomes of transiently overexpressed human PLAAT3-FLAG in human embryonic kidney 293 T (HEK293T) cells was incubated with MB064, followed by sodium dodecyl sulfate polyacrylamide gel electrophoresis (SDS-PAGE) and fluorescence scanning. A fluorescent band was observed at the expected MW of 18 kDa, which overlapped with a band visualized by the FLAG-tag antibody and was absent in mock-transfected cells (Figure 2A). The labeling was probe- and protein-concentration-dependent (Figure 2B) and was optimal at pH 8, which is consistent with previously reported pH optimum of PLAAT3 activity.^{14,22} Site-directed mutagenesis of the catalytic Cys113 into alanine or serine abolished or significantly reduced labeling, respectively, whereas its expression was not substantially altered as witnessed by FLAG-tag antibodies (Figure 2C). Of note, MB064 was also able to cross-react with PLAAT2, PLAAT3 and PLAAT5 (Figure 2D). Finally, it was tested whether MB064 could also label endogenously expressed PLAAT3. To this end, MB064 was incubated with freshly isolated mouse white adipose tissue (WAT) and brown adipose tissue (BAT) extracts. A fluorescent band was observed at the expected MW, which also overlapped with a band visualized by PLAAT3 antibodies (Figure 2E). Taken together, these results demonstrate that MB064 reacts with active human PLAAT3 to form a covalent bond with Cys113 and visualizes native mouse PLAAT3 in brown and white adipose tissue.

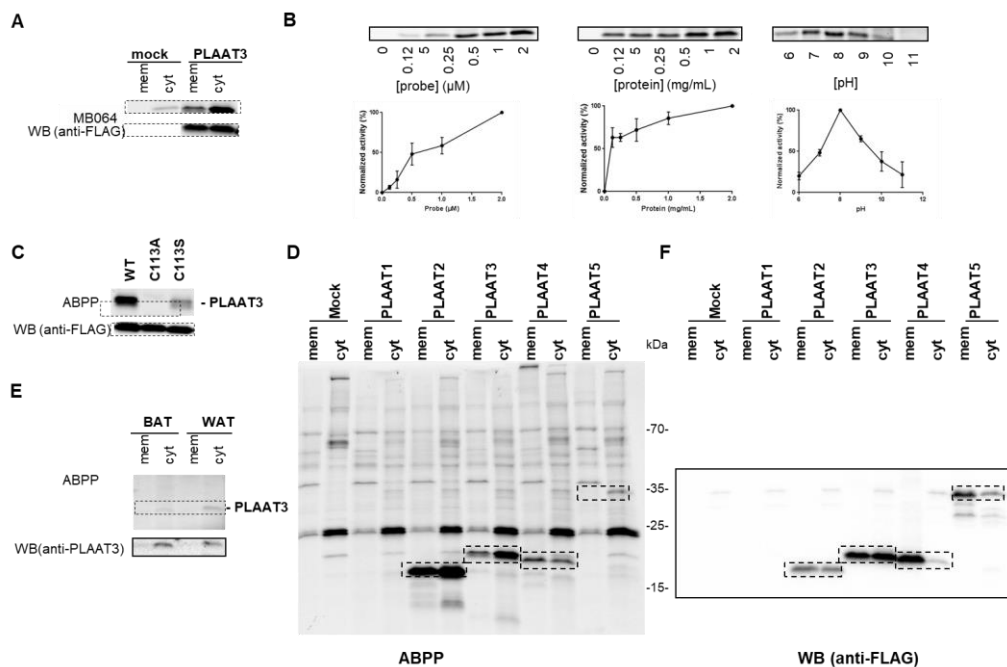


Figure 2. Characterization of MB064 as an ABP for PLAAT3. (A) ABPP using MB064 with PLAAT3 membrane (mem) or cytosol (cyt) proteome (1 mg/mL) transiently overexpressed in HEK293T cells and Western blot of the ABPP gel using an anti-FLAG antibody. (B) ABPP condition optimization for human PLAAT3 cytosol proteome using MB064. For the probe concentration test, 0.5 mg/mL protein lysate was used. For the protein concentration test, probe of 500 nM was used. (C) ABPP using MB064 with different human PLAAT3 constructs, and Western blot of the ABPP gel using an anti-FLAG antibody. (D) ABPP using probe MB064 on HRASLS protein family members (transiently overexpressed in HEK293T cells). (E) Labelling of endogenous PLAAT3 in WAT and BAT cytosol proteome by MB064, and Western blot of the ABPP gel using an anti-PLAAT3 antibody. (F) Western blot of the ABPP gel using an anti-FLAG antibody. All HRASLS family members except PLAAT1 were successfully overexpressed in HEK293T cells and the overexpressed proteins could be labelled by probe MB064.

Having identified MB064 as a suitable chemical probe targeting PLAAT3, it was decided to screen a small focused library of 50 lipase inhibitors representatively selected from a compound library as in our previous study²³ at 10 μ M in a competitive ABPP format. This led to discovery of 4-(4-chlorophenyl)-2-oxo-N-phenethylbutanamide, an α -ketoamide (compound **1**) as a hit that almost completely abolished PLAAT3 labeling at 10 μ M (Figure 3A).

Compound **1** was resynthesized using previously reported procedures and tested in a concentration-response ABPP assay. Compound **1** displayed a half-maximum inhibitory concentration ($\text{pIC}_{50} \pm \text{SEM}$) of 6.0 ± 0.1 ($n=3$). Furthermore, it demonstrated similar activity on the other proteins of the *HRASLS*-gene family (PLAAT2, PLAAT3 and PLAAT5) with a pIC_{50} in the range of 6.0-6.2 (Figure 3A and Table 1). Next, the inhibitory activity

of compound **1** was confirmed in a previously reported orthogonal biochemical fluorescence assay that uses the Green/Red Bodipy PC-A2 as a surrogate substrate (with a K_M of $7.8 \pm 2.2 \mu\text{M}$) and cytosol PLAAT3 fraction of HEK293T cells overexpressing human PLAAT3.⁸ Compound **1** displayed a K_i of 80 nM (95% confidence interval CI: 72-96 nM) (Figure 3B). α -Ketoamides have previously been reported to inhibit serine hydrolases expressed in the brain.²⁴⁻²⁷ To determine the selectivity of compound **1** on endogenously expressed serine hydrolases, a competitive ABPP experiment was performed in mouse brain proteomes using the broad-spectrum serine hydrolase ABPs, fluorophosphonate (FP)-TAMRA, and MB064. Compound **1** (10 μM) did not reduce the labeling of any proteins in mouse brain targeted by FP-TAMRA or MB064 (Figure 3C). Taken together, these results indicate that α -ketoamide **1** is a selective inhibitor of PLAAT3 and its family members.

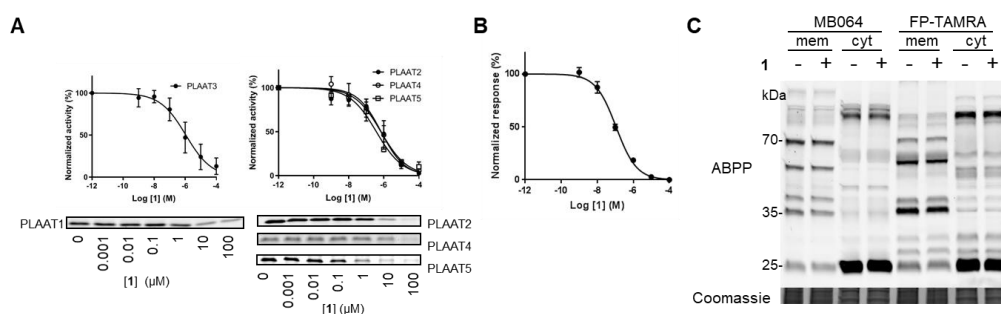


Figure 3. Discovery and biochemical characterization of compound **1**. (A) Dose-response curves for **1** on PLAAT3 (left) and other HRASLS family members, PLAAT2, PLAAT4 and PLAAT5 (right) measured by competitive ABPP using cytosol proteome prepared from transfected HEK293T cells with probe MB064. Under the curves are the corresponding ABPP gels: concentration-dependent inhibition of **1** against different proteins ($n=3$). (B) Dose-response curve of **1** for PLAAT3 (cytosol proteome prepared from PLAAT3 overexpressing HEK293T cells) with the PC-A2 fluorescent substrate assay ($n = 3$). (C) Selectivity of **1** against MB064 and FP-TAMRA in mouse brain membrane (mem) and cytosol (cyt) proteome. Coomassie was used as a protein loading control. Minus sign (-) indicates control (with DMSO), plus sign (+) indicates with compound **1** at 10 μM .

Table 1. $pIC_{50} \pm \text{SEM}$ ($n = 3$) of compound **1** against HRASLS protein family members from the ABPP assay.

Compound	PLAAT3	PLAAT2	PLAAT4	PLAAT5
1	6.0 ± 0.1	6.2 ± 0.1	6.2 ± 0.1	6.4 ± 0.1

2.3 Conclusions

In conclusion, in this chapter, an activity-based protein profiling assay has been developed to label PLAAT3 *in vitro*, using MB064. Thereafter, this method was applied to screen inhibitors for PLAAT3. α -Ketoamides were discovered as the first selective PLAAT3 inhibitors.

2.4 Experimental procedures

Plasmids. Full-length human cDNA of PLAAT3, PLAAT1, PLAAT2, PLAAT4 and PLAAT5 (from Prof. N. Ueda's lab) were cloned into mammalian expression vector pcDNA3.1, containing genes for ampicillin and neomycin resistance. The inserts were cloned in frame with a C-terminal FLAG-tag and site-directed mutagenesis was used to remove restriction by silent point mutations. Two step PCR mutagenesis was performed to substitute the active site cysteine for an alanine (A) or serine (S) in the hPLAAT3-FLAG, hPLAAT2, PLAAT4 and PLAAT5, respectively to obtain the corresponding mutants. Plasmids were isolated from transformed XL-10 Z-competent cells (Maxi Prep kit: Qiagen) and sequenced at the Leiden Genome Technology Center. Sequences were analyzed and verified (CLC Main Workbench).

Cell culture

General. HEK293T cells were kept in culture at 37 °C under 7% CO₂ in DMEM containing phenol red, stable glutamine, 10% (v/v) New Born Calf Serum (Thermo Fisher), and penicillin and streptomycin (200 μ g/mL each; Duchefa). Medium was refreshed every 2-3 days and cells were passaged twice a week at 80-90% confluence. Cells lines were purchased from ATCC and were regularly tested for mycoplasma contamination.

Transient transfection. Transient transfection was performed as previously described.²⁸ In brief, HEK293T cells were seeded in 15cm petri dishes one day prior to transfection. Prior to transfection, culture medium was aspirated and a minimal amount of medium was added. A 3:1 (m/m) mixture of polyethyleneimine (PEI, 1 mg/mL) (60 μ g/15-cm dish) and plasmid DNA (20 μ g/dish) was prepared in serum free culture medium and incubated for 15 min at RT. Transfection was performed by dropwise addition of the PEI/DNA mixture to the cells. Transfection with the empty pcDNA3.1 vector was used to generate control samples (mock groups). After 24 h, medium was refreshed. Medium was aspirated 72 h post-transfection and cells were harvested by resuspension in PBS. Cells were pelleted by centrifugation (5 min, 1,000 g) and the pellet was washed with PBS. Supernatant was discarded and cell pellets were snap-frozen in liquid nitrogen and stored at -80 °C until sample preparation.

Sample preparation

Cell membrane and cytosol proteome preparation. Cell pellets were thawed on ice, resuspended in cold lysis buffer (50 mM Tris HCl, pH 8, 2 mM DTT, 1 mM MgCl₂, 2.5 U/mL benzonase) and incubated on ice (30 min). The membrane and cytosolic fractions of the cell lysate were separated by ultracentrifugation (100.000 g, 45 min, 4 °C, Beckman Coulter, Ti 70.1 rotor). The supernatant was collected (cytosolic fraction) and the membrane pellet was resuspended in cold storage buffer (50 mM Tris HCl, pH 8, 2 mM DTT) by thorough pipetting and passage through an insulin needle (29G). Protein concentrations were determined by a Quick Start™ Bradford Protein Assay or Qubit™ protein assay (Invitrogen). Samples were flash frozen in liquid nitrogen and stored at -80 °C until further use.

Mouse tissue proteome preparation. Mouse brains (C57Bl6) were isolated according to guidelines approved by the ethical committee of Leiden University (DEC#13191), frozen in liquid nitrogen, and stored at -80 °C until further use. Tissues were thawed on ice, dounce homogenized in cold lysis buffer (50 mM Tris HCl, pH 8, 2 mM DTT, 1 mM MgCl₂, 2.5 U/mL benzonase) and incubated on ice (15 min), followed by low-speed centrifugation (2500 g, 3 min, 4°C) to remove debris. After high-speed centrifugation (100.000 x g, 45 min, 4°C) the supernatant was collected as the cytosol proteome, flash frozen in liquid nitrogen and stored at -80 °C until further use.

Mouse white or brown adipose tissue (C57Bl6) were isolated according to guidelines approved by the ethical committee of Leiden University (DEC#13191) and were immediately dounce homogenized in cold lysis buffer, followed by low-speed spin (2500 g, 3 min, 4°C) to remove the debris. The membrane and cytosol proteome were prepared followed by the same procedure as for the mouse brains described above.

Activity based protein profiling on transiently transfected HEK293T cell lysate. Gel-based activity based protein profiling (ABPP) was performed with minor alterations of the previously reported protocol.²⁸ For ABPP assays on HEK293T cells overexpressing PLAAT3, the cytosol proteome (0.5 mg/mL, 20 µL) was pre-incubated with vehicle (DMSO) or inhibitor (0.5 µL in DMSO, 30 min, RT) followed by an incubation with the activity based probe MB064 (final concentration: 250 nM, 20 min, RT). The incubation protocols for PLAAT2, PLAAT3 and PLAAT5 were similar except for the protein concentration (0.25 mg/mL, 1 mg/mL, 1 mg/mL, respectively) and probe concentration (250 nM, 500 nM, 500 nM). Final concentrations for the inhibitors were indicated in the main text and figure legends. Only cytosol proteome was used for the dose-response test in ABPP or substrate assay. Reactions were quenched with 7 µL of 4x Laemmli buffer (5 µL, 240 mM Tris (pH 6.8), 8% (w/v) SDS, 40% (v/v) glycerol, 5% (v/v) β-mercaptoethanol, 0.04% (v/v) bromophenol blue). 10 µL sample per reaction was resolved on a 10 % or 15% acrylamide SDS-PAGE gel (180 V, 70 min). Gels were scanned using a ChemiDoc MP

system with Cy3 and Cy5 multichannel settings (605/50 and 695/55, filters respectively) and stained with Coomassie after scanning. Experiments were done 3 times individually. Fluorescence was normalized to Coomassie staining and quantified with Image Lab (Bio-Rad). IC₅₀ curves were fitted with Graphpad Prism® 7 (Graphpad Software Inc.).

Activity based protein profiling on mouse brain proteome. Mouse brain membrane or cytosol proteome (2 mg/mL, 20 µL) was incubated with vehicle (DMSO) or inhibitor (0.5 µL in DMSO, 30 min, RT) followed by an incubation with the activity based probe MB064 (final concentration: 500 nM, 20 min, RT) or FP-TAMRA (Thermo Fisher, 88318, final concentration: 500 nM, 20min, RT). The reaction was quenched with 7 µL of 4x Laemmli buffer and the proteins were resolved and visualized using the same procedures as for the transfected HEK293T cells.

Activity based protein profiling on mouse adipose tissue. Brown or white adipose tissue cytosol proteome (1 mg/mL, 20 µL) was incubated with vehicle (DMSO) or inhibitor (0.5 µL in DMSO, 30 min, RT) followed by an incubation with the activity based probe MB064 (final concentration: 2 µM, 20 min, RT). The reaction was quenched with 7 µL of 4x Laemmli buffer and the proteins were resolved and visualized using the same procedures as for the transfected HEK293T cells.

Western Blot. Western blots were performed as previously reported.²⁹ After the ABPP assay, the proteins on the SDS-PAGE gel were transferred to a membrane using a Trans-Blot Turbo™ Transfer system (Bio-Rad). For anti-FLAG antibody, Membranes were washed with TBS (50 mM Tris, 150 mMNaCl) and blocked with 5% milk in TBST (50 mM Tris, 150 mMNaCl, 0.05% Tween 20) for 1 hat RT (anti-FLAG antibody) or overnight at 4 °C (for anti-PLAAT3 antibody). Membranes were then incubated with primary antibody in 5% milk TBST for 1 h at RT, washed with TBST, incubated with matching secondary antibody in 5% milk TBST for 1 h at RT and subsequently washed with TBST and TBS. The blot was developed in the dark using an imaging solution (10 mL luminal solution, 100 µL ECL enhancer and 3 µL 30% H₂O₂). Chemiluminescence was visualized using a ChemiDoc XRS (BioRad) with standard chemiluminescence settings. For anti-PLAAT3 antibody, the protocol was similar except that PBS or PBST were used as the washing buffer and blocking buffer instead of TBS or TBST, respectively.

Primary antibodies: monoclonal mouse-anti-PLAAT3 (1:200, Abnova, H00011145-M02), monoclonal mouse-anti-FLAG (1:5000, Sigma Aldrich, F3156). Secondary antibodies: HRP-coupled-goat-anti-mouse (1:5000, Santa Cruz, sc2005).

qPCR. For the qPCR experiments, NucleoSpin® RNA kit was used for the total RNA isolation, the transferase (Thermo Scientific Maxima Reverse Transcriptase) was used for cDNA synthesis and the 2x SYBR Green qPCR Master (bimake.com) was used for qPCR

following the manufactures protocols. Primers used were listed in the supplementary figures. The experiment was carried out in duplicate and repeated twice.

Fluorescent substrate assay. The fluorescent substrate assay was based on a previously reported method.⁸ Liposomes were prepared by slowly injecting a concentrated solution of the substrate Red/Green Bodipy PC-A2 (2.5 mM, in DMSO, Invitrogen, A10072), DOPC (10 mM in ethanol, Avanti Polar Lipids, Alabaster, AL) and DOPG (10mM in ethanol, Avanti Polar Lipids, Alabaster, AL) into the assay buffer (50 mM Tris HCl pH 8, 1 mM CaCl₂, 100 mMNaCl).

Relevant concentrations of compounds were prepared in DMSO. The cytosolic protein fraction of HEK293T cells transiently overexpressing PLAAT3 was diluted to 0.6 mg/mL in assay buffer. 50 µL of protein dilution was added in a dark flat-bottom Greiner 96-well plate and incubated with the compounds or vehicle for 30 min at RT. A sample with mock transfected cytosolic protein lysate incubated with DMSO was incorporated for background subtraction. 50 µL of the substrate liposome solution was added (Bodipy PC-A2, final concentration: 2.5 µM) and the fluorescence measurement was started immediately on a TECAN infinite M1000 pro (37 °C, scanning, continuous scanning for 1 h; excitation 488 nm, emission 530 nm). A standard curve of Bodipy FL C5 (D3834, Invitrogen) (the cleavage product of Bodipy PC-A2) was used for evaluating the amount of substrate conversion). The enzyme activity rates were calculated from the steady-state measured in the first 10 min of the reaction. The assay was carried out in duplicate and repeated twice. The data were corrected by the background of mock lysate, normalized by the residual protein activity at 100 µM and then evaluated using GraphPad Prism® 7.

2.5 References

1. Hajnal, A.; Klemenz, R.; Schafer, R., Subtraction cloning of H-rev107, a gene specifically expressed in H-ras resistant fibroblasts. *Oncogene* **1994**, *9* (2), 479-490.
2. Roder, K.; Kim, K. H.; Sul, H. S., Induction of murine H-rev107 gene expression by growth arrest and histone acetylation: involvement of an Sp1/Sp3-binding GC-box. *Biochem. Biophys. Res. Commun.* **2002**, *294* (1), 63-70.
3. Sers, C.; Emmenegger, U.; Husmann, K.; Bucher, K.; Andres, A. C.; Schafer, R., Growth-inhibitory activity and downregulation of the class II tumor-suppressor gene H-rev107 in tumor cell lines and experimental tumors. *J. Cell Biol.* **1997**, *136* (4), 935-44.
4. DiSepio, D.; Ghosn, C.; Eckert, R. L.; Deucher, A.; Robinson, N.; Duvic, M.; Chandraratna, R. A. S.; Nagpal, S., Identification and characterization of a retinoid-induced class II tumor suppressor growth regulatory gene. *Proc. Natl. Acad. Sci. U. S. A.* **1998**, *95* (25), 14811-14815.
5. Wang, L.; Yu, W.; Ren, X.; Lin, J.; Jin, C.; Xia, B., ¹H, ¹³C, and ¹⁵N resonance assignments of the N-terminal domain of human TIG3. *Biomol. NMR Assign.* **2012**, *6* (2), 201-203.
6. Golczak, M.; Kiser, P. D.; Sears, A. E.; Lodowski, D. T.; Blaner, W. S.; Palczewski, K., Structural basis for the acyltransferase activity of lecithin:retinol acyltransferase-like proteins. *J. Biol. Chem.* **2012**, *287* (28), 23790-807.
7. Golczak, M.; Sears, A. E.; Kiser, P. D.; Palczewski, K., LRAT-specific domain facilitates vitamin A metabolism by domain swapping in HRASLS3. *Nat. Chem. Biol.* **2015**, *11* (1), 26-32.
8. Pang, X. Y.; Cao, J.; Addington, L.; Lovell, S.; Battaile, K. P.; Zhang, N.; Rao, J. L.; Dennis, E. A.; Moise, A. R., Structure/function relationships of adipose phospholipase A2 containing a cys-his-his catalytic triad. *J. Biol. Chem.* **2012**, *287* (42), 35260-35274.
9. Ren, X. B.; Lin, J. A.; Jin, C. W.; Xia, B., Solution structure of the N-terminal catalytic domain of human H-REV107-A novel circularly permuted NlpC/P60 domain. *FEBS Lett.* **2010**, *584* (19), 4222-4226.
10. Hsu, T. H.; Chu, C. C.; Jiang, S. Y.; Hung, M. W.; Ni, W. C.; Lin, H. E.; Chang, T. C., Expression of the class II tumor suppressor gene RIG1 is directly regulated by p53 tumor suppressor in cancer cell lines. *FEBS Lett.* **2012**, *586* (9), 1287-1293.
11. Roder, K.; Latasa, M. J.; Sul, H. S., Silencing of the mouse H-rev107 gene encoding a class II tumor suppressor by CpG methylation. *J. Biol. Chem.* **2002**, *277* (34), 30543-30550.
12. Hummasti, S.; Hong, C.; Bensinger, S. J.; Tontonoz, P., HRASLS3 is a PPAR gamma-selective target gene that promotes adipocyte differentiation. *J. Lipid Res.* **2008**, *49* (12), 2535-2544.
13. Jin, X.-H.; Uyama, T.; Wang, J.; Okamoto, Y.; Tonai, T.; Ueda, N., cDNA cloning and characterization of human and mouse Ca²⁺-independent phosphatidylethanolamine N-acyltransferases. *BBA-Mol. Cell Biol. L.* **2009**, *1791* (1), 32-38.

14. Duncan, R. E.; Sarkadi-Nagy, E.; Jaworski, K.; Ahmadian, M.; Sul, H. S., Identification and Functional Characterization of Adipose-specific Phospholipase A2 (AdPLA). *J. Biol. Chem.* **2008**, *283* (37), 25428-25436.
15. Uyama, T.; Jin, X.-H.; Tsuboi, K.; Tonai, T.; Ueda, N., Characterization of the human tumor suppressors TIG3 and HRASLS2 as phospholipid-metabolizing enzymes. *BBA-Mol. Cell Biol. L.* **2009**, *1791* (12), 1114-1124.
16. Jaworski, K.; Ahmadian, M.; Duncan, R. E.; Sarkadi-Nagy, E.; Varady, K. A.; Hellerstein, M. K.; Lee, H.-Y.; Samuel, V. T.; Shulman, G. I.; Kim, K.-H.; de Val, S.; Kang, C.; Sul, H. S., AdPLA ablation increases lipolysis and prevents obesity induced by high-fat feeding or leptin deficiency. *Nat. Med.* **2009**, *15*, 159.
17. Nazarenko, I.; Schäfer, R.; Sers, C., Mechanisms of the HRSL3 tumor suppressor function in ovarian carcinoma cells. *J. Cell Sci.* **2007**, *120* (8), 1393.
18. Elling, U.; Wimmer, R. A.; Leibbrandt, A.; Urkard, T. B.; Michlits, G.; Leopoldi, A.; Micheler, T.; Abdeen, D.; Zhuk, S.; Aspalter, I. M.; Handl, C.; Liebergesell, J.; Hubmann, M.; Husa, A. M.; Kinzer, M.; Schuller, N.; Wetzels, E.; van de Loo, N.; Martinez, J. A. Z.; Estoppey, D.; Riedl, R.; Yang, F. T.; Fu, B. Y.; Dechat, T.; Ivics, Z.; Agu, C. A.; Bell, O.; Blaas, D.; Gerhardt, H.; Hoepfner, D.; Stark, A.; Penninger, J. M., A reversible haploid mouse embryonic stem cell biobank resource for functional genomics. *Nature* **2017**, *550* (7674), 114-118.
19. Sers, C.; Emmenegger, U.; Husmann, K.; Bucher, K.; Andres, A. C.; Schafer, R., Growth-inhibitory activity and downregulation of the class II tumor-suppressor gene H-rev107 in tumor cell lines and experimental tumors. *J. Cell Biol.* **1997**, *136* (4), 935-944.
20. Liu, Y. S.; Patricelli, M. P.; Cravatt, B. F., Activity-based protein profiling: the serine hydrolases. *Proc. Natl. Acad. Sci. U. S. A.* **1999**, *96* (26), 14694-14699.
21. Staring, J.; von Castelmur, E.; Blomen, V. A.; van den Hengel, L. G.; Brockmann, M.; Baggen, J.; Thibaut, H. J.; Nieuwenhuis, J.; Janssen, H.; van Kuppeveld, F. J. M.; Perrakis, A.; Carette, J. E.; Brummelkamp, T. R., PLA2G16 represents a switch between entry and clearance of Picornaviridae. *Nature* **2017**, *541* (7637), 412-416.
22. Uyama, T.; Morishita, J.; Jin, X. H.; Okamoto, Y.; Tsuboi, K.; Ueda, N., The tumor suppressor gene H-Rev107 functions as a novel Ca²⁺-independent cytosolic phospholipase A(1/2) of the thiol hydrolase type. *J. Lipid Res.* **2009**, *50* (4), 685-693.
23. Baggelaar, M. P.; den Dulk, H.; Florea, B. I.; Fazio, D.; Bernabò, N.; Raspa, M.; Janssen, A. P. A.; Scavizzi, F.; Barboni, B.; Overkleeft, H. S.; Maccarrone, M.; van der Stelt, M., ABHD2 Inhibitor identified by activity-based protein profiling reduces acrosome reaction. *ACS Chem. Biol.* **2019**, *14* (10), 2295-2304.

24. Aoyagi, T.; Nagai, M.; Ogawa, K.; Kojima, F.; Okada, M.; Ikeda, T.; Hamada, M.; Takeuchi, T., Poststatin, a new inhibitor of prolyl endopeptidase, produced by *Streptomyces viridochromogenes* MH534-30F3. *J. Antibiot.* **1991**, *44* (9), 949-955.
25. Fusetani, N.; Matsunaga, S.; Matsumoto, H.; Takebayashi, Y., Bioactive marine metabolites. 33. Cyclotheonamides, potent thrombin inhibitors, from a marine sponge *Theonella* sp. *J. Am. Chem. Soc.* **1990**, *112* (19), 7053-7054.
26. Nakao, Y.; Matsunaga, S.; Fusetani, N., Three more cyclotheonamides, C, D, and E, potent thrombin inhibitors from the marine sponge *Theonella-swinhoei*. *Bioorg. Med. Chem.* **1995**, *3* (8), 1115-1122.
27. Nakao, Y.; Oku, N.; Matsunaga, S.; Fusetani, N., Cyclotheonamides E2 and E3, new potent serine protease inhibitors from the marine sponge of the genus *Theonella*. *J. Nat. Prod.* **1998**, *61* (5), 667-670.
28. Baggelaar, M. P.; Janssen, F. J.; van Esbroeck, A. C. M.; den Dulk, H.; Allara, M.; Hoogendoorn, S.; McGuire, R.; Florea, B. I.; Meeuwenoord, N.; van den Elst, H.; van der Marel, G. A.; Brouwer, J.; Di Marzo, V.; Overkleeft, H. S.; van der Stelt, M., Development of an activity-based probe and in silico design reveal highly selective inhibitors for diacylglycerol lipase-alpha in brain. *Angew. Chem.-Int. Edit.* **2013**, *52* (46), 12081-12085.
29. van Esbroeck, A. C. M.; Janssen, A. P. A.; Cognetta, A. B.; Ogasawara, D.; Shpak, G.; van der Kroeg, M.; Kantae, V.; Baggelaar, M. P.; de Vrij, F. M. S.; Deng, H.; Allara, M.; Fezza, F.; Lin, Z.; van der Wel, T.; Soethoudt, M.; Mock, E. D.; den Dulk, H.; Baak, I. L.; Florea, B. I.; Hendriks, G.; de Petrocellis, L.; Overkleeft, H. S.; Hankemeier, T.; De Zeeuw, C. I.; Di Marzo, V.; Maccarrone, M.; Cravatt, B. F.; Kushner, S. A.; van der Stelt, M., Activity-based protein profiling reveals off-target proteins of the FAAH inhibitor BIA 10-2474. *Science* **2017**, *356* (6342), 1084-1087.

2.6 Supplementary Information

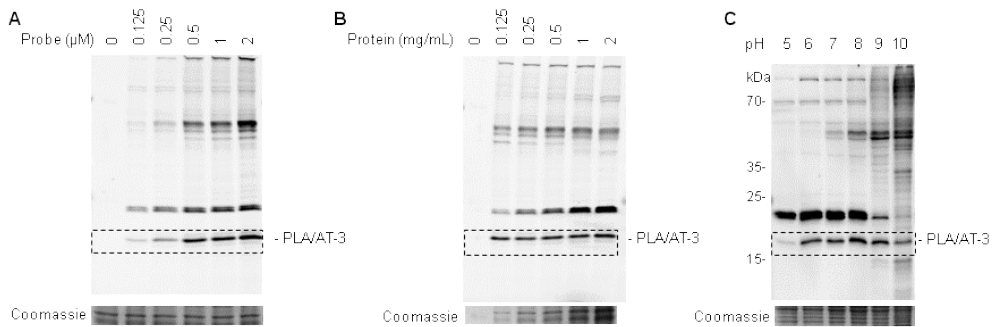


Figure S1. ABPP condition optimization for human PLAAT3 cytosol proteome using MB064. For the probe concentration test, 0.5 mg/mL protein lysate was used. For the protein concentration test, probe of 500 nM was used. Coomassie staining was used as a protein loading control. The lysis buffer with a pH 8 gives the optimal fluorescence signal.

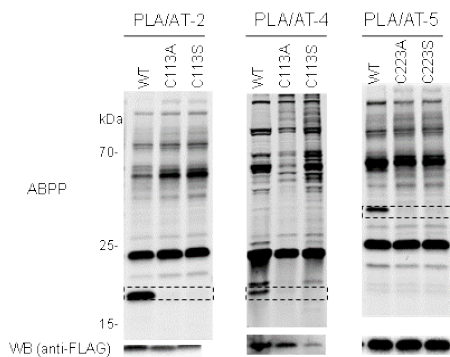


Figure S2. ABPP using MB064 (500 nM) with different enzyme constructs (cytosol fraction from transiently transfected in HEK293T cells) at the same protein concentration, respectively; and western blot of the ABPP gel using an anti-FLAG antibody.

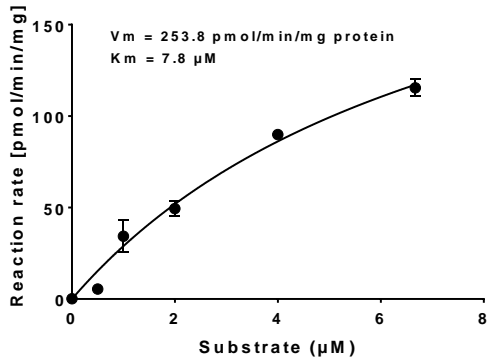


Figure S3. Phospholipase A2 activity of hPLAAT3. Red/Green BODIPY PC-A2 was used to measure the rate of reaction as a function of substrate concentration. The enzyme kinetic data V_{max} and K_m were calculated through sum-of-squares non-linear regression.

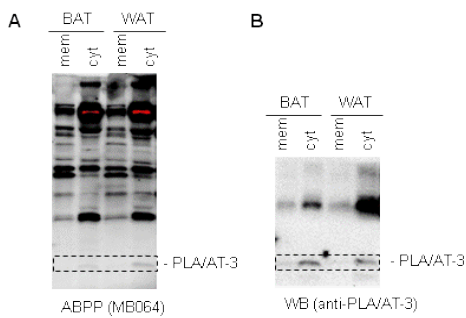


Figure S4. ABPP (A) using MB064 ($2 \mu\text{M}$) with BAT or WAT membrane (mem) or cytosol (cyt) proteome at the same protein concentration, and western blot (B) of the ABPP gel using an anti-PLAAT3 antibody.

3

Structure activity relationship of α -ketoamides on phospholipase-acyltransferases: discovery of LEI110

3.1 Introduction

The human phospholipase A/acyl transferase (PLAAT) family consists of five members (namely, PLAAT1-5) of which two are absent in rodents (i.e. PLAAT2, and PLAAT4).^{1,2} PLAAT enzymes show structural homology to lecithin retinol acyl transferase (LRAT) and belong to the Nlpc/P60 superfamily of cysteine proteases.³ The members of the PLAAT family share a highly conserved NCEHFV peptidic sequence, which includes the catalytically active cysteine residue.⁴ The catalytic cysteine forms a catalytic triad with two N-terminal histidines in PLAAT2-5 and an N-terminal histidine together with an asparagine in PLAAT1. PLAATs possess Ca²⁺-independent phospholipase activity *in vitro* with both phosphatidylcholine (PC) and phosphatidylethanolamine (PE) acting as substrates. All members also exhibit *O*-acyl transferase activity with preference for the *sn*-1 position of lysophosphatidylcholine (lysoPC) as well as *N*-acyltransferase activity with the ability to produce *N*-acylphosphatidylethanolamines (NAPEs) through catalysis of the acyl chain transfer from the *sn*-1 position of glycerophospholipids to the amine function of PE.² All enzymes, except PLAAT3, show a preference for PLA₁ activity (hydrolysis of phospholipids to produce 2-acyl-lysophospholipids and fatty acids) over PLA₂ activity (hydrolysis of the *sn*-2 position of membrane glycerophospholipids to liberate arachidonic acid). Depending on the assay conditions the substrate preference of PLAAT3 may shift. For example, Duncan *et al.* reported that PLAAT3 has a preference for the *sn*-2 position with a moderate Ca²⁺-dependency,⁵ while Uyama *et al.* found primarily hydrolysis of the fatty acyl at the *sn*-1 position.⁶

The structures of PLAAT2 and PLAAT3 have been solved through X-ray crystallography.⁷ Both proteins contain three alpha helices separated from a four stranded anti-parallel beta sheet. The proteins also contain a C-terminal transmembrane hydrophobic domain, with the exception of PLAAT5, which was proposed to anchor the protein in the lipid membrane. The C-terminal domain of these proteins has been shown to be required for subcellular localization, as the truncated form of the PLAAT3-GFP fusion protein has been found to be evenly diffused in COS-7 cells. The full length fusion protein on the other hand showed a predominantly perinuclear localization and to a lesser extent localization in the cytoplasm.⁵ In contrast, in HEK293 and HeLa cells PLAAT3 localization has been shown to be associated with peroxisomes.⁸ Furthermore, deletion of the hydrophobic transmembrane C-terminal domain of PLAAT3 resulted in a total loss of phospholipase activity.⁵

PLAAT1 is predominantly expressed in human testes, skeletal muscle, and heart. Overexpression of PLAAT1 was shown to inhibit the growth of H-Ras-transformed NIH3T3 fibroblasts.⁹ Furthermore, hypermethylation of CpG islands in the 5' region of the PLAAT1 gene, causing reduced expression of the protein, has also been shown in multiple gastric cancers.¹⁰ A relatively high *N*-acyltransferase activity has been observed *in vitro*, compared to PLAAT2-5.¹¹ The

physiological role of the enzyme however has yet to be studied. PLAAT2 is expressed primarily in the human colon, small intestine, stomach, trachea and kidneys.¹² Overexpression of this protein resulted in reduced colony formation in HCT166 colon cancer cells, HeLa cervical cancer cells, and MCF-7 breast cancer cells. Moreover, overexpression of PLAAT2 in HtTA cervical cancer cells resulted in suppression of RAS activation and increased cell death. This effect was found to be dependent on the C-terminal hydrophobic domain. The enzyme was determined to have primarily *N*-acyltransferase activity *in vitro* and preferred the *sn*-1 position of PC as acyl donor.¹³ The physiological role of PLAAT2 has not been characterized, which is partly due to a lack of inhibitors.

PLAAT3 is the most studied member of the PLAAT proteins. The *in vivo* relevance of PLAAT3 has not been well studied, but a mouse model constitutively lacking the *hrasls3* gene has been generated.¹⁴ Ablation of PLAAT3 prevented obesity caused by high fat diet feeding or leptin deficiency, thus establishing PLAAT3 as a potential target for the treatment of obesity. PLAAT3 deficient mice exhibited a higher rate of lipolysis, due to decreased levels of prostaglandin E₂ (PGE₂) that were most likely caused by a decrease in arachidonic acid levels. In addition, increased fatty acid oxidation in adipose tissue was also reported. Currently, there are no pharmacological tools to study the effects of acute and dynamic inhibition of PLAAT3.

The expression of PLAAT4 was decreased in a variety of primary human tumors, and cancer cell lines.¹⁵ Similarly to other PLAAT members, this enzyme inhibited H-RAS mediated signaling. PLAAT4 primarily functions as a phospholipase *in vitro* and the activity has been observed to be dependent on the C-terminal domain.^{2, 16} It is expressed in high levels in differentiated human keratinocytes where it regulates cell survival through interaction with type 1 transglutaminase (TG1), the enzyme responsible for the cornified envelope formation. In addition, reduced expression of PLAAT4 can be observed in psoriasis.¹⁷ Currently, there are no chemical tools to study the effects of acute and dynamic inhibition of PLAAT4.

PLAAT5 primarily shows *N*-acyltransferase activity over *O*-acyltransferase and PLA1/2 *in vitro*.² It has been observed in rat spermatocytes although its function remains unknown.¹⁸ As mentioned earlier, the enzyme is structurally different from the other PLAAT proteins as it does not contain the C-terminal transmembrane domain and therefore is predominantly found in the cytosol.¹⁹ The physiological function of the enzyme remains unknown. Furthermore, it is also unknown if PLAAT5 acts as a tumor suppressor similar to the other PLAAT members. Ueda and coworkers overexpressed PLAAT5 in COS-7 cells and found that this protein could catalyze the formation of radioactive NAPE via transferring the radioactive acyl group from PC to PE. The activity of PLAAT5 was mainly found in cytosolic fraction and not stimulated by Ca²⁺-ions.¹⁹

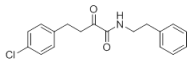
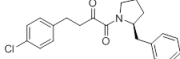
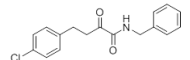
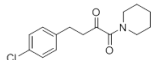
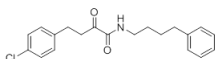
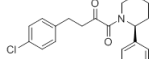
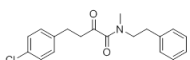
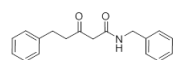
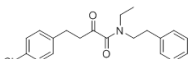
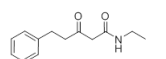
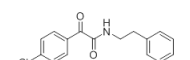
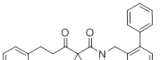
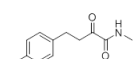
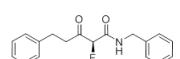
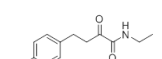
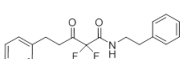
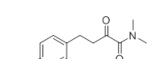
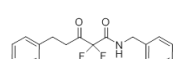
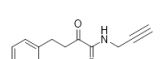
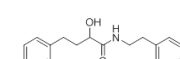
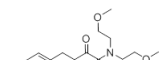
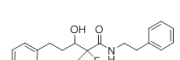
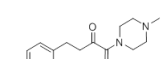
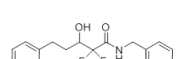
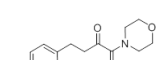
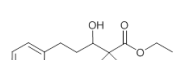
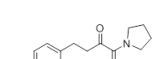
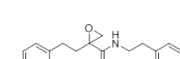
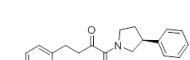
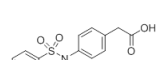
In chapter 3, an activity based protein profiling (ABPP) method was developed to measure PLAAT activity. Screening of a focused library resulted in the discovery of α -ketoamide **1** as a selective PLAAT inhibitor. In this chapter, a set of 63 analogues of compound **1** was tested for

their potency against PLAAT3, PLAAT4 and PLAAT5 using competitive ABPP, which led to the discovery of LEI110 as a potent and selective inhibitor for PLAAT3.

3.2 Results and discussion

To obtain a structure-activity relationship of α -ketoamides on PLAAT activity, an ABPP method was employed as developed in **Chapter 3**. In short, cytosol fractions of human embryonal kidney 293T cells (HEK293T) transiently overexpressing recombinant human PLAAT3, PLAAT4 or PLAAT5 were incubated with test compounds at 10 μ M for 30 min and then with probe MB064 for another 20 min. The proteins were then resolved by sodium dodecyl sulfate polyacrylamide gel electrophoresis (SDS PAGE) and the residual protein activity was visualized by in-gel fluorescence scanning. First, a small set of structural analogues (**2-30**) of compound **1** were tested at a single concentration of 10 μ M. The following structure-activity relationship could be derived (see Table 1). Compared to compound **1**, reducing the linker length either at the amine part (**2**) or α -keto part (**6**) reduced inhibitory activity. Of note, compound **2** showed selectivity for PLAAT3 over PLAAT4/5. Conversely, increasing the spacer length at the amine part increased the inhibitory activity (**3**). The inhibitory activity was abolished when the amide was methylated (**4, 9**) or ethylated (**5**). Substitution of 2-phenethylamine with various primary amines (**7,8,10**) retained activity, but secondary amines (**9, 11-18**) did not yield promising inhibitors. β -Ketoamides (**19, 20**) and α -(di)fluoro-substituted β -ketoamides (**21-24**) or reduced analogues (**26-28**) were not active. Importantly, reduction of the α -keto to the hydroxyl group in compound **25** led to a decrease in activity, suggesting that the α -keto forms an important interaction with the enzymes. Replacement of the α -keto warhead by an epoxide as an alternative electrophile did not yield an active inhibitor (**29**). Finally, compound **30** showed weak inhibitory activity. From these results, it is concluded that the α -keto and a secondary amide are essential for PLAAT inhibition.

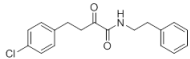
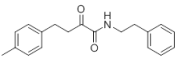
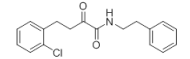
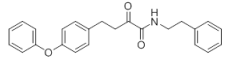
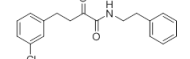
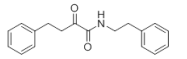
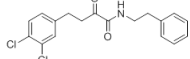
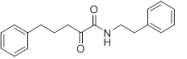
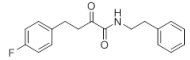
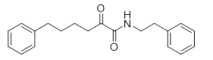
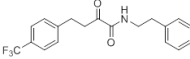
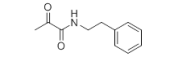
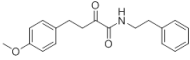
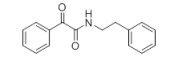
Table 1. The pIC₅₀ values of compounds **1-30** with standard deviations.

ID	Structure	PLAAT3	4	5	ID	Structure	PLAAT3	4	5
1		6.0±0.2	6.2±0.1	6.4±0.1	16		<5	<5	<5
2		5.8±0.1	<5	<5	17		<5	<5	<5
3		6±0.1	5.8±0.1	6.7±0.1	18		<5	<5	<5
4		<5	<5	<5	19		<5	<5	<5
5		<5	<5	<5	20		<5	<5	<5
6		<5	<5	<5	21		<5	<5	<5
7		5.2±0.1	5.4±0.1	6.1±0.1	22		<5	<5	<5
8		5.1±0.1	5.4±0.1	6±0.1	23		<5	<5	<5
9		<5	<5	<5	24		<5	<5	<5
10		<5	<5	5.6±0.1	25		<5	<5	<5
11		<5	<5	<5	26		<5	<5	<5
12		<5	<5	<5	27		<5	<5	<5
13		<5	<5	<5	28		<5	<5	<5
14		<5	<5	<5	29		<5	<5	<5
15		<5	<5	<5	30		<5	<5	<5

In the next compound set, the phenethylamine was kept constant and different groups were incorporated at the other side of the molecule (Table 2). The inhibitors were tested

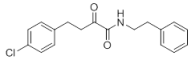
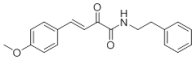
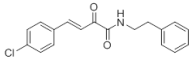
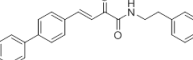
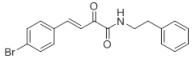
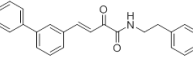
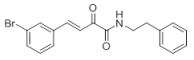
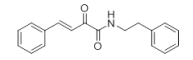
at five different concentrations (0.01, 0.1, 1, 10, and 100 μM) against PLAAT 3-5 and the dose-response curve was plotted to determine the pIC_{50} . Changing the location of the chlorine substituent to the *ortho*- (**31**) or *meta*-position (**32**) did not increase the potency compared to compound **1**. Incorporation of a 3,4-dichloro-substituent (**33**) slightly increased the inhibitory activities against these three enzymes. None of the other substituents (F, Me, OMe, CF_3) at the *para*-position (**34-38**) gave better inhibitors. However, removal of the chlorine (compound **39**) or elimination of the 4-Cl-phenyl moiety (compound **42**) led to an inactive compound at PLAAT3, but not at PLAAT5. Different linker lengths between the phenyl and the α -ketone (**40, 41, 43**) were explored. Notably, compound **40** with a three-carbon linker showed increased potency for PLAAT3 and 5.

Table 2. The pIC_{50} values of compound **1**, **31-43** with standard deviations.

ID	Structure	PLAAT3	4	5	ID	Structure	PLAAT3	4	5
1		6.0 \pm 0.2	6.2 \pm 0.1	6.4 \pm 0.1	37		5.7 \pm 0.1	5.8 \pm 0.1	5.6 \pm 0.1
31		5.7 \pm 0.1	5.6 \pm 0.1	5.8 \pm 0.1	38		5.4 \pm 0.1	5.9 \pm 0.1	6.9 \pm 0.1
32		5.8 \pm 0.1	5.9 \pm 0.1	5.9 \pm 0.1	39		<5	5.5 \pm 0.1	6.0 \pm 0.1
33		7.0 \pm 0.2	6.0 \pm 0.1	7.0 \pm 0.1	40		6.4 \pm 0.1	6.2 \pm 0.1	7.0 \pm 0.1
34		5.3 \pm 0.1	5.0 \pm 0.1	5.8 \pm 0.1	41		6.0 \pm 0.1	5.8 \pm 0.1	6.8 \pm 0.1
35		5.1 \pm 0.1	5.6 \pm 0.1	6.5 \pm 0.1	42		<5	<5	<5
36		5.5 \pm 0.1	5.9 \pm 0.1	5.9 \pm 0.1	43		<5	<5	<5

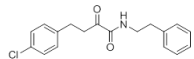
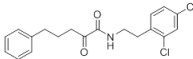
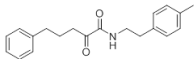
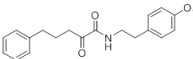
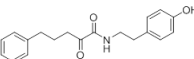
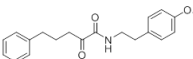
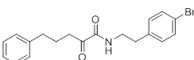
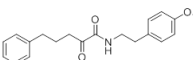
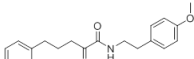
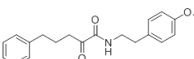
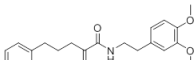
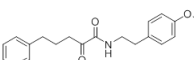
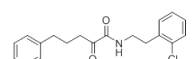
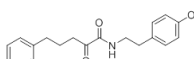
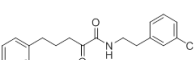
Next, a series of β,γ -unsaturated α -ketoamides (**44-50**, Table 3) were tested to explore the effect of restricting the conformation of the alkyl linker. None of these compounds showed improved potency against PLAAT3-5. The structure-activity relationship (Table 2 and 3) indicates that the 3-phenylpropyl moiety (shown in compound **40**) is the optimal fragment for the α -keto side.

Table 3. The pIC₅₀ values of compound **1**, **44-50** with standard deviations.

ID	Structure	PLAAT3	4	5	ID	Structure	PLAAT3	4	5
1		6.0±0.2	6.2±0.1	6.4±0.1	47		5.3±0.1	5.6± 0.07	6.0±0.1
44		5.6±0.1	5.6±0.1	6.2±0.1	48		5.2±0.1	5.0± 0.1	5.6±0.1
45		5.6±0.1	5.2±0.1	6.2± 0.1	49		5.5±0.1	5.6± 0.1	6.0±0.1
46		<5	5.1± 0.1	5.5± 0.1	50		5.8±0.1	5.0± 0.1	5.2±0.2

Finally, with the optimal fragment (3-phenylpropyl) for the α -keto side in hand, it was decided to optimize the phenethylamine moiety (Table 4). Incorporation of small substituents on the *para*-position (**51-54**) resulted in different bioactivities. 4-Methyl-substituted compound (**51**) and 4-bromo analog (**53**) showed substantially increased inhibitory potency for PLAAT3 and PLAAT5 (pIC₅₀: 7.0±0.1 and 7.4±0.1, respectively), whereas more polar substituents, such as *p*-hydroxyl (**52**), 4-methoxy (**54**), 3,4-dimethoxy (**55**) did not increase the potency. Of note, *para*-substitution increased also the selectivity for PLAAT5. The 2-chloro analogue (**56**) showed decreased potency, while the 3-chloro (**57**) and 2,4-dichloro (**58**) derivatives showed increased potency for PLAAT3,5 and slightly decreased potency for PLAAT4. Finally, various aromatic rings (**59-64**) were incorporated at the *para*-position of the phenethylamine via an ether linkage. Compound **59** (phenyl-), **62** (6-(trifluoromethyl)pyridin-3-yl), **63** (5-(trifluoromethyl)pyridin-2-yl) and **64** (2-chloropyrimidin-4-yl) all showed increased inhibitory activities against PLAAT3-5.

Table 4. The pIC₅₀ values of compound **1**, **51-64** with standard deviations.

ID	Structure	PLAAT3	4	5	ID	Structure	PLAAT3	4	5
1		6.0±0.2	6.2±0.1	6.4±0.1	58		6.6±0.1	6.1±0.1	7.2±0.1
51		7.0±0.1	5.9±0.1	7.4±0.1	59		7.2±0.1	7.3±0.1	7.4±0.2
52		5.8±0.1	5.6±0.1	6.8±0.10	60		6.6±0.1	6.2±0.1	7.2±0.1
53		6.8±0.1	6.7±0.1	8.0±0.1	61		5.7±0.1	5.9±0.1	6.6±0.1
54		6.1±0.1	5.8±0.1	7.1±0.1	62		6.8±0.1	7.1±0.1	7.1±0.1
55		6.0±0.2	5.2±0.1	6.5±0.1	63		7.0±0.1	6.8±0.1	7.6±0.1
56		5.9±0.1	5.6±0.1	6.1±0.2	(LEI110) 64		6.6±0.1	6.7±0.1	7.1±0.1
57		6.7±0.1	6.0±0.1	7.3±0.1					

In order to gain insight in the molecular interactions of α -ketoamides with PLAAT3, LEI110 (**63**) and **1** were docked in a PLAAT3 crystal structure (PDB: 4DOT).⁷ It was envisioned that the electrophilic ketone of LEI110 and **1** could act through a reversible covalent mechanism with the active site Cys113 forming a hemithioacetal adduct (Figure 1B), similar to other reported α -ketoamide inhibitors.²⁰ This adduct was generated in silico for LEI110 and **1** after which molecular dynamics simulation was performed (Figure 1A). Hydrogen bonding of the oxyanion with His23 was observed in both cases, as well as π - π stacking with Tyr21. The extension of the ketone alkyl chain by one methylene allows for a more optimal π -cation interaction with Arg18 for LEI110, compared to **1**. Furthermore, the introduction of the pyridyl moiety in LEI110 enables an additional hydrogen bond with the Tyr21-OH. These docking results provide a potential explanation for the 10-fold increase in activity seen for LEI110.

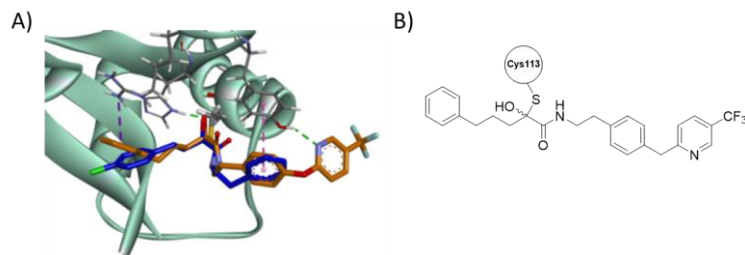


Figure 1. (A) Structure-guided modeling of **1** and LEI110. Compounds **1** (blue) and LEI110 (orange) in complex with PLAAT3, covalently bound to Cys113. Green dotted lines represent a hydrogen bond, pink and purple represent π -interactions. (B) the structure of the hemithioacetal adduct of LEI110.

3.3 Conclusions

In this chapter, an ABPP assay method was used to profile the inhibitory activities of the pan-PLAAT inhibitor **1** and 63 designed analogs and a structure-activity relationship was also developed. Based on the screening results of library 1 (Table 1), it was found that the α -keto and the secondary amide were essential for inhibition. Screening the focused compound libraries 2 (Table 2) and 3 (Table 3) with variation of the α -keto side of the molecule, the 3-phenylpropyl moiety (shown in compound **40**) is found to be the optimal fragment from the α -keto side. Further efforts were focused on the optimization of the phenethylamine moiety while having the 3-phenylpropyl moiety at the α -keto side. In the end, compound **52** and **53** were identified as potent and selective inhibitors for PLAAT5. Compound **51** and **63** (LEI110) were identified as potent and selective inhibitors for PLAAT3 and 5. Molecular dynamics simulations of LEI110 in the reported crystal structure of PLAAT3 provided insight in the potential ligand-protein interactions to explain its binding mode. LEI110 is the most potent and selective PLAAT3 inhibitor reported to date and provides a good starting point for further structure-based inhibitor development for PLAAT3.

4.4 Experimental procedures

Plasmids. Full-length human cDNA of PLAAT3 (kindly provided by Prof. N. Ueda, Department of Biochemistry, School of Medicine, Kagawa University, 1750-1 Ikenobe, Miki, Kagawa 761-0793, Japan) was cloned into mammalian expression vector pcDNA3.1, containing genes for ampicillin and neomycin resistance. The inserts were cloned in frame with a C-terminal FLAG-tag and site-directed mutagenesis was used to remove restriction by silent point mutations. Plasmids were isolated from transformed XL-10 Z-competent cells (Maxi Prep kit: Qiagen) and sequenced at the Leiden Genome Technology Center. Sequences were analyzed and verified (CLC Main Workbench).

Cell culture

General. HEK293T cells were kept in culture at 37 °C under 7% CO₂ in DMEM containing phenol red, stable glutamine, 10% (v/v) newborn calf serum (Thermo Fisher), and penicillin and streptomycin (200 µg/mL each; Duchefa). Medium was refreshed every 2-3 days and cells were passaged twice a week at 80-90% confluence. Cells lines were purchased from ATCC and were regularly tested for mycoplasma contamination.

Transient transfection. Transient transfection was performed as previously described.²¹ In brief, HEK293T cells were seeded in 15-cm petri dishes one day prior to transfection. Prior to transfection, culture medium was aspirated and a minimal amount of medium was added. A 3:1 (m/m) mixture of polyethyleneimine (PEI, 1 mg/mL) (60 µg/15-cm dish) and plasmid DNA (20 µg/dish) was prepared in serum free culture medium and incubated for 15 min at RT. Transfection was performed by dropwise addition of the PEI/DNA mixture to the cells. Transfection with the empty pcDNA3.1 vector was used to generate control samples (mock groups). After 24 h, medium was refreshed. Medium was aspirated 72 h post-transfection and cells were harvested by resuspension in PBS. Cells were pelleted by centrifugation (5 min, 1,000 g) and the pellet was washed with PBS. The supernatant was discarded and the cell pellets were snap-frozen in liquid nitrogen and stored at -80 °C until sample preparation.

Sample preparation

Cell membrane and cytosol proteome preparation. Cell pellets were thawed on ice, resuspended in cold lysis buffer (50 mM Tris HCl, pH 8, 2 mM DTT, 1 mM MgCl₂, 2.5 U/mL benzonase) and incubated on ice (30 min). The cell lysate was collected and centrifuged (100.000 g, 45 min, 4 °C, Beckman Coulter, Ti 70.1 rotor). The supernatant was collected (cytosolic fraction) and the membrane pellet was resuspended in cold storage buffer (50 mM Tris HCl, pH 8, 2 mM DTT) by thorough pipetting and passage through an insulin needle (29G). Protein concentrations were determined by a Quick Start™ Bradford

Protein Assay or QubitTM protein assay (Invitrogen). Samples were flash frozen in liquid nitrogen and stored at -80 °C until further use.

Activity based protein profiling on transiently transfected HEK293T cell lysate. Gel-based activity based protein profiling (ABPP) was performed with minor alterations of the previously reported protocol.²¹ For ABPP assays on HEK293T cells overexpressing PLAAT3, the cytosol proteome (0.5 mg/mL, 20 μ L) was pre-incubated with vehicle (DMSO) or inhibitor (0.5 μ L in DMSO, 30 min, RT) followed by an incubation with the activity based probe MB064 (final concentration: 250 nM, 20 min, RT). Final concentrations for the inhibitors are indicated in the main text and figure legends. Only cytosol proteome was used for the dose-response test in ABPP or substrate assay. Reactions were quenched with 7 μ L of 4x Laemmli buffer (5 μ L, 240 mM Tris (pH 6.8), 8% (w/v) SDS, 40% (v/v) glycerol, 5% (v/v) β -mercaptoethanol, 0.04% (v/v) bromophenol blue). 10 μ L sample per reaction was resolved on a 10% or 15% acrylamide SDS-PAGE gel (180 V, 70 min). Gels were scanned using a ChemiDoc MP system with Cy3 and Cy5 multichannel settings (605/50 and 695/55, filters respectively) and stained with Coomassie after scanning. All experiments were performed 3 times. Fluorescence was normalized to Coomassie staining and quantified with Image Lab (Bio-Rad). IC₅₀ curves were fitted with Graphpad Prism[®] 7 (Graphpad Software Inc.).

Computational Chemistry

Ligand preparation. Molecular structures of LEI110 and **1** were prepared for docking using Ligprep from Schrödinger.²² Default Ligprep settings were applied: states of heteroatoms were generated using Epik at a pH 7 \pm 2.²³ No tautomers were created by the program, which resulted in one standardized structure per ligand.

Protein preparation. The x-ray structure of PLAAT3 was extracted from the PDB (PDB ID: 4DOT).⁷ The apo protein structure was prepared for docking with the Protein Preparation tool from the Schrödinger 2017-4 suite. Waters were removed and default protein preparation settings were applied: explicit hydrogens were added and states of heteroatoms were generated using Epik at a pH 7 \pm 2, resulting in a protonated state of binding pocket His23. Additionally, missing side chains and loops were added using Prime,²⁴ but none were detected.

Docking. As the PLAAT3 lacked a co-crystallized ligand, induced-fit docking was applied to induce the PLAAT3 binding pocket into a ligand-binding conformation. Both LEI110 and **1** were docked with induced-fit, resulting in 39 different pocket conformations. Induced-fit docking was followed by covalent docking of LEI110 and **1** to Cys113 in all 39 generated pocket conformations. Compounds were docked using the Schrödinger 2017-4 suite²⁵ with SP precision. The ten poses with the lowest docking scores were manually

examined and one pose per ligand was selected. Selection was based on docking score, frequency of recurring poses, and interactions made between the ligand and the protein.

Molecular dynamics. The selected LEI110 and **1** poses in complex with PLAAT3 were simulated with molecular dynamics using Desmond Molecular Dynamics System from Schrödinger.²⁶ The system was setup using solvent model SPC and OPLS3 force field. The simulation was performed at a temperature of 300 Kelvin and a pressure of 1.01 bar. Triplicate runs were executed with a runtime of 100 ns per run. The simulations showed that PLAAT3 remained stable when in complex with LEI110 and **1**.

3.5 References

1. Jin, X.-H.; Uyama, T.; Wang, J.; Okamoto, Y.; Tonai, T.; Ueda, N., cDNA cloning and characterization of human and mouse Ca^{2+} -independent phosphatidylethanolamine N-acyltransferases. *BBA-Mol. Cell Biol. L.* **2009**, *1791* (1), 32-38.
2. Uyama, T.; Ikematsu, N.; Inoue, M.; Shinohara, N.; Jin, X. H.; Tsuboi, K.; Tonai, T.; Tokumura, A.; Ueda, N., Generation of N-acylphosphatidylethanolamine by members of the phospholipase A/acyltransferase (PLA/AT) family. *J. Biol. Chem.* **2012**, *287* (38), 31905-19.
3. Anantharaman, V.; Aravind, L., Evolutionary history, structural features and biochemical diversity of the NlpC/P60 superfamily of enzymes. *Genome Biol.* **2003**, *4* (2), R11.
4. Kiser, P. D.; Golczak, M.; Palczewski, K., Chemistry of the retinoid (visual) cycle. *Chem. Rev.* **2014**, *114* (1), 194-232.
5. Duncan, R. E.; Sarkadi-Nagy, E.; Jaworski, K.; Ahmadian, M.; Sul, H. S., Identification and functional characterization of adipose-specific phospholipase A2 (AdPLA). *J. Biol. Chem.* **2008**, *283* (37), 25428-25436.
6. Uyama, T.; Morishita, J.; Jin, X. H.; Okamoto, Y.; Tsuboi, K.; Ueda, N., The tumor suppressor gene H-Rev107 functions as a novel Ca^{2+} -independent cytosolic phospholipase A(1/2) of the thiol hydrolase type. *J. Lipid Res.* **2009**, *50* (4), 685-693.
7. Golczak, M.; Kiser, P. D.; Sears, A. E.; Lodowski, D. T.; Blaner, W. S.; Palczewski, K., Structural basis for the acyltransferase activity of lecithin:retinol acyltransferase-like proteins. *J. Biol. Chem.* **2012**, *287* (28), 23790-807.
8. Uyama, T.; Ichi, I.; Kono, N.; Inoue, A.; Tsuboi, K.; Jin, X. H.; Araki, N.; Aoki, J.; Arai, H.; Ueda, N., Regulation of peroxisomal lipid metabolism by catalytic activity of tumor suppressor H-rev107. *J. Biol. Chem.* **2012**, *287* (4), 2706-18.
9. Akiyama, H.; Hiraki, Y.; Noda, M.; Shigeno, C.; Ito, H.; Nakamura, T., Molecular cloning and biological activity of a novel Ha-Ras suppressor gene predominantly expressed in skeletal muscle, heart, brain, and bone marrow by differential display using clonal mouse EC cells, ATDC5. *J. Biol. Chem.* **1999**, *274* (45), 32192-7.
10. Ito, H.; Akiyama, H.; Shigeno, C.; Nakamura, T., Isolation, characterization, and chromosome mapping of a human A-C1 Ha-Ras suppressor gene (HRASLS). *Cytogenet. Cell Genet.* **2001**, *93* (1-2), 36-9.
11. Uyama, T.; Inoue, M.; Okamoto, Y.; Shinohara, N.; Tai, T.; Tsuboi, K.; Inoue, T.; Tokumura, A.; Ueda, N., Involvement of phospholipase A/acyltransferase-1 in N-acylphosphatidylethanolamine generation. *Biochim. Biophys. Acta* **2013**, *1831* (12), 1690-701.
12. Shyu, R. Y.; Hsieh, Y. C.; Tsai, F. M.; Wu, C. C.; Jiang, S. Y., Cloning and functional characterization of the HRASLS2 gene. *Amino acids* **2008**, *35* (1), 129-37.

13. Uyama, T.; Jin, X.-H.; Tsuboi, K.; Tonai, T.; Ueda, N., Characterization of the human tumor suppressors TIG3 and HRASLS2 as phospholipid-metabolizing enzymes. *BBA-Mol. Cell Biol. L.* **2009**, *1791* (12), 1114-1124.
14. Jaworski, K.; Ahmadian, M.; Duncan, R. E.; Sarkadi-Nagy, E.; Varady, K. A.; Hellerstein, M. K.; Lee, H.-Y.; Samuel, V. T.; Shulman, G. I.; Kim, K.-H.; de Val, S.; Kang, C.; Sul, H. S., AdPLA ablation increases lipolysis and prevents obesity induced by high-fat feeding or leptin deficiency. *Nat. Med.* **2009**, *15*, 159.
15. DiSepio, D.; Ghosn, C.; Eckert, R. L.; Deucher, A.; Robinson, N.; Duvic, M.; Chandraratna, R. A. S.; Nagpal, S., Identification and characterization of a retinoid-induced class II tumor suppressor growth regulatory gene. *Proc. Natl. Acad. Sci. U. S. A.* **1998**, *95* (25), 14811-14815.
16. Wu, C. C.; Shyu, R. Y.; Wang, C. H.; Tsai, T. C.; Wang, L. K.; Chen, M. L.; Jiang, S. Y.; Tsai, F. M., Involvement of the prostaglandin D2 signal pathway in retinoid-inducible gene 1 (RIG1)-mediated suppression of cell invasion in testis cancer cells. *Biochim. Biophys. Acta* **2012**, *1823* (12), 2227-36.
17. Duvic, M.; Helekar, B.; Schulz, C.; Cho, M.; DiSepio, D.; Hager, C.; DiMao, D.; Hazarika, P.; Jackson, B.; Breuer-McHam, J.; Young, J.; Clayman, G.; Lippman, S. M.; Chandraratna, R. A.; Robinson, N. A.; Deucher, A.; Eckert, R. L.; Nagpal, S., Expression of a retinoid-inducible tumor suppressor, Tazarotene-inducible gene-3, is decreased in psoriasis and skin cancer. *Clin. Cancer Res.* **2000**, *6* (8), 3249-59.
18. Yamano, Y.; Asano, A.; Ohyama, K.; Ohta, M.; Nishio, R.; Morishima, I., Expression of the Ha-ras suppressor family member 5 gene in the maturing rat testis. *Biosci. Biotech. Bioch.* **2008**, *72* (5), 1360-3.
19. Jin, X. H.; Okamoto, Y.; Morishita, J.; Tsuboi, K.; Tonai, T.; Ueda, N., Discovery and characterization of a Ca²⁺-independent phosphatidylethanolamine N-acyltransferase generating the anandamide precursor and its congeners. *J. Biol. Chem.* **2007**, *282* (6), 3614-23.
20. De Risi, C.; Pollini, G. P.; Zanirato, V., Recent developments in general methodologies for the synthesis of α -ketoamides. *Chem. Rev.* **2016**, *116* (5), 3241-3305.
21. Baggelaar, M. P.; Janssen, F. J.; van Esbroeck, A. C. M.; den Dulk, H.; Allara, M.; Hoogendoorn, S.; McGuire, R.; Florea, B. I.; Meeuwenoord, N.; van den Elst, H.; van der Marel, G. A.; Brouwer, J.; Di Marzo, V.; Overkleeft, H. S.; van der Stelt, M., Development of an activity-based probe and in silico design reveal highly selective inhibitors for diacylglycerol lipase-alpha in brain. *Angew. Chem.-Int. Edit.* **2013**, *52* (46), 12081-12085.
22. Schrödinger. Release 2017-4, LigPrep, Schrödinger, LLC, New York, NY, **2017**.
23. Schrödinger. Release 2017-4, Epik, Schrödinger, LLC, New York, NY, **2017**.
24. Schrödinger. Release 2017-4: Prime, Schrödinger, LLC, New York, NY, **2017**.

25. Schrödinger. Small-Molecule Drug Discovery Suite 2017-4, Schrödinger, LLC, New York, NY, **2017**.
26. Schrödinger. Release 2017-4: Desmond Molecular Dynamics System, D. E. Shaw Research, New York, NY, **2017**. Maestro-Desmond Interoperability Tools, Schrödinger, New York, NY, 2017.

4

Biochemical and cellular profiling of LEI110

4.1 Introduction

The previous two chapters together outline the pathway to the discovery of a selective PLAAT3 inhibitor. PLAATs play an important role in lipid metabolism and biosynthesis of NAE phospholipids and studies on their individual contribution to these physiological processes are required, both for fundamental understanding and for unveiling their potential as therapeutic targets in obesity and/or the common cold. Recent immunoprecipitation studies have shown that PLAAT3 binds to peroxin-19 (Pex19), a protein known to function as a chaperone in the transport of peroxisomal membrane proteins.¹ Overexpression of PLAAT3 causes almost complete disappearance of peroxisomes in mammalian cells within 24 h, which further supports the regulatory role of PLAAT3 in the oxidation of fatty acids. Interestingly, the catalytically inactive point mutant of PLAAT3 (C113S) was neither able to disrupt the binding of Pex19 to other peroxisomal membrane proteins nor the peroxisomal function itself, while retaining the ability to bind Pex19. Therefore it has been suggested that PLAAT3 could exert its inhibitory effect through hydrolysis of peroxisomal membrane lipids, although more data is necessary to confirm this hypothesis. The dysregulation of peroxisomal function by PLAAT3 is in accordance with the observed phenotype of PLAAT3 deficient mice as elimination of adipocyte peroxisomes by ablation of a peroxin essential to peroxisome biogenesis, Pex5, in mice was reported to result in increased fat mass and a reduced rate of lipolysis in white adipose tissue (WAT).²

LEI 110 (Figure 1B), discovered by research in the previous **chapter 3** provides the potential means to do, at least for its preferred target, PLAAT3. For this potential to bear out, its behavior in live cells needs to be mapped. This chapter details studies performed to this end and entailing biochemical and cellular profiling of LEI110.

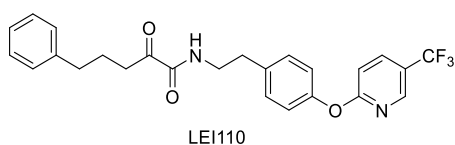


Figure 1. Chemical structure of LEI110.

4.2 Results and discussion

In **chapter 3**, 2-oxo-5-phenyl-N-(4-((5-(trifluoromethyl)pyridin-2-yl)oxy)phenethyl)-pentanamide (LEI110) was discovered as a PLAAT3 inhibitor with a $pIC_{50} = 7.0 \pm 0.1$ in the ABPP-assay. In order to gain insight into the selectivity over other members of this protein family, LEI110 was tested against other PLAATs. The results showed that LEI110 was also active on PLAAT2 (pIC_{50} : 6.8), PLAAT4 (pIC_{50} : 6.8) and PLAAT5 (pIC_{50} : 7.6), (Figure 2A, Table 1). LEI110 was tested in a fluorescent substrate assay. In this assay, the

cytosolic protein fraction of HEK293T cells transiently overexpressing PLAAT3 was diluted to 0.6 mg/mL in assay buffer (50 mM Tris-HCl pH 8, 1 mM CaCl₂, 100 mM NaCl). 50 μ L of protein dilution was added in a dark flat-bottom Greiner 96-well plate and incubated with the LEI110 at different concentrations. 50 μ L of the substrate liposome solution, which was prepared by slowly adding a concentrated solution of the substrate Red/Green Bodipy PC-A2 (2.5 mM in DMSO), DOPC (10 mM in ethanol, Avanti Polar Lipids, Alabaster, AL) and DOPG (10 mM in ethanol, Avanti Polar Lipids, Alabaster, AL) into the assay buffer, was added (Bodipy PC-A2, final concentration: 2.5 μ M) and the fluorescence measurement was started immediately on a TECAN infinite M1000 pro. A standard curve of Bodipy FL C5 (D3834, Invitrogen) was used for evaluating the amount of substrate conversion. LEI110 demonstrated a K_i of 20 nM (95% CI: 17-24 nM) (Figure 2B). The selectivity of LEI110 was profiled in mouse brain membrane and cytosol proteome with probe MB064 and FP-TAMRA, respectively. The results showed that LEI110 was selective over brain serine hydrolases as determined with a gel-based ABPP assay (Figure 2C).

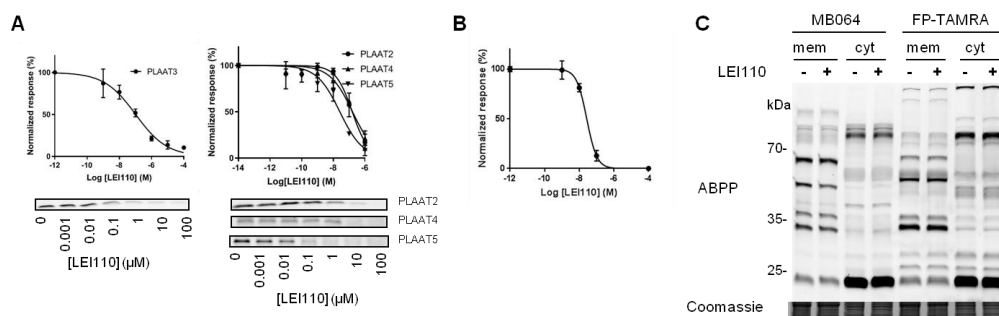


Figure 2. Biochemical characterization of LEI110. (A) Dose-response curves of LEI110 against PLAAT3 and other PLAAT family members with probe MB064. (B) Dose-response curve of LEI110 for PLA2G16 with the PC-A2 fluorescent substrate assay. (C) Selectivity of LEI110 against MB064 (2 μ M) and FP-TAMRA in mouse brain membrane (mem) and cytosol (cyt) proteome. Coomassie staining was used as a protein loading control. – indicates control (with DMSO), + indicates with LEI110 at 10 μ M.

Table 1. $pIC_{50} \pm SEM$ (n = 3) of compound **1** and LEI110 against HRASLS protein family members from the ABPP assay.

Compound	PLAAT3	PLAAT2	PLAAT4	PLAAT5
1	6.0 \pm 0.1	6.2 \pm 0.1	6.2 \pm 0.1	6.4 \pm 0.1
LEI110	7.0 \pm 0.1	6.8 \pm 0.1	6.8 \pm 0.1	7.6 \pm 0.1

PLAAT3 is endogenously expressed in brown and white adipose tissue and its activity could be visualized by MB064 (Figure 3A). Therefore it was decided to test whether compound **1** and LEI110 were able to block PLAAT3 activity in adipose tissue. Indeed,

both compounds completely abolished labeling of native PLAAT3 by MB064, whereas the labeling of other proteins in brown and white adipose tissue was not affected (Figure 3A). The selectivity of LEI110 in adipose tissue was confirmed in a chemical proteomics assay using MB108 (THL-biotin, Figure 3B) and FP-biotin (Figure 3C), respectively (Figure 3D and 3E, respectively). Based on its activity and selectivity profile, it was decided to test LEI110 in a cellular assay to investigate how the PLAAT3 product formation was affected by this inhibitor. To this end, human PLAAT3 was transfected in U2OS cells which were then incubated with vehicle (DMSO) or LEI110 (10 μ M) in serum-free conditions. This led to a time-dependent increase in arachidonic acid, a product of PLAAT3, as determined by targeted lipidomics, which could be almost completely abolished by LEI110 (Figure 3F). Taken together, the results indicate that LEI110 is a potent, selective and cell-permeable PLAAT3 inhibitor.

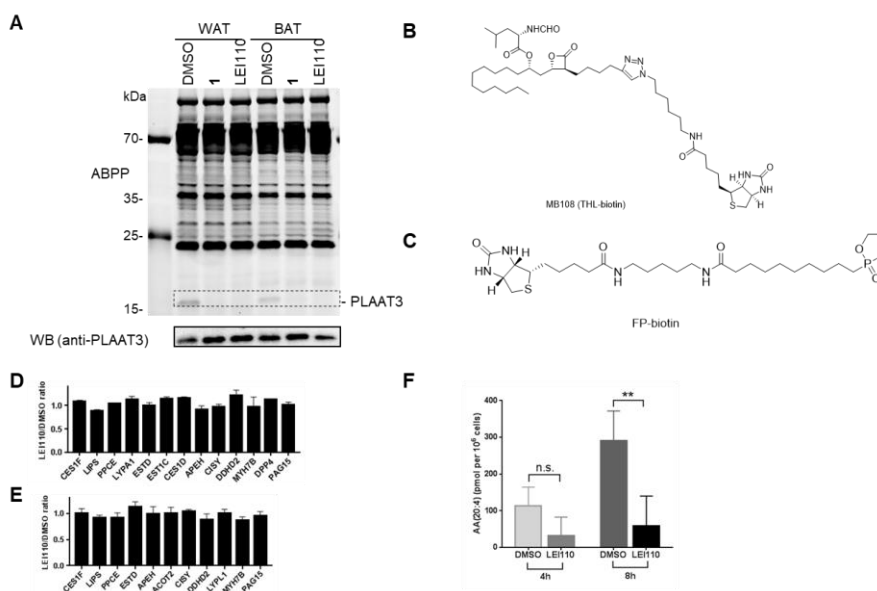


Figure 3. (A) Competitive ABPP of compound **1** and LEI110 against endogenous PLAAT3 using MB064 in the cytosol proteome of mouse WAT and BAT and Western blot of the ABPP gel using an anti-PLAAT3 antibody. Both inhibitors block the activity of PLAAT3 at 10 μ M. (B) Chemical structure of MB108 (THL-biotin). (C) Chemical structure of FP-biotin. (D) MB108 and FP-biotin based chemoproteomic analysis of serine hydrolase activities in the mouse WAT cytosol proteome treated with LEI110 (10 μ M). (E) MB108 and FP-biotin based chemoproteomic analysis of serine hydrolase activities in the mouse BAT cytosol proteome treated with LEI110 (10 μ M). (F) *In situ* treatment of U2OS cells overexpressing PLAAT3 with LEI110 (10 μ M, 4 h or 8 h) reduced arachidonic acid (AA) levels that were induced by PLAAT3.

Genetic studies have previously demonstrated that PLAAT3 regulates lipolysis;^{3, 4} therefore it was decided to test LEI110 phenotypic assay with human hepatocytes.

Stimulation of HepG2 cells with oleic acid induces steatosis that eventually results in lipid droplet formation, as visualized by Adipored, which is a widely used *in vitro* model to study fatty liver disease.^{5, 6} Since PLAAT3 activity could not be visualized in HepG2 cells using the ABPP method which was described in **chapter 2** and this may be probably due to its low abundance, a quantitative RT-PCR method was used to confirm PLAAT3 mRNA expression in HepG2 cells (Table 2). Of note, relatively high level of mRNA for PLAAT3 (Ct value: 24.1) was found when compared to PLAAT1 (Ct value: 34.0), PLAAT2 (Ct value: 32.3) and PLAAT4 (Ct value: 30.8). In addition, the selectivity of LEI110 in HepG2 cells was confirmed in a chemical proteomics assay with MB108 and FP-biotin (Figure 4A). Next, HepG2 cells were incubated with LEI110 (10 μ M) before oleic acid treatment and a reduction in lipid droplet formation was observed, which indicates that LEI110 modulates lipolysis (Figure 4B). This is in line with previous reports showing that PLAAT3 modulates lipid metabolism in HepG2 cells or adipocytes.^{3, 7}

Table 2. Summary table of the Ct values in qPCR analysis for different *HRASLS*-gene detection in HepG2 cells (*GAPDH* as the house-keeping gene)

Gene name	<i>GAPDH</i>	<i>PLAAT1</i>	<i>PLAAT2</i>	<i>PLAAT3</i>	<i>PLAAT4</i>	<i>PLAAT5</i>
Ct values	15.0 \pm 0.3	34.0 \pm 0.3	32.2 \pm 0.5	24.1 \pm 0.4	30.8 \pm 0.4	n.d.*

* n.d. indicates not determined

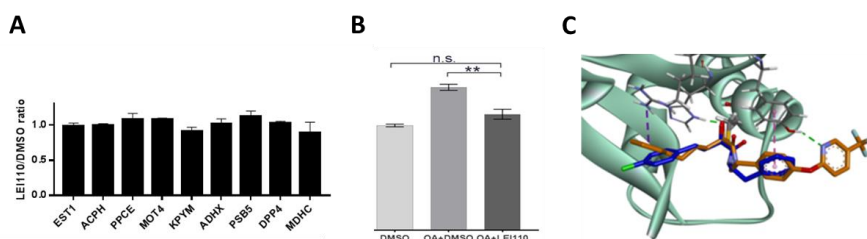


Figure 4. Biochemical characterization of compound LEI110. (A) MB108 and FP-biotin based chemoproteomic analysis of serine hydrolase activities in HepG2 cell lysate proteome treated with LEI110 (10 μ M). (B) *In situ* treatment of HepG2 cells with LEI110 (10 μ M, 24 h) reversed the lipid accumulation in the cells induced by oleic acid (OA, 100 μ M, 24 h). (C) Structure-guided modelling of **1** and LEI110. Compounds **1** (blue) and LEI110 (orange) in complex with PLAAT3, covalently bound to Cys113. Green dotted lines represent a hydrogen bond, pink and purple represent π -interactions. Data represent mean values \pm SEM for at least 3 replicates. *, $p < 0.05$, **, $p < 0.01$, ***, $p < 0.001$ using Student's t-test.

4.3 Conclusions

In summary, here it was shown that LEI110, a potent PLAAT3 inhibitor ($K_i = 20$ nM), reduces cellular arachidonic acid levels in PLAAT3-overexpressing U2OS cells and oleic acid-induced steatosis in human HepG2 cells. Gel-based ABPP and chemical proteomics showed that LEI110 is a selective pan-inhibitor of the HRASLS-family of thiol hydrolases (i.e. PLAAT2, PLAAT3 and PLAAT5). α -Ketoamides have previously been employed as pharmacophore for the inhibition of hydrolases⁸⁻¹⁰ and are incorporated in marketed drugs for the treatment of the viral infection with hepatitis C (e.g., boceprevir);^{11, 12} therefore, it is anticipated that LEI110 constitutes an excellent starting point for the structure-based drug development of novel molecular therapies for obesity and/or common cold.

4.4 Experimental procedures

Plasmids. Full-length human cDNA of PLAAT3, A-C1, PLAAT2, PLAAT4 and PLAAT5 (from Prof. N. Ueda's lab) were cloned into mammalian expression vector pcDNA3.1, containing genes for ampicillin and neomycin resistance. The inserts were cloned in frame with a C-terminal FLAG-tag. Two-step PCR mutagenesis was performed to substitute the active site cysteine for an alanine (A) or serine (S) in the PLAAT3-FLAG, PLAAT2, PLAAT4 and PLAAT5, respectively to obtain the corresponding mutants. Plasmids were isolated from transformed XL-10 Goldcompetent cells (Maxi Prep kit: Qiagen) and sequenced at Macrogen. Sequences were analyzed and verified (CLC Main Workbench).

Cell culture

General. HEK293T, U2OS and HepG2 cells were kept in culture at 37 °C under 7% CO₂ in DMEM containing phenol red, stable glutamine, 10% (v/v) New Born Calf Serum (Thermo Fisher), and penicillin and streptomycin (200 µg/mL each; Duchefa). Medium was refreshed every 2-3 days and cells were passaged twice a week at 80-90% confluence. Cells lines were purchased from ATCC and were regularly tested for mycoplasma contamination.

Transient transfection. Transient transfection was performed as previously described.¹³ In brief, HEK293T cells were seeded in 15-cm petri dishes one day prior to transfection. Prior to transfection, culture medium was aspirated and a minimal amount of medium was added. A 3:1 (m/m) mixture of polyethyleneimine (PEI, 1 mg/mL) (60 µg/15-cm dish) and plasmid DNA (20 µg/dish) was prepared in serum free culture medium and incubated for 15 min at RT. Transfection was performed by dropwise addition of the PEI/DNA mixture to the cells. Transfection with the empty pcDNA3.1 vector was used to generate control samples (mock groups). After 24 h, medium was refreshed. Medium was aspirated 72 h post-transfection and cells were harvested by resuspension in PBS. Cells were pelleted by centrifugation (5 min, 1,000 g) and the pellet was washed with PBS. Supernatant was discarded and cell pellets were snap-frozen in liquid nitrogen and stored at -80 °C until sample preparation.

For Figure 3F, a slightly altered procedure and a different cell line was used: one day prior to transfection, U2OS cells were seeded in 6-cm dishes. After 24 h, a mixture of polyethyleneimine (PEI, 1 mg/mL) (8 µg/6-cm dish) and plasmid DNA (2.7 µg/dish) were incubated in serum free culture medium (15 min, RT), and then added dropwise to the cells. After 24 h, medium was aspirated and cells were washed once with serum free medium. New serum free medium supplemented with DMSO (final concentration 0.1%,

v/v) or LEI110 (final concentration: 10 μ M) were added in the dishes. After 4 or 8 h incubation at 37 °C under 7% CO₂, cells were harvested for lipidomics analysis.

In situ treatment on HepG2 cells. For Figure 3E, a liver hepatocellular carcinoma cell line HepG2 cells was used. One day prior to treatment, HepG2 cells were seeded in a 48-well plate. After 24 h, the medium was aspirated and cells were treated with 100 μ M oleic acid (OA) or DMSO in the absence or presence of LEI110 (final concentration: 10 μ M). After 24 h, medium was aspirated and cells were washed once with PBS, then AdipoRed Assay Reagent (3% in PBS, PT-7009, Lonza) was added. After 10 min, place the plate in the fluorimeter (Tecan infinite M1000 pro), and measure the fluorescence in a 3 x 3 grid with excitation at 485 nm and emission at 572 nm.

Sample preparation

Cell membrane and cytosol proteome preparation. Cell pellets were thawed on ice, resuspended in cold lysis buffer (50 mM Tris-HCl pH 8, 2 mM DTT, 1 mM MgCl₂, 2.5 U/mL benzonase) and incubated on ice (30 min). The cell lysate was collected and centrifuged (100.000 g, 45 min, 4 °C, Beckman Coulter, Ti 70.1 rotor). The supernatant was collected (cytosolic fraction) and the membrane pellet was resuspended in cold storage buffer (50 mM Tris HCl, pH 8, 2 mM DTT) by thorough pipetting and passage through an insulin needle (29G). Protein concentrations were determined by a Quick Start™ Bradford Protein Assay or Qubit™ protein assay (Invitrogen). Samples were flash frozen in liquid nitrogen and stored at -80 °C until further use.

Mouse tissue proteome preparation. Mouse brains (C57Bl6) were isolated according to guidelines approved by the ethical committee of Leiden University (DEC#13191), frozen in liquid nitrogen, and stored at -80 °C until use. Tissues were thawed on ice, dounce homogenized in cold lysis buffer (50 mM Tris HCl, pH 8, 2 mM DTT, 1 mM MgCl₂, 2.5 U/mL benzonase) and incubated on ice (15 min), followed by low-speed centrifugation (2500 g, 3 min, 4°C) to remove debris. After high-speed centrifugation (100.000 g, 45 min, 4°C) the supernatant was collected as the cytosol proteome, flash frozen in liquid nitrogen and stored at -80 °C for further use.

Mouse white or brown adipose tissue (C57Bl6) were isolated according to guidelines approved by the ethical committee of Leiden University (DEC#13191) and were immediately dounce homogenized in cold lysis buffer, followed by low-speed spin (2500 g, 3 min, 4°C) to remove the debris. The membrane and cytosol proteome were prepared followed by the same procedure as for the mouse brains described above.

Activity based protein profiling on transiently transfected HEK293T cell lysate. Gel-based activity based protein profiling (ABPP) was performed with minor alterations of

the previously reported protocol.¹³ For ABPP assays on HEK293T cells overexpressing PLAAT3, the cytosol proteome (0.5 mg/mL, 20 μ L) was pre-incubated with vehicle (DMSO) or inhibitor (0.5 μ L in DMSO, 30 min, RT) followed by an incubation with the activity based probe MB064 (final concentration: 250 nM, 20 min, RT). The incubation protocols for HRASLS2, RARRES3 and iNAT were similar except for the protein concentration (0.25 mg/mL, 1 mg/mL, 1 mg/mL, respectively) and probe concentration (250 nM, 500 nM, 500 nM). Final concentrations for the inhibitors are indicated in the main text and figure legends. Only cytosol proteome was used for the dose-response test in ABPP or substrate assay. Reactions were quenched with 7 μ L of 4x Laemmli buffer (5 μ L, 240 mM Tris (pH 6.8), 8% (w/v) SDS, 40% (v/v) glycerol, 5% (v/v) β -mercaptoethanol, 0.04% (v/v) bromophenol blue). 10 μ L sample per reaction was resolved on a 10% or 15% acrylamide SDS-PAGE gel (180 V, 70 min). Gels were scanned using a ChemiDoc MP system with Cy3 and Cy5 multichannel settings (605/50 and 695/55, filters respectively) and stained with Coomassie after scanning. Experiments were done 3 times individually. Fluorescence was normalized to Coomassie staining and quantified with Image Lab (Bio-Rad). IC₅₀ curves were fitted with Graphpad Prism[®] 7 (Graphpad Software Inc.).

Activity based protein profiling on mouse brain proteome. Mouse brain membrane or cytosol proteome (2 mg/mL, 20 μ L) was incubated with vehicle (DMSO) or inhibitor (0.5 μ L in DMSO, 30 min, RT) followed by an incubation with the activity based probe MB064 (final concentration: 500 nM, 20 min, RT) or FP-TAMRA (Thermo Fisher, 88318, final concentration: 500 nM, 20min, RT). The reaction was quenched with 7 μ L of 4x Laemmli buffer and the proteins were resolved and visualized using the same procedures as for the transfected HEK293T cells.

Activity based protein profiling on mouse adipose tissue. Brown or white adipose tissue cytosol proteome (1 mg/mL, 20 μ L) was incubated with vehicle (DMSO) or inhibitor (0.5 μ L in DMSO, 30 min, RT) followed by an incubation with the activity based probe MB064 (final concentration: 2 μ M, 20 min, RT). The reaction was quenched with 7 μ L of 4x Laemmli buffer and the proteins were resolved and visualized using the same procedures as for the transfected HEK293T cells.

Western Blot. Western blots were performed as previously reported.⁷ After the ABPP assay, the proteins on the SDS-PAGE gel were transferred to a PVDF membrane using a Trans-Blot Turbo™ Transfer system (Bio-Rad). For anti-FLAG antibody, membranes were washed with TBS (50 mM Tris, 150 mM NaCl) and blocked with 5% milk in TBST (50 mM Tris, 150 mM NaCl, 0.05% Tween 20) for 1 h at RT (anti-FLAG antibody) or overnight at 4 °C (for anti-PLAAT3 antibody). Membranes were then incubated with primary antibody in 5% milk TBST for 1 h at RT, washed with TBST, incubated with matching secondary antibody in 5% milk TBST for 1 h at RT and subsequently washed with TBST and TBS. The

blot was developed in the dark using an imaging solution (10 mL luminal solution, 100 μ L ECL enhancer and 3 μ L 30% H_2O_2). Chemiluminescence was visualized using a ChemiDoc MP (BioRad) with standard chemiluminescence settings. For anti-PLAAT3 antibody, the protocol was similar except that PBS or PBST were used as the washing buffer and blocking buffer instead of TBS or TBST, respectively.

Primary antibodies: monoclonal mouse-anti-PLAAT3 (1:200, Abnova, H00011145-M02), monoclonal mouse-anti-FLAG (1:5000, Sigma Aldrich, F3156). Secondary antibodies: HRP-coupled-goat-anti-mouse (1:5000, Santa Cruz, sc2005).

qPCR. For the qPCR experiments, NucleoSpin[®] RNA kit (Macherey-Nagel) was used for the total RNA isolation, the transcriptase (Thermo Scientific Maxima Reverse Transcriptase) was used for cDNA synthesis and the 2x SYBR Green qPCR Master (Bimake) was used for qPCR following the manufacturer's protocols. Primers used were listed in the supplementary figures. The experiment was carried out in duplicate and repeated twice.

Fluorescent substrate assay. The fluorescent substrate assay was based on a previously reported method.¹⁴ Liposomes were prepared by slowly injecting a concentrated solution of the substrate Red/Green Bodipy PC-A2 (2.5 mM, in DMSO, Invitrogen, A10072), DOPC (10 mM in ethanol, Avanti Polar Lipids, Alabaster, AL) and DOPG (10mM in ethanol, Avanti Polar Lipids, Alabaster, AL) into the assay buffer (50 mM Tris-HCl pH 8, 1 mM $CaCl_2$, 100 mM NaCl).

Relevant concentrations of compounds are prepared in DMSO. The cytosolic protein fraction of HEK293T cells transiently overexpressing PLAAT3 was diluted to 0.6 mg/mL in assay buffer. 50 μ L of protein dilution was added in a dark flat-bottom Greiner 96-well plate and incubated with the compounds or vehicle for 30 min at RT. A sample with mock transfected cytosolic protein lysate incubated with DMSO was incorporated for background subtraction. 50 μ L of the substrate liposome solution was added (Bodipy PC-A2, final concentration: 2.5 μ M) and the fluorescence measurement was started immediately on a TECAN infinite M1000 pro (37 °C, continuous scanning for 1 h; excitation 488 nm, emission 530 nm). A standard curve of Bodipy FL C5 (D3834, Invitrogen) (the cleavage product of Bodipy PC-A2) was used for evaluating the amount of substrate conversion). The enzyme activity rates were calculated from the steady-state measured in the first 10 min of the reaction. The assay was carried out in duplicate and repeated twice. The data were corrected by the background of mock lysate, normalized by the residual protein activity at 100 % and then evaluated using GraphPad Prism[®] 7.

Targeted lipidomics

Targeted lipidomics was performed as described previously with minor modifications.^{7, 15} In brief, lipids were extracted using liquid-liquid extraction method (MTBE: Methyl *tert*-butyl ether) from *in situ* treated U2OS cells (hPLAAT3-construct transiently expressed, 4 or 8 h, 10 μ M LEI110 or vehicle (0.1% DMSO) treatment). The resulting samples are separated and quantified using LC-MS/MS platform.

Activity-based proteomics

Activity-based proteomics was performed based on previously described procedures.^{16, 17} In summary, mouse adipose tissue cytosol proteome or HepG2 cell cytosol proteome (250 μ L at 1.0 mg/mL) was incubated with vehicle (2% DMSO) or inhibitor (LEI110, 10 μ M, 30 min, RT). The heat-inactivated proteome were used for background correction. The proteomes were then labeled with MB108 (THL-biotin) or FP-Biotin (sc-215056A, 10 μ M, 20 min, RT), enriched using avidin (pulldown) and on-bead digestion. The resulting peptides are measured, identified and quantified by LC-MS/MS.

Statistical methods

All data are shown as the mean \pm SEM where applicable. A Student's t-test (unpaired, two-tailed) was used to determine differences between two groups. All statistical analyses were conducted using Excel or GraphPad Prism version 7, and a p-value less than 0.05 was considered significant throughout unless indicated otherwise.

A sample size of $n = 3$ was sufficient to detect $\geq 50\%$ inhibition of protein labeling with a 20% standard deviation and a power of 80% at a $p < 0.05$. Routinely, a protein is considered to be an off-target, if 50% inhibition of activity is reached at 10 μ M.

4.5. References

1. Uyama, T.; Kawai, K.; Kono, N.; Watanabe, M.; Tsuboi, K.; Inoue, T.; Araki, N.; Arai, H.; Ueda, N., Interaction of phospholipase A/acyltransferase-3 with Pex19p: a possible involvement in the down-regulation of peroxisomes. *J. Biol. Chem.* **2015**, *290* (28), 17520-34.
2. Martens, K.; Bottelbergs, A.; Peeters, A.; Jacobs, F.; Espeel, M.; Carmeliet, P.; Van Veldhoven, P. P.; Baes, M., Peroxisome deficient aP2-Pex5 knockout mice display impaired white adipocyte and muscle function concomitant with reduced adrenergic tone. *Mol. Genet. Metab.* **2012**, *107* (4), 735-47.
3. Jaworski, K.; Ahmadian, M.; Duncan, R. E.; Sarkadi-Nagy, E.; Varady, K. A.; Hellerstein, M. K.; Lee, H.-Y.; Samuel, V. T.; Shulman, G. I.; Kim, K.-H.; de Val, S.; Kang, C.; Sul, H. S., AdPLA ablation increases lipolysis and prevents obesity induced by high-fat feeding or leptin deficiency. *Nat. Med.* **2009**, *15*, 159.
4. Tsai, F. M.; Chen, M. L.; Wang, L. K.; Lee, M. C., H-rev107 regulates cytochrome P450 reductase activity and increases lipid accumulation. *PLoS One* **2015**, *10* (9).
5. Gibbons, G. F.; Khurana, R.; Odwell, A.; Seelaender, M. C. L., Lipid balance in HepG2 cells - active synthesis and impaired mobilization. *J. Lipid Res.* **1994**, *35* (10), 1801-1808.
6. Park, J. Y.; Kim, Y.; Im, J. A.; Lee, H., Oligonol suppresses lipid accumulation and improves insulin resistance in a palmitate-induced in HepG2 hepatocytes as a cellular steatosis model. *BMC Complem.. Altern. M.* **2015**, *15*.
7. van Esbroeck, A. C. M.; Janssen, A. P. A.; Cognetta, A. B.; Ogasawara, D.; Shpak, G.; van der Kroeg, M.; Kantae, V.; Baggelaar, M. P.; de Vrij, F. M. S.; Deng, H.; Allara, M.; Fezza, F.; Lin, Z.; van der Wel, T.; Soethoudt, M.; Mock, E. D.; den Dulk, H.; Baak, I. L.; Florea, B. I.; Hendriks, G.; de Petrocellis, L.; Overkleeft, H. S.; Hankemeier, T.; De Zeeuw, C. I.; Di Marzo, V.; Maccarrone, M.; Cravatt, B. F.; Kushner, S. A.; van der Stelt, M., Activity-based protein profiling reveals off-target proteins of the FAAH inhibitor BIA 10-2474. *Science* **2017**, *356* (6342), 1084-1087.
8. Yuan, W.; Wong, C. H.; Haeggstroem, J. Z.; Wetterholm, A.; Samuelsson, B., Novel tight-binding inhibitors of leukotriene A4 hydrolase. *J. Am. Chem. Soc.* **1992**, *114* (16), 6552-6553.
9. Patel, D. F., (CA, US), Gless, Richard D. (Oakland, CA, US), Hsu, Heather Webb K. (San Francisco, CA, US), Anandan, Sampath Kumar (Fremont, CA, US), Aavula, Bhaskar R. (Pleasanton, CA, US) Soluble epoxide hydrolase inhibitors. **2008**.
10. Shen, H. C., Soluble epoxide hydrolase inhibitors: a patent review. *Expert Opin. Ther. Patents* **2010**, *20* (7), 941-956.
11. Ascione, A., Boceprevir in chronic hepatitis C infection: a perspective review. *Ther. Adv. Chronic Dis.* **2012**, *3* (3), 113-121.
12. Butt, A. A.; Kanwal, F., Boceprevir and telaprevir in the management of hepatitis C virus-infected patients. *Clin. Infect. Dis.* **2012**, *54* (1), 96-104.

13. Baggelaar, M. P.; Janssen, F. J.; van Esbroeck, A. C. M.; den Dulk, H.; Allara, M.; Hoogendoorn, S.; McGuire, R.; Florea, B. I.; Meeuwenoord, N.; van den Elst, H.; van der Marel, G. A.; Brouwer, J.; Di Marzo, V.; Overkleeft, H. S.; van der Stelt, M., Development of an activity-based probe and in silico design reveal highly selective inhibitors for diacylglycerol lipase- α in brain. *Angew. Chem.-Int. Edit.* **2013**, *52* (46), 12081-12085.
14. Pang, X. Y.; Cao, J.; Addington, L.; Lovell, S.; Battaile, K. P.; Zhang, N.; Rao, J. L.; Dennis, E. A.; Moise, A. R., Structure/function relationships of adipose phospholipase A2 containing a cys-his-his catalytic triad. *J. Biol. Chem.* **2012**, *287* (42), 35260-74.
15. Kantae, V.; Nahon, K. J.; Straat, M. E.; Bakker, L. E. H.; Harms, A. C.; van der Stelt, M.; Hankemeier, T.; Jazet, I. M.; Boon, M. R.; Rensen, P. C. N., Endocannabinoid tone is higher in healthy lean South Asian than white Caucasian men. *Sci. Rep.* **2017**, *7* (1), 7558.
16. Baggelaar, M. P.; Chameau, P. J. P.; Kantae, V.; Hummel, J.; Hsu, K. L.; Janssen, F.; van der Wel, T.; Soethoudt, M.; Deng, H.; den Dulk, H.; Allara, M.; Florea, B. I.; Di Marzo, V.; Wadman, W. J.; Kruse, C. G.; Overkleeft, H. S.; Hankemeier, T.; Werkman, T. R.; Cravatt, B. F.; van der Stelt, M., Highly selective, reversible inhibitor identified by comparative chemoproteomics modulates diacylglycerol lipase activity inneurons. *J. Am. Chem. Soc.* **2015**, *137* (27), 8851-8857.
17. van Rooden, E. J.; Florea, B. I.; Deng, H.; Baggelaar, M. P.; van Esbroeck, A. C. M.; Zhou, J.; Overkleeft, H. S.; van der Stelt, M., Mapping in vivo target interaction profiles of covalent inhibitors using chemical proteomics with label-free quantification. *Nat. Protoc.* **2018**, *13* (4), 752-767.

4.6 Supporting Information

Table S1. Summary table of the primers used for the qPCR analysis with their corresponding gene names.

Accession Number	Gene name	Forward(5'–3')	Reverse (5'–3')
XM_011544751	<i>HRASL5</i>	GTTCCGTCCTGGCTATCAGC	CTGCATTTTCACCAGGGCCT
XM_011545120	<i>HRASL2</i>	GAGACTTGGAGACCTGATTGA	GCTTGTTATTGACCCTGTAG
XM_006718426	<i>PLA2G16</i>	AGCGAAATCGAGCCTGG	CCAGATGAACCACATATCCA
NM_004585	<i>RARRES3</i>	AGCTGATCCACAACAAGAG	CCAGATGGATCACGTAGCCA
XM_011544751	<i>HRASL5</i>	AATTGGCTATGAGCACTGG	AGACGACTGTATTTCAACCAC

5

**Development of a PLA2G4E assay and subsequent application
in hit identification**

5.1 Introduction

In 1996, Piomelli and coworkers characterized the Ca^{2+} -dependent biosynthesis of *N*-acylphosphatidylethanolamines (NAPE) in cortical neurons and rat brain tissue.^{1, 2} The enzyme responsible for the Ca^{2+} -dependent formation of NAPEs remained elusive until Cravatt and colleagues showed that PLA2G4E (also known as cPLA₂ε) was able to transfer an acyl chain from the *sn*-1 position of phosphatidylcholine (PC) to the amine of phosphatidylethanolamine (PE), thereby effectively producing NAPEs.³

PLA2G4E was previously discovered in a comprehensive homology search against murine genome and EST databases and annotated as a phospholipase A (PLA).⁴ It belongs to the cytosolic phospholipase A2 group IV (PLA2G4) proteins, a subfamily from the PLA2 proteins, which catalyze the hydrolysis of the *sn*-2 acyl bond of phospholipids, thereby releasing fatty acids. This leads to a cascade of lipid second messengers, which regulates a wide variety of physiological responses and plays an important role in diseases, such as cancer.⁵ There are six members in this protein family, namely PLA2G4A, PLA2G4B, PLA2G4C, PLA2G4D, PLA2G4E and PLA2G4F. These proteins are structurally similar. They all contain a N-terminal C2 domain (except PLA2G4C) and a C-terminal catalytic domain. The C2 domain has a binding site for intracellular Ca^{2+} . When calcium ions bind, the protein is transported from the cytosol to the Golgi membrane, which is needed for catalytic activity.⁶ The catalytic pocket contains a Ser/Asp dyad which lays in the α/β hydrolase fold.^{6, 7} In contrast to the other family members, PLA2G4E has a strong preference for catalyzing the *N*-acyltransferase reactions over phospholipid hydrolysis.

PLA2G4E has high mRNA expression levels in heart, skeletal muscle, testis and thyroid and low expression in brain and stomach. PLA2G4E was previously found to play an important role within the clathrin-independent transport pathway, which is involved in the uptake and recycling of cargo proteins, such as MHC-I.⁸ Two isoforms of human PLA2G4E (hPLA2G4E-A and hPLA2G4E-B) have been identified. Their activity is potently stimulated by phosphatidylserine (PS).⁹ Endogenous PS and other anionic phospholipids (such as phosphatidic acid and phosphatidylinositol 4,5-bisphosphate) affect the localization and enzyme activity of PLA2G4E.¹⁰ Currently, there are no inhibitors of PLA2G4E available that could help to elucidate the biological role of PLA2G4E. In this chapter, competitive activity based protein profiling (ABPP) is used to identify the first inhibitors of PLA2G4E.

5.2 Results and discussion

To test whether the fluorescently labeled fluorophosphonate probe TAMRA-FP could be used in a competitive ABPP experiment, TAMRA-FP was incubated with the membrane fraction of human embryonic kidney 293T (HEK293T) cells that transiently overexpressed human PLA2G4E fused to a FLAG-tag. Resolving the proteins by sodium dodecyl sulfate polyacrylamide gel

electrophoresis (SDS-PAGE) and in-gel fluorescent scanning revealed a fluorescent band at the expected MW, which overlapped with a band visualized by the FLAG-tag antibody. This band was absent in mock-transfected cells (Figure 2A, left). The labeling was dependent on both the probe and protein concentration (Figure 2A, right panels). A protein concentration of 0.25 $\mu\text{g}/\mu\text{L}$ and probe concentration of 0.05 μM were chosen as the optimal ABPP conditions. Removal of Ca^{2+} -ions from the incubation buffer resulted in a strong decrease in labeling, thereby confirming the Ca^{2+} -dependency of the enzyme activity (Figure 2B). Fluorescent labeling of the protein was optimal at 3 mM Ca^{2+} and at pH 8.0 (Figure 2C-D). A 5 min incubation was sufficient to generate a robust fluorescent signal. Taken together, these results demonstrated that TAMRA-FP can efficiently label active human PLA2G4E and optimal ABPP assay conditions were found that could be used to identify inhibitors of PLA2G4E.

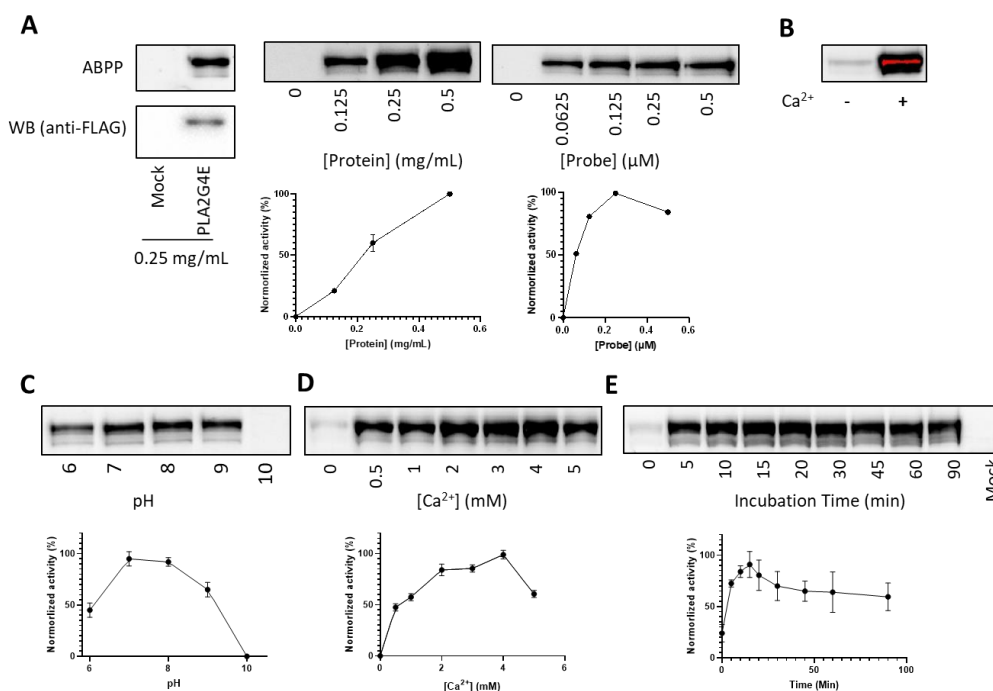


Figure 2. (A) Confirmation of hPLA2G4E overexpression with ABPP and western blot (left) and ABPP labeling of hPLA2G4E with probe TAMRA-FP at different probe or protein concentrations (right) (N=2). For protein concentration optimization 500 nM TAMRA-FP was used. For probe concentration optimization 0.25 mg/mL protein was used. (B) Gel-based ABPP to test the difference in labeling with TAMRA-FP (0.5 μM , 20 min at RT) on the membrane fraction of hPLA2G4E (1 $\mu\text{g}/\mu\text{L}$) overexpression lysate in the presence or absence of calcium (CaCl_2 , 3 mM). (C, D, E) Optimization of ABPP conditions for hPLA2G4E using probe TAMRA-FP. For pH optimization 500 nM TAMRA-FP, 1 mg/mL protein and 3 mM CaCl_2 were used; for Ca^{2+} concentration optimization 500 nM TAMRA-FP and 0.5 mg/mL protein were used; for incubation time optimization 62.5 nM TAMRA-FP, 0.25 mg/mL protein and 3 mM CaCl_2 were used (N=2).

Next, a focused library of 223 compounds¹¹ was screened at 10 μM in a competitive gel-based ABPP format. Compounds that inhibited fluorescent labeling of PLA2G4E over 50% were retested. Eight compounds (**6**, **7**, **8**, **45**, **177**, **180**, **195** and **196**) reduced protein activity by more than 80% and were designated as potential hits (Figure 3; Table 1). These compounds could be divided into two different clusters based on their scaffolds: compounds **45**, **177**, **180**, **195** and **196** belong to the triazoleurea class of inhibitors, whereas compounds **6-8** constitute the bromoenol lactone class.

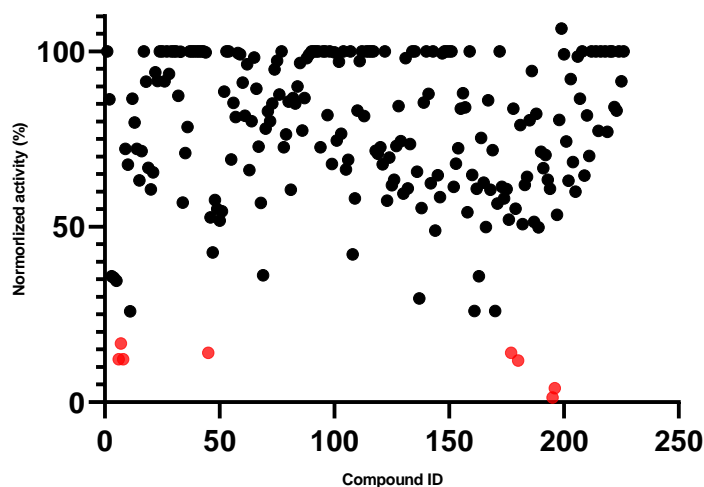
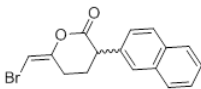
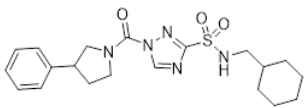
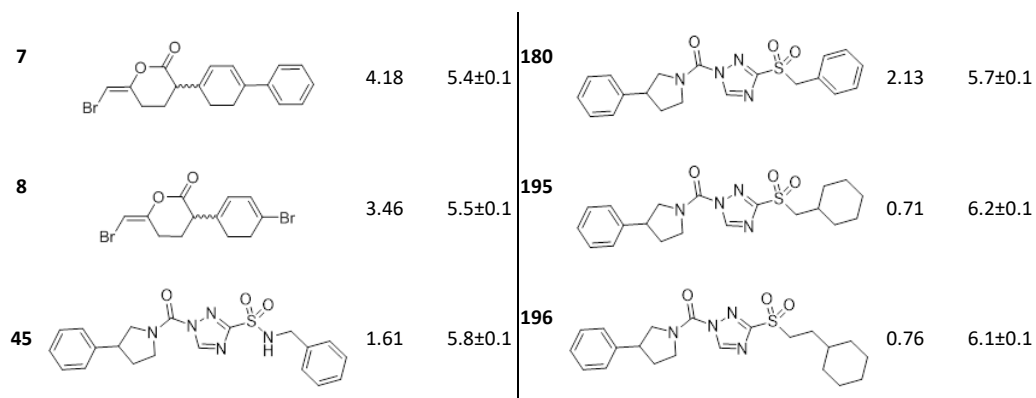


Figure 3. Summary of all tested compounds (10 μM) with corrected residual protein activity of hPLA2G4E (N=1). The data is presented in percentage (%) and lower percentage indicates higher inhibitory activity. The potential hits (>80% inhibition) are highlighted in red.

The compounds showing more than 80% inhibition at 10 μM were tested in a concentration-response manner to determine their IC_{50} values (Table 1). (The IC_{50} curves are shown in Figure S1).

Table 1. The chemical structures, IC_{50} values and pIC_{50} values with standard deviations of 8 inhibitors of hPLA2G4E (N=3).

ID	Structures	IC_{50} (μM)	pIC_{50}	ID	Structures	IC_{50} (μM)	pIC_{50}
6		5.04	5.3 ± 0.1	177		1.56	5.8 ± 0.1



Compound **195** and **196** were the most potent inhibitors with pIC₅₀ values of 6.2 ± 0.1 and 6.1 ± 0.1, respectively. In order to better profile the selectivity of these compounds, not only the most compounds (**195** and **196**) but also compounds from other scaffolds (**6-8** and **45**) were subjected to gel-based ABPP using mouse brain membrane and cytosol proteome (Figure 4).

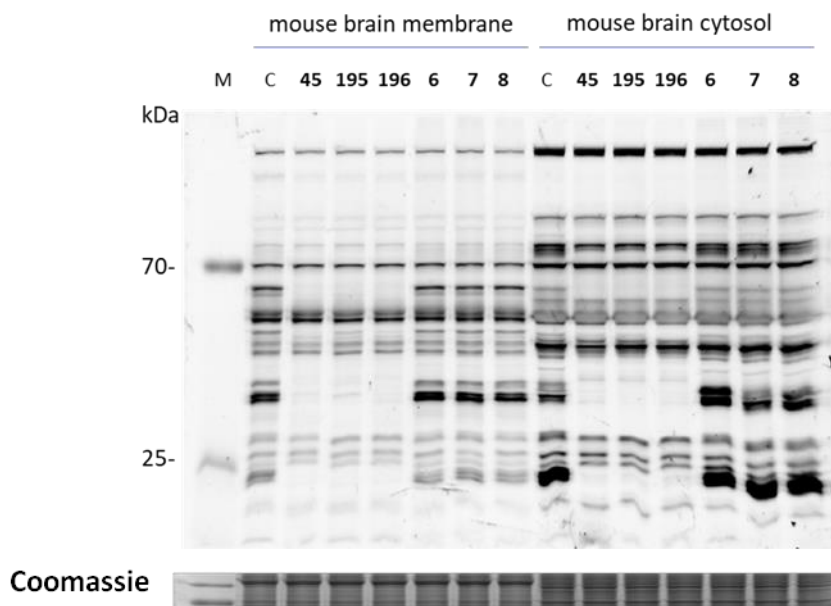


Figure 4. Selectivity of six inhibitors on mouse brain membrane and cytosol. The results of ABPP gel of the inhibitors (10 μM of **6**, **7**, **8**, **45**, **195** and **196**) on mouse brain proteins of the membrane and cytosol (2.5 μg/μL). This is detected by reactions with TAMRA-FP (0.5 μM, 20 min at RT). The samples have been loaded on a 10% SDS-PAGE gel. Coomassie staining was done as protein loading control.

At 10 μM, compounds **45**, **195** and **196** reduced fluorescence labeling of proteins with a MW around 25, 35, 60 and 75 kDa in the mouse brain membrane proteome. Compounds

6-8 showed no off-targets at 10 μM . Of note, compound **6** increases the labeling of a protein at around 35 kDa in the cytosol. Overall, the compounds **6-8** are more selective than compounds **45**, **195** and **196**.

To gain more insight into the selectivity of these compounds over the other proteins of the PLA2G4 family an ABPP method was developed as described above for mouse PLA2G4A-D and human PLA2G4A, C and D. In total, four proteins (mPLA2G4B, hPLA2G4C, mPLA2G4C and mPLA2G4D) could be successfully labeled (Figure 5) (See SI Figure S2 for optimization results).

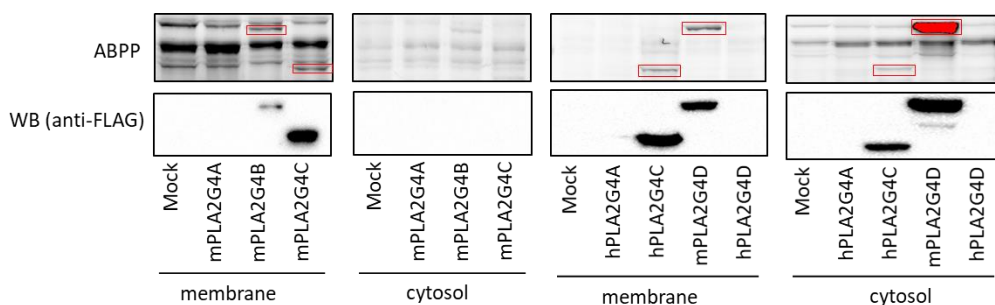


Figure 5. Gel-based ABPP for PLA2G4 protein family members. mPLA2G4B, mPLA2G4C, hPLA2G4C, and mPLA2G4D could be labelled with TAMRA-FP (0.5 μM , 20 min at RT). The samples were loaded on a 10% SDS-PAGE gel. The labeled PLA2G4 proteins are marked with a red box.

Neither of the eight compounds showed any activity on mPLA2G4B and mPLA2G4C (Table S1). Five compounds inhibited mPLA2G4D with more than 80% and were tested in a concentration-response manner (Table 2, inhibition curves in Figure S3). Compounds **6-8** showed submicromolar activity on mPLA2G4D (pIC_{50} : 6.1-6.3), whereas compounds **195** and **196** showed somewhat lower activity ($\text{pIC}_{50} < 6$).

Table 2. pIC_{50} values for the compounds which showed inhibition for mPLA2G4D (N=3).

compound	6	7	8	195	196
$\text{pIC}_{50} + \text{S.D.}$	6.3 ± 0.1	6.3 ± 0.1	6.1 ± 0.1	5.8 ± 0.1	5.8 ± 0.1

5.3 Conclusions

This chapter reported on the discovery of the first inhibitors of PLA2G4E. A competitive, gel-based ABPP method for PLA2G4E using TAMRA-FP was successfully developed and applied to screen a focused library of lipase inhibitors. This resulted in the discovery of two clusters of inhibitors with different scaffolds. The triazoleurea inhibitors were the most potent inhibitors with submicromolar activity, whereas the bromoenol lactone inhibitors were less potent, but more selective as determined by gel-based ABPP using mouse brain proteomes. Optimization of the potency and selectivity of the inhibitors is required to be able to use them to study the biological role of PLA2G4E in an acute and dynamic setting with these novel tools.

5.4 Experimental procedures

Plasmids. Full-length human cDNA of PLA2G4A, C-E, and mouse cDNA of PLA2G4A-D were cloned into mammalian expression vector pcDNA3.1, containing genes for ampicillin and neomycin resistance. The inserts were cloned in frame with a C-terminal FLAG-tag and site-directed mutagenesis was used to remove restriction sites by silent point mutations. Plasmids were isolated from transformed XL-10 Z-competent cells (Maxi Prep kit: Qiagen) and sequenced at the Leiden Genome Technology Center. Sequences were analyzed and verified (CLC Main Workbench).

Cell culture

General. HEK293T cells were kept in culture at 37 °C under 7% CO₂ in DMEM containing phenol red, stable glutamine, 10% (v/v) New Born Calf Serum (Thermo Fisher), and penicillin and streptomycin (200 µg/mL each; Duchefa). Medium was refreshed every 2-3 days and cells were passaged twice a week at 80-90% confluence. Cell lines were purchased from ATCC and were regularly tested for mycoplasma contamination.

Transient transfection. Transient transfection was performed as previously described.¹² In brief, HEK293T cells were seeded in 15-cm petri dishes one day prior to transfection. Prior to transfection, culture medium was aspirated and a minimal amount of medium was added. A 3:1 (m/m) mixture of polyethyleneimine (PEI, 1 mg/mL) (60 µg/15-cm dish) and plasmid DNA (20 µg/dish) was prepared in serum free culture medium and incubated for 15 min at RT. Transfection was performed by dropwise addition of the PEI/DNA mixture to the cells. Transfection with the empty pcDNA3.1 vector was used to generate control samples (mock groups). After 24 h, medium was refreshed. Medium was aspirated 72 h post-transfection and cells were harvested by resuspension in PBS. Cells were pelleted by centrifugation (5 min, 1,000 × *g*) and the pellet was washed with PBS. Supernatant was discarded and cell pellets were snap-frozen in liquid nitrogen and stored at -80 °C until sample preparation.

Sample preparation

Cell membrane and cytosol proteome preparation. Cell pellets were thawed on ice, resuspended in cold lysis buffer (50 mM Tris HCl, pH 8, 2 mM DTT, 1 mM MgCl₂, 25 U/mL benzonase) and incubated on ice (30 min). The cell lysate was collected and centrifuged (100,000 × *g*, 45 min, 4 °C, Beckman Coulter, Ti 70.1 rotor). The supernatant was collected (cytosolic fraction) and the pellet (membrane fraction) was resuspended in cold storage buffer (50 mM Tris HCl, pH 8, 2 mM DTT) by thorough pipetting and passage through an insulin needle (29G). Protein concentrations were determined by a Quick Start™

Bradford Protein Assay or Qubit™ protein assay (Invitrogen). Samples were flash frozen in liquid nitrogen and stored at -80 °C until further use.

Activity based protein profiling on transiently transfected HEK293T cell lysate. Gel-based activity based protein profiling (ABPP) was performed with minor alterations of the previously reported protocol.¹² For ABPP assays on HEK293T cells overexpressing the corresponding PLA2G4 proteins, the cytosol proteome (0.5 mg/mL, 20 µL) was pre-incubated with vehicle (DMSO) or inhibitor (0.5 µL in DMSO, 30 min, RT) followed by an incubation with the activity based probe TAMRA-FP for 5 min (PLA2G4E) or 20 min (PLA2G4A-D). Final concentrations for the inhibitors were indicated in the main text and figure legends. Reactions were quenched with 7 µL of 4x Laemmli buffer (5 µL, 240 mM Tris (pH 6.8), 8% (w/v) SDS, 40% (v/v) glycerol, 5% (v/v) β-mercaptoethanol, 0.04% (v/v) bromophenol blue). 10 µL sample per reaction was resolved on a 10 % or 15% acrylamide SDS-PAGE gel (180 V, 70 min). Gels were scanned using a ChemiDoc MP system with Cy3 and Cy5 multichannel settings (605/50 and 695/55, filters respectively) and stained with Coomassie after scanning. Experiments were done 3 times individually. Fluorescence was normalized to Coomassie staining and quantified with Image Lab (Bio-Rad). IC₅₀ curves were fitted with Graphpad Prism® 7 (Graphpad Software Inc.).

Western Blot. Western blots were performed as previously reported.¹³ After the ABPP assay, the proteins on the SDS-PAGE gel were transferred to a membrane using a Trans-Blot Turbo™ Transfer system (Bio-Rad). For anti-FLAG antibody, Membranes were washed with TBS (50 mM Tris, 150 mM NaCl) and blocked with 5% milk in TBST (50 mM Tris, 150 mM NaCl, 0.05% Tween 20) for 1 h at RT. Membranes were then incubated with primary mouse anti-flag (0.02%) antibody in 5% milk TBST for 1 h at RT, washed with TBST, incubated with matching secondary antibody goat anti-mouse (0.02%) in 5% milk TBST for 1 h at RT and subsequently washed with TBST and TBS. The blot was developed in the dark using an imaging solution (10 mL luminol solution, 100 µL ECL enhancer and 3 µL 30% H₂O₂). Chemiluminescence was visualized using a ChemiDoc XRS (BioRad) with standard chemiluminescence settings.

Primary antibodies: monoclonal mouse-anti-FLAG (1:5000, Sigma Aldrich, F3156).
Secondary antibodies: HRP-coupled-goat-anti-mouse (1:5000, Santa Cruz, sc2005).

5.5 References

1. Cadas, H.; Gailllet, S.; Beltramo, M.; Venance, L.; Piomelli, D., Biosynthesis of an endogenous cannabinoid precursor in neurons and its control by calcium and cAMP. *J. Neurosci.* **1996**, *16* (12), 3934-3942.
2. Cadas, H.; di Tomaso, E.; Piomelli, D., Occurrence and biosynthesis of endogenous cannabinoid precursor, N-arachidonoyl phosphatidylethanolamine, in rat brain. *J. Neurosci.* **1997**, *17* (4), 1226-1242.
3. Ogura, Y.; Parsons, W. H.; Kamat, S. S.; Cravatt, B. F., A calcium-dependent acyltransferase that produces N-acyl phosphatidylethanolamines. *Nat. Chem. Biol.* **2016**, *12* (9), 669-71.
4. Ohto, T.; Uozumi, N.; Hirabayashi, T.; Shimizu, T., Identification of novel cytosolic phospholipase A2s, murine cPLA2 δ , ϵ , and ζ , Which form a gene cluster with cPLA2 β . *J. Biol. Chem.* **2005**, *280* (26), 24576-24583.
5. Lucas, K. K.; Dennis, E. A., Distinguishing phospholipase A2 types in biological samples by employing group-specific assays in the presence of inhibitors. *Prostag. Oth. Lipid M.* **2005**, *77* (1-4), 235-248.
6. Dennis, E. A.; Cao, J.; Hsu, Y. H.; Magrioti, V.; Kokotos, G., Phospholipase A2 enzymes: physical structure, biological function, disease implication, chemical inhibition, and therapeutic intervention. *Chem. Rev.* **2011**, *111* (10), 6130-6185.
7. Ghosh, M.; Tucker, D. E.; Burchett, S. A.; Leslie, C. C., Properties of the Group IV phospholipase A2 family. *Prog. Lipid Res.* **2006**, *45* (6), 487-510.
8. Capestrano, M.; Mariggio, S.; Perinetti, G.; Egorova, A. V.; Iacobacci, S.; Santoro, M.; Di Pentima, A.; Iurisci, C.; Egorov, M. V.; Di Tullio, G.; Buccione, R.; Luini, A.; Polishchuk, R. S., Cytosolic phospholipase A(2)epsilon drives recycling through the clathrin-independent endocytic route. *J. Cell. Sci.* **2014**, *127* (P5), 977-993.
9. Hussain, Z.; Uyama, T.; Kawai, K.; Binte Mustafiz, S. S.; Tsuboi, K.; Araki, N.; Ueda, N., Phosphatidylserine-stimulated production of N-acyl-phosphatidylethanolamines by Ca²⁺-dependent N-acyltransferase. *BBA-Mol. Cell Biol. L.* **2018**, *1863* (5), 493-502.
10. Binte Mustafiz, S. S.; Uyama, T.; Hussain, Z.; Kawai, K.; Tsuboi, K.; Araki, N.; Ueda, N., The role of intracellular anionic phospholipids in the production of N-acyl-phosphatidylethanolamines by cytosolic phospholipase A2 ϵ . *J. Biol. Chem.* **2019**, *165* (4), 343-352.
11. Baggelaar, M. P.; den Dulk, H.; Florea, B. I.; Fazio, D.; Bernabò, N.; Raspa, M.; Janssen, A. P. A.; Scavizzi, F.; Barboni, B.; Overkleeft, H. S.; Maccarrone, M.; van der Stelt, M., ABHD2 Inhibitor identified by activity-based protein profiling reduces acrosome reaction. *ACS Chem. Biol.* **2019**, *14* (10), 2295-2304.

12. Baggelaar, M. P.; Janssen, F. J.; van Esbroeck, A. C. M.; den Dulk, H.; Allara, M.; Hoogendoorn, S.; McGuire, R.; Florea, B. I.; Meeuwenoord, N.; van den Elst, H.; van der Marel, G. A.; Brouwer, J.; Di Marzo, V.; Overkleeft, H. S.; van der Stelt, M., Development of an activity-based probe and in silico design reveal highly selective inhibitors for diacylglycerol lipase-alpha in brain. *Angew. Chem.-Int. Edit.* **2013**, *52* (46), 12081-12085.
13. van Esbroeck, A. C. M.; Janssen, A. P. A.; Cognetta, A. B.; Ogasawara, D.; Shpak, G.; van der Kroeg, M.; Kantae, V.; Baggelaar, M. P.; de Vrij, F. M. S.; Deng, H.; Allara, M.; Fezza, F.; Lin, Z.; van der Wel, T.; Soethoudt, M.; Mock, E. D.; den Dulk, H.; Baak, I. L.; Florea, B. I.; Hendriks, G.; de Petrocellis, L.; Overkleeft, H. S.; Hankemeier, T.; De Zeeuw, C. I.; Di Marzo, V.; Maccarrone, M.; Cravatt, B. F.; Kushner, S. A.; van der Stelt, M., Activity-based protein profiling reveals off-target proteins of the FAAH inhibitor BIA 10-2474. *Science* **2017**, *356* (6342), 1084-1087.

5.6 Supplementary Information

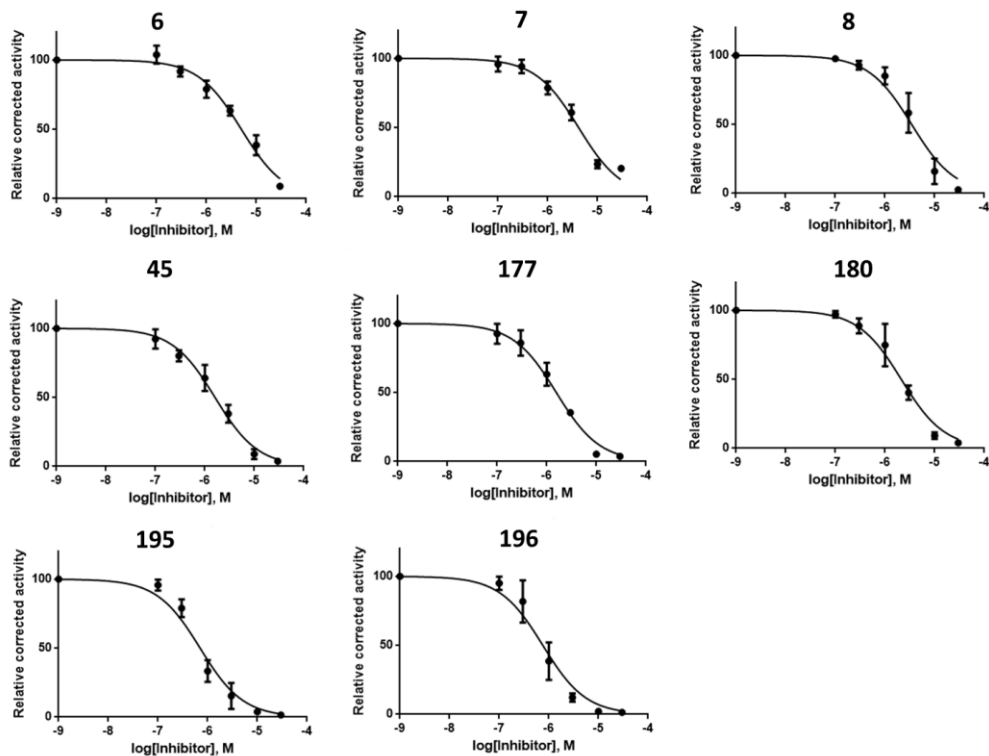


Figure S1. Dose response curves of compounds which have been tested on hPLA2G4E (N=3).

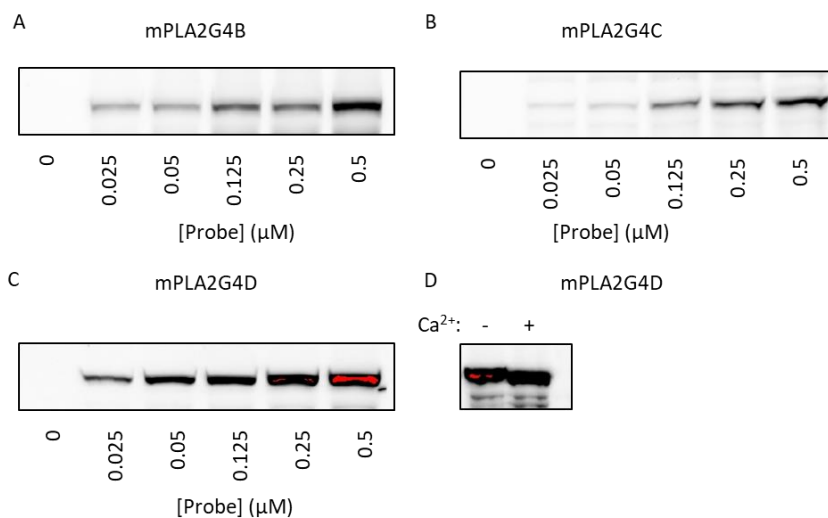


Figure S2. Optimization of ABPP for mPLA2G4B, mPLA2G4C and mPLA2G4D. (A)&(B) Gel-based ABPP for optimization of the TAMRA-FP concentration (0; 0.025; 0.05; 0.125; 0.25; 0.5 μ M, 20 min at RT) for the reaction with the cytosol fraction of mPLA2G4B and mPLA2G4C (1 μ g/ μ L). (C) Gel-based ABPP for the TAMRA-FP concentration (0; 0.0125; 0.025; 0.05; 0.125; 0.25 μ M, 20 min at RT) for the cytosol fraction of mPLA2G4D (0.5 μ g/ μ L). (D) Gel-based ABPP for the difference of with and without calcium (3 mM) on mPLA2G4D (1.0 μ g/ μ L) labelling by TAMRA-FP (0.5 μ M, 20 min at RT). The samples are loaded on a 10% SDS-PAGE gel and Coomassie staining was used for the protein loading correction.

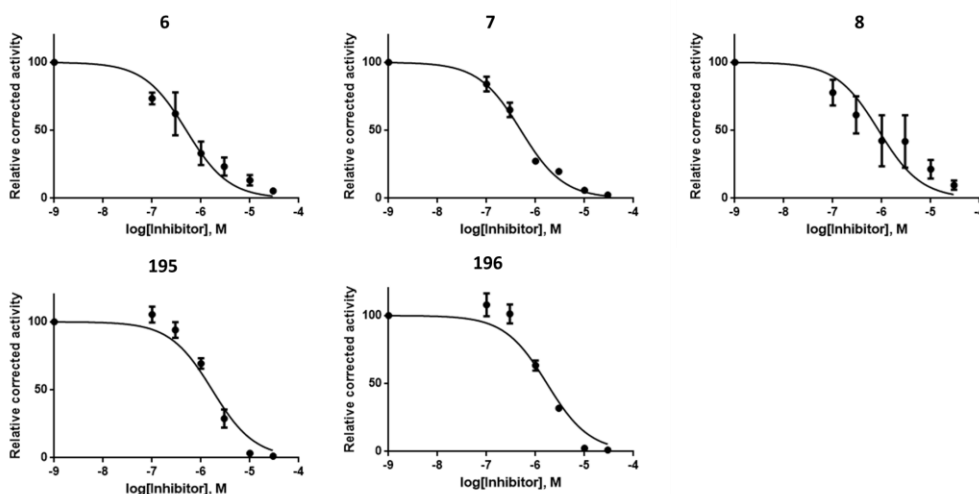


Figure S3. Dose response curves of compounds which have been tested on mPLA2G4D (N=3).

Table S1. Inhibitory activity of selected 8 compounds against mPLA2GB, mPLA2GC and mPLA2GD, respectively, in the gel-based ABPP assay. The data shows the residual protein activity in percentage and lower percentage number indicates high inhibitory activity of the inhibitor at 10 μ M (N=1).

	6	7	8	45	177	180	195	196
mPLA2GB	100	98	90	63	62	60	58	71
mPLA2GC	100	89	82	100	100	100	100	98
mPLA2GD	14	6	12	58	41	28	8	4

6

Summary and future prospects

6.1 Summary

In **Chapter 1**, the endocannabinoid anandamide (*N*-arachidonylethanolamine, AEA) is described as an endogenous ligand capable of activating the cannabinoid receptors. A part from AEA, several other structurally related *N*-Acylethanolamines (NAEs), such as Palmitoylethanolamide (PEA), Oleoylethanolamide (OEA), Stearoylethanolamide (SEA) and Docosahexaenylethanolamide (DHEA), and their biosynthetic pathways were introduced. *N*-acyltransferases (NAT) perform the first rate-limiting step in the biosynthesis of NAEs. There are two classes of NATs: Ca²⁺-dependent NAT (Ca-NAT) and Ca²⁺-independent NATs (PLAAT1-5).¹ Recently, Cravatt and colleagues showed that PLA2G4E (also known as cPLA₂ε) is a Ca-NAT and transfers an acyl chain from the *sn*-1 position of phosphatidylcholine (PC) to the amine of phosphatidylethanolamine (PE), thereby effectively producing NAPEs.² PLA2G4E belongs to the family of cytosolic phospholipase A2 group IV (PLA2G4) proteins, of which there are six members (PLA2G4A, PLA2G4B, PLA2G4C, PLA2G4D, PLA2G4E and PLA2G4F). In contrast to the other family members, PLA2G4E has a strong preference for catalyzing the *N*-acyltransferase reaction over phospholipid hydrolysis.

The human phospholipase A/acyl transferase (PLAAT1-5) family consists of five members (namely, PLA/AT 1-5) of which two are absent in rodents (i.e. PLAAT2 and PLAAT4).^{3,4} They are the protein products of the *Hrasls* genes.⁵ PLAATs possess Ca²⁺ independent phospholipase activity *in vitro* with both phosphatidylcholine (PC) and phosphatidylethanolamine (PE) acting as substrates. All members also exhibit O-acyl transferase activity with preference for the *sn*-1 position of lysophosphatidylcholine (lyso-PC) as well as *N*-acyltransferase activity with the ability to produce *N*-acylphosphatidylethanolamines (NAPEs) through catalysis of the acyl chain transfer from the *sn*-1 position of glycerophospholipids to the amine function of PE.⁴ All enzymes, except PLAAT3, show a preference for PLA1 activity over PLA2 activity. Depending on the assay conditions the substrate preference of PLAAT3 may shift.

Taken together, PLAAT and PLA2G4E are involved in the main biosynthetic pathways of NAEs, which make them highly interesting drug targets when there is a need to manipulate the level of NAEs in a disease-related situation.⁶⁻⁸ The aim of the research described in this thesis focused on the development of activity-based protein profiling assays to identify inhibitors for these enzymes.

In **Chapter 2**, activity-based probe (ABP) MB064, previously developed for monitoring diacylglycerol lipase-α/β activity, was used to profile the activity of PLAAT3 enzyme. MB064 was able to label endogenous PLAAT3 in an activity-dependent manner in brown and white adipose tissue. A small focused library of 50 lipase inhibitors was screen at 10 μM in a competitive ABPP format using recombinant overexpressed protein to discover inhibitors for PLAAT3. This resulted in the discovery of an α-ketoamide (compound **1**) that almost completely inhibited the

activity of PLAAT3 at 10 μM . Compound **1** inhibited also other members of PLAAT family, but was selective over other serine hydrolases.

In **Chapter 3** the hit optimization and structure activity relationships of the α -ketoamide inhibitors are described. It was shown that the α -keto and the substituent on the amide group were crucial for the inhibitory activity. The 3-phenylpropanyl moiety (as depicted in compound **37**) was found to be the optimal fragment as the α -keto substituent. Compounds **49** and **50** were potent and selective inhibitors for PLAAT5, whereas compound **48** and **60** (also named LEI110) were identified as potent and selective inhibitors for PLAAT3 and 5.

In **Chapter 4** the biological profiling of LEI110 is described. LEI110 was found to be a potent, selective and cell permeable inhibitor of PLAAT3. It reduced cellular arachidonic acid levels in PLAAT3 overexpressing U2OS cells and oleic acid-induced steatosis in human HepG2 cells. To gain insight in the molecular interactions of α -ketoamides with PLAAT3, LEI110 and **1** were docked in a PLAAT3 crystal structure. LEI110 and **1** were covalently attached to Cys113 and a molecular dynamics simulation was performed. It was observed that the oxyanion could form a hydrogen bond with His23, as well as π - π stacking with Tyr21. It is anticipated that LEI110 constitutes an excellent starting point for the structure-based drug development of novel molecular therapies for obesity and/or common cold.

Chapter 5 reports on the development of an ABPP assay to profile the activity of PLA2G4E with TAMRA-FP. A library of more than 200 compounds was screened at 10 μM for human PLA2G4E. Eight inhibitors showed less than 20% residual activity of human PLA2G4E. ESC386 and ESC387 were the most potent inhibitors with pIC_{50} values of 6.2 ± 0.1 and 6.1 ± 0.1 , respectively. These compounds represent the first-in-class inhibitors of PLA2G4E and form an excellent starting point for further probe development.

6.2 Future prospects.

Although the competitive gel-based APPP assay was successful in the identification of novel inhibitors for PLAAT2-5⁹ and PLA2G4E, it cannot be used for high throughput screening. In a classical competitive ABPP assay the workflow is labor intensive and requires the separation of proteins on SDS-PAGE, which is not compatible with an HTS-assay.¹⁰ Therefore, there is an urgent need to develop plate-based assays for high-throughput screening. One option would be to use a fluorescence polarization assay, which has been widely used in the small molecular screening and drug development.¹¹ Fluorescence polarization activity-based protein profiling (FluoPol-ABPP) was first developed by Cravatt and co-workers to screen for inhibitors of uncharacterized enzymes.¹² The ABP, which contains a small fluorophore, rotates quickly and emit depolarized light when it does not bind to the target protein. Once bound to the target protein, the probe rotates slowly and emits polarized light. This technology was

introduced to address the limitation of traditional competitive ABPP methods. This assay format was also recently applied to identify inhibitors for human non-lysosomal glucosylceramidase (GBA2).¹³ In these FluoPol-ABPP studies, tetramethylrhodamine (TMR) was used as a fluorescent dye. MB064 contains a BODIPY-dye, which is very lipophilic and not compatible with screening membrane proteins, such as the PLA2G4E and PLAATs, in solution. Therefore, it would be of interest to synthesize a new probe (Figure 1B) in which the BODIPY is replaced by TMR, to be used in FluoPol-ABPP assays. To determine the selectivity profile of the hits, it is advised to perform competitive ABPP with brain membrane and soluble proteomes with the classical gel-based format.

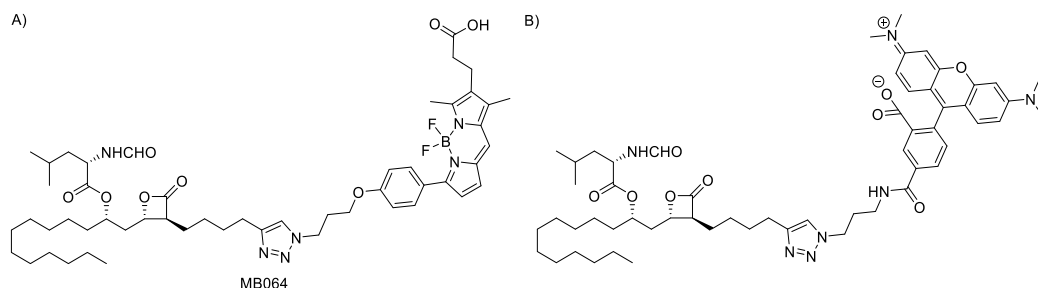


Figure 1. (A) Chemical structure of probe MB064; (B) Proposed new probe for FluoPol-ABPP.

Furthermore, there is still a need for more potent and selective inhibitors for each of the individual PLAAT proteins.⁹ Since the crystal structure of PLAAT3 has been reported,¹⁴ and the docking study of LEI-110 captured the structure activity relationship of the alpha-ketoamide series, one could use structure-based drug design and homology models of the other PLAATs to develop new and more potent and selective inhibitors for PLAAT3 and PLAAT5.

Alternatively, targeting an allosteric site at a protein represents a novel strategy in drug development to generate more selective compounds.¹⁵⁻¹⁷ Proteins from the same family usually share a highly conserved catalytic domain, which makes it very difficult to generate selective inhibitors when they target the active site.¹⁸ However, allosteric binding sites may be more diverse among proteins within the same family. PLAAT1-5 also share a highly conserved catalytic domain and the current inhibitors target the active site, therefore it would be interesting to investigate with structure-based methods whether potential allosteric sites in PLAATs exist and can be exploited for drug discovery purposes.

With potent inhibitor LEI110 in hand, the biological consequence of inhibiting PLAAT in cells and animal models can be studied in further detail. It has been shown that the dysregulation of the endocannabinoid system (ECS) is associated with the progress of

gynecological disorders and cancer.⁷ For example, in ovarian cancers, AEA was found in the follicular fluid after ovarian stimulation by hormones.¹⁹ So it would be interesting to treat ovarian cancer cells with LEI110 and study the maturation of follicles and oocytes. It is also unknown whether cellular NAPes and NAEs are affected by LEI110 treatment. An activity-based probe can also be designed based on LEI110 (Figure 2). This probe can be applied to visualize the PLAAT activity both in cell lysates and living cells.

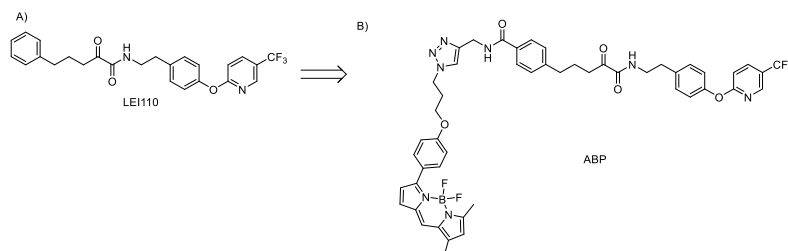


Figure 2. (A) Chemical structure of probe LEI110; (B) Proposed activity-based probe.

In summary, in this thesis an activity-based probe was discovered that could visualize the activity of PLAATs. With an optimized gel-based ABPP assay in hand, screening of a compound library led to the discovery of alpha-ketoamides as a hit for PLAAT3. Through extensive structural modifications of the hit, LEI110 was identified as the most potent inhibitor ($K_i = 20\text{nM}$) for PLAAT3. LEI110 reduced cellular arachidonic acid levels in PLAAT3 overexpressing U2OS cells and oleic acid-induced steatosis in human HepG2 cells. Gel-based ABPP and chemical proteomics showed that LEI110 is a selective pan-inhibitor of the *Hrasls*-family of thiol hydrolases (i.e. PLAAT2, PLAAT3 and PLAAT5). LEI110 could be an excellent starting point for the structure-based drug development of novel molecular therapies for obesity and/or common cold. In addition, a competitive, gel-based ABPP method for PLA2G4E using TAMRA-FP was successfully developed and applied to screen a focused library of lipase inhibitors. This resulted in the discovery of two clusters of inhibitors with different scaffolds. Optimization of the potency and selectivity of the inhibitors is required to the study of the biological role of PLA2G4E in an acute and dynamic setting with these novel tools. Together these novel chemical tools and methods will allow for a better understanding of the biosynthesis of the NAPes and to study their biological role.

6.3 References

1. Hussain, Z.; Uyama, T.; Tsuboi, K.; Ueda, N., Mammalian enzymes responsible for the biosynthesis of N-acylethanolamines. *BBA-Mol. Cell Biol. L.* **2017**, *1862* (12), 1546-1561.
2. Ogura, Y.; Parsons, W. H.; Kamat, S. S.; Cravatt, B. F., A calcium-dependent acyltransferase that produces N-acyl phosphatidylethanolamines. *Nat. Chem. Biol.* **2016**, *12* (9), 669-671.
3. Jin, X.-H.; Uyama, T.; Wang, J.; Okamoto, Y.; Tonai, T.; Ueda, N., cDNA cloning and characterization of human and mouse Ca²⁺-independent phosphatidylethanolamine N-acyltransferases. *BBA-Mol. Cell Biol. L.* **2009**, *1791* (1), 32-38.
4. Uyama, T.; Ikematsu, N.; Inoue, M.; Shinohara, N.; Jin, X. H.; Tsuboi, K.; Tonai, T.; Tokumura, A.; Ueda, N., Generation of N-acylphosphatidylethanolamine by members of the phospholipase A/acyltransferase (PLA/AT) family. *J. Biol. Chem.* **2012**, *287* (38), 31905-31919.
5. Mardian, E. B.; Bradley, R. M.; Duncan, R. E., The HRASLS (PLA/AT) subfamily of enzymes. *J. Biomed. Sci.* **2015**, *22* (1), 99.
6. Pistis, M.; Muntoni, A. L., Roles of N-acylethanolamines in brain functions and neuropsychiatric diseases. In *Endocannabinoids and Lipid Mediators in Brain Functions*, Melis, M., Ed. Springer International Publishing: Cham, **2017**; pp 319-346.
7. Luschnig, P.; Schicho, R., Cannabinoids in gynecological Diseases. *Med. Cannabis and Cannabinoids* **2019**, *2* (1), 14-21.
8. Skaper, S. D.; Di Marzo, V., Endocannabinoids in nervous system health and disease: the big picture in a nutshell. *Philos. Trans. R. Soc. Lon. B. Biol. Sci.* **2012**, *367* (1607), 3193-200.
9. Zhou, J.; Mock, E. D.; Martella, A.; Kantae, V.; Di, X.; Burggraaff, L.; Baggelaar, M. P.; Al-Ayed, K.; Bakker, A.; Florea, B. I.; Grimm, S. H.; den Dulk, H.; Li, C. T.; Mulder, L.; Overkleeft, H. S.; Hankemeier, T.; van Westen, G. J. P.; van der Stelt, M., Activity-based protein profiling identifies α -ketoamides as inhibitors for phospholipase A2 Group XVI. *ACS Chem. Biol.* **2019**, *14* (2), 164-169.
10. Wang, S.; Tian, Y.; Wang, M.; Wang, M.; Sun, G.-B.; Sun, X.-B., Advanced activity-based protein profiling application strategies for drug development. *Front. Pharmacol.* **2018**, *9*, 353-353.
11. Lea, W. A.; Simeonov, A., Fluorescence polarization assays in small molecule screening. *Expert Opin. Drug Dis.* **2011**, *6* (1), 17-32.
12. Bachovchin, D. A.; Brown, S. J.; Rosen, H.; Cravatt, B. F., Identification of selective inhibitors of uncharacterized enzymes by high-throughput screening with fluorescent activity-based probes. *Nat. Biotechnol.* **2009**, *27* (4), 387-94.
13. Lahav, D.; Liu, B.; van den Berg, R.; van den Nieuwendijk, A.; Wennekes, T.; Ghisaidoobe, A. T.; Breen, I.; Ferraz, M. J.; Kuo, C. L.; Wu, L.; Geurink, P. P.; Ovaa, H.; van der Marel, G. A.; van der Stelt, M.; Boot, R. G.; Davies, G. J.; Aerts, J.; Overkleeft, H. S., A fluorescence polarization

activity-based protein profiling assay in the discovery of potent, selective inhibitors for human nonlysosomal glucosylceramidase. *J. Am. Chem. Soc.* **2017**, *139* (40), 14192-14197.

14. Golczak, M.; Kiser, P. D.; Sears, A. E.; Lodowski, D. T.; Blaner, W. S.; Palczewski, K., Structural basis for the acyltransferase activity of lecithin:retinol acyltransferase-like proteins. *J. Biol. Chem.* **2012**, *287* (28), 23790-807.

15. Srinivasan, B.; Forouhar, F.; Shukla, A.; Sampangi, C.; Kulkarni, S.; Abashidze, M.; Seetharaman, J.; Lew, S.; Mao, L.; Acton, T. B.; Xiao, R.; Everett, J. K.; Montelione, G. T.; Tong, L.; Balaram, H., Allosteric regulation and substrate activation in cytosolic nucleotidase II from *Legionella pneumophila*. *FEBS J.* **2014**, *281* (6), 1613-1628.

16. Srinivasan, B.; Rodrigues, J. V.; Tonddast-Navaei, S.; Shakhnovich, E.; Skolnick, J., Rational design of novel allosteric dihydrofolate reductase inhibitors showing antibacterial effects on drug-resistant *Escherichia coli* escape variants. *ACS Chem. Biol.* **2017**, *12* (7), 1848-1857.

17. Srinivasan, B.; Tonddast-Navaei, S.; Roy, A.; Zhou, H.; Skolnick, J., Chemical space of *Escherichia coli* dihydrofolate reductase inhibitors: new approaches for discovering novel drugs for old bugs. *Med. Res. Rev.* **2019**, *39* (2), 684-705.

18. Orengo, C. A.; Thornton, J. M., Protein families and their evolution-a structural perspective. *Annu. Rev. Biochem.* **2005**, *74* (1), 867-900.

19. El-Talatini, M. R.; Taylor, A. H.; Konje, J. C., The relationship between plasma levels of the endocannabinoid, anandamide, sex steroids, and gonadotrophins during the menstrual cycle. *Fertil. Steril.* **2010**, *93* (6), 1989-1996.

Chinese summary

小结

Inhibitor discovery of phospholipase and N-acyltransferases

磷脂酶和 N-酰基转移酶抑制剂的发现

在**第一章**中，内源性大麻素（N-花生四烯酸乙醇胺，AEA）被认为是一种能够激活大麻素受体的内源性配体。除了 AEA，还介绍了其他几种与 AEA 结构类似的 N-酰基乙醇胺（NAE），例如棕榈酰基乙醇酰胺（PEA），油酰基乙醇酰胺（OEA），硬脂酰基乙醇酰胺（SEA）和二十二碳六烯基乙醇酰胺（DHEA），以及它们的生物合成途径。N-酰基转移酶（NAT）在 NAE 的生物合成中的第一步限速步骤中发挥作用。NATs 有两类： Ca^{2+} 依赖型的 NAT（Ca-NAT）和非 Ca^{2+} 依赖型的 NAT（PLAAT1-5）。最近，Cravatt 及其同事报道了 PLA2G4E（也称为 cPLA2 ϵ ）也是一种 Ca-NAT。该蛋白可以将酰基链从磷脂酰胆碱（PC）的 sn-1 位置转移到磷脂酰乙醇胺（PE）的胺基上，从而有效地产生 NAPEs。PLA2G4E 属于胞质磷脂酶 A2 IV 组（PLA2G4）蛋白家族，该家族中有六个成员（PLA2G4A, PLA2G4B, PLA2G4C, PLA2G4D, PLA2G4E 和 PLA2G4F）。与其他家族成员不同的是，与磷脂水解反应相比，PLA2G4E 对 N-酰基转移反应有很强的选择性。

人类磷脂酶 A / 酰基转移酶（PLAAT1-5）家族由五个成员组成（即 PLAAT 1-5），其中两个在啮齿动物中不存在（即 PLAAT2 和 PLAAT4）。它们是 Hras1s 基因编码的蛋白质。PLAATs 在体外具有非 Ca^{2+} 依赖型的磷脂酶活性，反应的底物为磷脂酰胆碱（PC）和磷脂酰乙醇胺（PE）。所有蛋白质成员都具有 O-酰基转移酶活性，并优先选择溶血磷脂酰胆碱（lyso-PC）的 sn-1 位置。这些蛋白同时也具有 N-酰基转移酶的活性：通过将甘油磷脂的 sn-1 位置的酰基链转移到 PE 的胺基上来生成 N-酰基磷脂酰乙醇胺（NAPE）。除 PLAAT3 外，所有酶均显示 PLA1 活性优于 PLA2 活性。在不同的测试条件下，PLAAT3 的底物偏好可能会发生变化。

总之，PLAAT 和 PLA2G4E 参与了 NAE 的主要生物合成途径，这使得在特定的疾病情况下如果需要操纵 NAE 的水平时，它们便成为非常好的药物靶标。本论文中的研究课题主要是开发基于活性的蛋白质谱的活性测试方法，并用该方法寻找这些酶的抑制剂。

在**第二章**中，之前开发用于监测二酰基甘油酯酶- α/β 活性的基于活性的探针（ABP）MB064 被用于分析 PLAAT3 蛋白的活性。MB064 能够以活性依赖性方式在棕色和白色脂肪组织中标记内源性 PLAAT3。使用竞争性 ABPP 的活性测试方法和重组过表达的蛋白质，以 10 μM 的浓度筛选一个包含 50 个脂肪酶抑制剂的化合物库来寻找 PLAAT3 的抑制剂。结果

发现了在 10 μM 时几乎完全抑制 PLAAT3 活性的 α -酮酰胺（化合物 1）。化合物 1 也抑制 PLAAT 家族的其他成员，但是对其他丝氨酸水解酶具有选择性。

在**第三章**中，描述了对 α -酮酰胺先导化合物的优化和构效关系。结果表明， α -酮基和酰胺基上的取代基对于抑制活性至关重要。发现 3-苯基丙烷基部分（如化合物 37 中所示）是作为 α -酮取代基的最佳片段。化合物 49 和 50 对 PLAAT5 有很强的抑制活性和选择性，而化合物 48 和 60（也称为 LEI110）是对 PLAAT3 和 5 都具有很强的抑制活性和选择性的抑制剂。

第四章中介绍了 LEI110 的生物学分析结果。LEI110 是对 PLAAT3 有效的，选择性的和细胞渗透性的抑制剂。在 PLAAT3 过表达的 U2OS 细胞中，LEI110 可以降低细胞花生四烯酸水平。在人类 HepG2 细胞中，LEI110 降低了中油酸诱导的脂肪变性。为了深入了解 α -酮酰胺与 PLAAT3 相互作用的分子机制，LEI110 和化合物 1 被对接到 PLAAT3 晶体结构中。LEI110 和化合物 1 共价连接到 Cys113，并进行了分子动力学模拟。观察到氧负离子可以与 His23 形成氢键，同时与 Tyr21 的 π - π 堆积作用。可以预期，LEI110 是针对肥胖和/或普通感冒的新型分子疗法的基于结构的药物开发的绝佳起点。

在**第五章**，开发了以 TAMRA-FP 为探针的 ABPP 测试方法来分析 PLA2G4E 的活性。在 10 μM 的浓度下，筛选了含有 200 多种化合物的化合物库，来寻找人类 PLA2G4E 的抑制剂。八个抑制剂显示人类 PLA2G4E 的残留活性不到 20%。ESC386 和 ESC387 是最有效的抑制剂， $p\text{IC}_{50}$ 值分别为 6.2 ± 0.1 和 6.1 ± 0.1 。这些化合物代表 PLA2G4E 的最新的抑制剂，为进一步的探针开发提供了非常好的起点。

第六章对本论文的实验工作进行了归纳和总结，并对未来的研究工作进行了展望。

Curriculum Vitae

Juan Zhou was born on 27th of November 1985 in Zhoukou, Henan province, China. In 2005, she was accepted by the Zhengzhou University after the National College Entrance Examination. She obtained her bachelor's diploma in pharmacy in 2009 and was admitted to the Graduate School of China Pharmaceutical University in the same year.

In 2009, she started her master program in Pharmacology at China Pharmaceutical University under the supervision of Prof. Dr. Feng Yu. Her research projects focused on the effect of metformin on liver in a rat model of Type 2 diabetes. She obtained her Master Degree in Science in 2012.

In September 2012, she started working in Department of Human Genetics, Leiden University Medical Center as a researcher. In May 2014, she started her PhD research project within the Bio-organic Synthesis group and then the Molecular Physiology group in Leiden Institute of Chemistry, Leiden University with financial support from the CSC. The research was conducted under the supervision of Prof. Dr. Mario van der Stelt and Prof. Dr. Herman Overkleeft. During her PhD research, she focused on the assay development and inhibitors discovery for PLAAT family protein. Part of her work was presented as poster at the CHAINS-Dutch chemistry conference (Veldhoven, 2015) and the ICRS-International Cannabinoid Research Society (2018, Leiden).

List of publications

1. Structure-Activity Relationship Studies of α -Ketoamides as Inhibitors of the Phospholipase A and Acyltransferase Enzyme Family. *J. Med. Chem.* 2020, 63 (17), 9340-9359.
Zhou, J.; Mock, E. D.; Al Ayed, K.; Di, X.; Kantae, V.; Burggraaff, L.; Stevens, A. F.; Martella, A.; Mohr, F.; Jiang, M.; van der Wel, T.; Wendel, T. J.; Ofman, T. P.; Tran, Y.; de Koster, N.; van Westen, G. J. P.; Hankemeier, T.; van der Stelt, M.
2. Activity-Based Protein Profiling Identifies α -Ketoamides as Inhibitors for Phospholipase A2 Group XVI. *ACS Chem. Biol.* 2019, 14 (2), 164-169.
Zhou, J.; Mock, E. D.; Martella, A.; Kantae, V.; Di, X.; Burggraaff, L.; Baggelaar, M. P.; Al-Ayed, K.; Bakker, A.; Florea, B. I.; Grimm, S. H.; den Dulk, H.; Li, C. T.; Mulder, L.; Overkleeft, H. S.; Hankemeier, T.; van Westen, G. J. P.; van der Stelt, M.
3. Mapping in vivo target interaction profiles of covalent inhibitors using chemical proteomics with label-free quantification. *Nat. Protoc.* **2018**, 13 (4), 752-767.
van Rooden, E. J.; Florea, B. I.; Deng, H.; Baggelaar, M. P.; van Esbroeck, A. C. M.; **Zhou, J.**; Overkleeft, H. S.; van der Stelt, M.,
4. Rapid and profound rewiring of brain lipid signaling networks by acute diacylglycerol lipase inhibition. *Proc. Natl. Acad. Sci. USA* **2016**, 113 (1), 26-33.
Ogasawara, D.; Deng, H.; Viader, A.; Baggelaar, M. P.; Breman, A.; den Dulk, H.; van den Nieuwendijk, A. M.; Soethoudt, M.; van der Wel, T.; **Zhou, J.**; Overkleeft, H. S.; Sanchez-Alavez, M.; Mori, S.; Nguyen, W.; Conti, B.; Liu, X.; Chen, Y.; Liu, Q. S.; Cravatt, B. F.; van der Stelt, M.